

https://dspace.org/

Analyses of cassava phytohormones in biotic responses during South African cassava mosaic virus infection

Mokoka, Oboikanyo Austin

2025-06

University of the Witwatersrand, Johannesburg

https://hdl.handle.net/10539/48752

Mokoka, Oboikanyo Austin. (2025). Analyses of cassava phytohormones in biotic responses during South African cassava mosaic virus infection. [Master's dissertation, University of the Witwatersrand, Johannesburg]. WIReDSpace. https://hdl.handle.net/10539/48752

Downloaded from a DSpace repository. https://dspace.org/



UNIVERSITY OF THE
WITWATERSRAND,
JOHANNESBURG

Analyses of cassava phytohormones in biotic responses during *South African cassava mosaic virus* infection

by

Oboikanyo Mokoka

(1899853)

Dissertation

Submitted in fulfilment of the requirements for the degree:

Master of Science

in

Molecular and Cell Biology

in the Faculty of Science, University of the Witwatersrand, Johannesburg, South Africa

Supervisor: Prof M.E.C. Rey

Co-supervisor: Dr. B.L. Sizani

09 June 2025

DECLARATION

I, **Oboikanyo Austin Mokoka (1899853)**, declare that this dissertation is my own, unaided work. It is being submitted for the Degree of Master of Science at the University of the Witwatersrand, Johannesburg. It has not been submitted before for any degree or examination at any other University.

Signature: 

9th day of June 2025 at Braamfontein, Johannesburg

ABSTRACT

Manihot esculenta Crantz (cassava) is a starch-rich perennial tuber crop that serves as a food source, in addition to having industrial applications. Concerningly, cassava is susceptible to infection by *South African cassava mosaic virus*, resulting in the development of cassava mosaic disease (CMD). As CMD results in significant losses of cassava yields, it poses a threat to food security. *South African cassava mosaic virus* (SACMV) encodes for multifunctional proteins that aid in infection and suppress host immune responses, which are coordinated by plant hormones. Phytohormones are activated during a pathogenic infection, and include salicylic acid (SA), jasmonic acid (JA), ethylene (ET), and abscisic acid (ABA).

The main aim of this research project was to quantify, using Ultra-High Pressure Liquid Chromatography-Mass Spectrometry (UHPLC-MS), the phytohormone levels of SA, JA, ABA, and ET in the CMD-susceptible T200 and CMD-tolerant TME3 across the three stages of SACMV infection, namely 12-, 32-, and 67-days post infection (dpi). This was to determine if these phytohormones contribute to either susceptibility or recovery, and to relate the hormone levels of the expression of SACMV genes and cassava hormone-related genes, assessed using reverse transcription quantitative polymerase chain reaction (RT-qPCR). Infection trials and subsequent gene expression studies revealed that T200 had a significantly higher SACMV load compared to TME3 at 32- and 67- dpi, and this correlated with the significantly higher expression of SACMV genes in T200. Additionally, the activities of these viral proteins promoted virus fitness in T200 via dysregulation of cell proliferation, promotion of viral replication and transmission, disruption of global metabolism, disruption of plant defences, and the suppression of post-transcriptional gene silencing (PTGS) and transcriptional gene silencing (TGS). Contrastingly, TME3 recovered by 67 dpi and was tolerant to SACMV infection. The quantification of hormone levels and assessment hormone-related gene expression revealed that TME3 relies on an early response of ABA- and JA-mediated PTGS and SA-driven defence, while its recovery is reliant on SA-, ET-, and JA-driven defence responses and the establishment of systemic acquired resistance (SAR). Lastly, following recovery, TME3 tolerates SACMV via induced systemic resistance (ISR) that is reliant on finetuned JA-, ET-, and ABA- signalling.

Keywords: geminiviruses, cassava mosaic disease, pathogenicity determinants, plant immunity, disease recovery, tolerance

DEDICATION

I dedicate this work to my grandmother, who left an indelible mark on her children, grandchildren, and great grandchildren.

Mmapitso Jacobeth Mokoka

(23 November 1937 – 17 December 2017)

In the end, I did as you asked of me: **I got educated, so that I may succeed in this life**.
I know I will.

Additionally, I dedicate this work to my friend,

Ntokozo Malebadi

(10 March 2000 – 02 March 2023)

You never got to see it work out for me after all. Your smile, humility, and empathy will never be forgotten.

ACKNOWLEDGEMENTS

- Firstly, I would like to thank and acknowledge **God** for giving me the strength, wisdom, and clarity of mind to be able to navigate through and complete this research project.
- I would like to acknowledge my supervisor, **Prof Chrissie Rey**, for your guidance, support, and patience as I conducted this fascinating research project, from which I have acquired indispensable skills and an expanded knowledge base.
- I would like to thank my co-supervisor, **Dr Bulelani Sizani**, for your guidance and helping me to develop my critical thinking. I will never forget how you impacted my way of seeing the complexity in everything. Thank you very much!
- Many great thanks to my colleagues in the School of Molecular and Cell Biology for insightful conversations, particularly **Mr Keelan Krinsky**, **Dr Nikita Nankoo**, and **Mr Dylan Moodley**. A special shout out to **Ms Aviwe Matsha**, **Mr Pusang King Sekgobela**, and **Mr Tlotliso Sello**.
- To my mom, **Kefilwe**, thank you for always encouraging me, as your belief allowed me to persevere through it all from start to finish. To my dad, **Karabo**, thank you for always helping me keep a steady head through the challenges I faced and for always helping me to navigate obstacles. Lastly, to my big sister, **Obakeng**, thank you for always believing in me and spurring me on, and for always being by my side. May we continue to motivate and inspire each other to succeed and get better each and every time.
- To my love, **Tsholofelo**, thank you for always believing in me, for always celebrating me, and for always encouraging me to live up to my potential. Your unwavering support, kindness, and faith carried me through the good times and the bad.
- To my friends, **Makhuparetjia Nyama**, **Phuti Mphaki**, **Pako Molope**, **Thabo Nkutha**, **Orefemetse Mfelang**, **Iman Kalakgosi**, **Letlhogonolo Tlhapane**, **Kgotso Mokau**, **Kopano Phutiyagae**, **Oratile Poane**, and **Kholofelo Matibidi**. I thank you for your tremendous support and constantly checking up on me. While I could not name everyone, I would like to thank all my friends for their encouragement, belief, support, and motivation.
- I would like to acknowledge and thank **Prof Ian Dubery**, **Dr Farhahna Allie**, and **Mrs Nombuso Buthelezi** from the University of Johannesburg for the collaborative contributions that they have to this research.
- Lastly, I would like to thank the **National Research Foundation**, **University of the Witwatersrand Postgraduate Merit Award**, and **LEAP-Agri** for funding.

TABLE OF CONTENTS

DECLARATION I

ABSTRACT II

DEDICATION III

ACKNOWLEDGEMENTS IV

TABLE OF CONTENTS V

LIST OF FIGURES IX

LIST OF TABLES XII

ABBREVIATIONS XIII

RESEARCH OUTPUTS XIX

CHAPTER 1: INTRODUCTION 1

1.1. GENERAL INTRODUCTION OF CASSAVA AND CASSAVA MOSAIC DISEASE 1

1.2. PROBLEM STATEMENT 2

1.3. RATIONALE OF THE STUDY 3

1.4. NOVELTY OF THE STUDY 6

1.5. HYPOTHESIS 6

1.6. RESEARCH QUESTIONS 6

1.7. AIMS AND OBJECTIVES 7

Aim 7

Specific objectives 7

1.8. STRUCTURE OF THE DISSERTATION 7

CHAPTER 2: LITERATURE REVIEW 9

2.1 OVERVIEW OF FOOD SECURITY 9

2.1.1 Food security in Africa *9*

2.1.2 The threat posed by climate change *9*

2.2 ***MANIHOT ESCULENTA*** **CRANTZ** 9

2.2.1 Brief overview of cassava and its uses *10*

2.2.2 General characteristics *10*

2.2.3 Global production *11*

2.2.4 Devastating impact of plant diseases in cassava *12*

2.3 CASSAVA MOSAIC GEMINIVIRUSES 14

2.3.1 General overview *14*

2.3.2 Genome organisation of begomoviruses and their pathogenicity determinants *14*

2.3.3 Prevalence of Cassava Mosaic Geminiviruses (CMGs) *16*

2.3.4 South African cassava mosaic virus *17*

2.4 PLANT DEFENCE AND IMMUNITY MECHANISMS 18

2.4.1. Basal Immunity *18*

2.4.2. PAMP-Triggered Immunity (PTI) and Effector-Triggered Immunity (ETI) *18*

2.4.3. Hypersensitive Response *20*

2.4.4. Systemic Acquired Resistance (SAR) and Induced Systemic Resistance (ISR) *20*

2.4.5. Transcriptional and Posttranscriptional Gene Silencing *20*

2.5 MOLECULAR SIGNALLING AND REGULATION OF DEFENCE PATHWAYS 21

2.5.1. Phytohormones *21*

Salicylic Acid 21

Jasmonic Acid 23

Ethylene 25

Abscisic Acid 27

Auxins 29

2.5.2. Reactive Oxygen Species and Nitric Oxide *30*

CHAPTER 3: MATERIALS AND METHODS **32**

3.1. METHODOLOGY FLOW CHART 32

3.2. REAGENTS AND MATERIALS 33

3.3. *AGROBACTERIUM TUMEFACIENS* C58C1 INFECTIOUS CLONE STOCKS 33

3.4. PLANT TISSUE CULTURE MAINTENANCE AND PROPAGATION 35

3.5. IN VIVO GENERATION OF PLANT TISSUE CULTURE 35

3.6. CASSAVA T200 AND TME3 INFECTION TRIALS 36

3.6.1. Preparation of infectious clones *36*

3.6.2. Agroinfection of T200 and TME3 ..... *36*

3.7. SAMPLE HARVESTING AND STORAGE 37
3.8. PRIMER DESIGN AND OPTIMISATION 37
3.8.1. Primer design for SACMV-specific ORFs *37*
3.8.2. Primer design for cassava hormone biosynthesis and response genes *38*
3.8.3. Primer efficiency *42*
3.9. DETECTION (CONVENTIONAL) PCR OF SACMV-INFECTED CASSAVA 44
3.10. VIRAL LOAD DETERMINATION 44
3.11. CDNA SYNTHESIS 46
3.11.1. RNA extraction *46*
3.11.2. Deoxyribonuclease (DNase) treatment *47*
3.11.3. First Strand synthesis *47*
3.12. GENE EXPRESSION STUDIES 48
3.13. QUANTIFICATION OF CASSAVA PHYTOHORMONES DURING INFECTION BY SACMV 50
3.13.1. Validation of hormone extraction protocol *50*
3.13.2. Percentage Recovery study *50*
3.13.3. Hormone extraction and quantification *51*
CHAPTER 4: RESULTS 53
4.1. QUALITY CONTROL 53
4.1.1. Confirmation of A. tumefaciens C58C1 clones harbouring either pBIN19-SACMV-DNA-A, pBIN19-SACMV-DNA-B, or empty pBIN19 vector *53*
4.1.2. Nucleic acid extractions *54*
4.1.3. Primer efficiency and specificity for SACMV genes *56*
4.1.4. Primer efficiency and specificity for selected cassava hormone-related genes *58*
4.2. SACMV INFECTION TRIALS IN T200 AND TME3 62
4.2.1. CMD progression and symptom severity in cassava T200 and TME3 ..... *62*
4.2.2. Detection PCR for confirmation of SACMV infection in T200 and TME3 ..... *63*
4.2.3. Viral load quantification in T200 and TME3 ..... *64*
4.3. DIFFERENTIAL EXPRESSION OF VIRAL ORFS AT 12-, 32-, AND 67-DPI IN SACMV-INFECTED T200 AND TME3 65

4.4. DIFFERENTIAL EXPRESSION OF HORMONE BIOSYNTHESIS AND RESPONSE GENES AT 12-, 32-, AND 67-DPI IN SACMV-INFECTED T200 AND TME3 66

4.5. HORMONE QUANTIFICATION AT 12- AND 32-DPI IN SACMV-INFECTED T200 AND TME3 69

4.5.1. Quantification of hormone production in T200 and TME3 at 12- and 32-dpi during SACMV-infection *69*

4.5.2. Comparison of hormone production in SACMV-infected T200 and SACMV-infected TME3 at 12- and 32-dpi *70*

CHAPTER 5: DISCUSSION 71

5.1. *SOUTH AFRICAN CASSAVA MOSAIC VIRUS* TITRE INFLUENCES CMD DEVELOPMENT IN CASSAVA AND IS ASSOCIATED WITH SYMPTOM SEVERITY AND RECOVERY 71

5.2. DIFFERENTIAL EXPRESSION OF VIRAL PATHOGENICITY DETERMINANTS CAN BE ASSOCIATED WITH CMD PROGRESSION AND SYMPTOM DEVELOPMENT 73

5.2.1. Expression of pathogenicity determinants involved in viral replication and cell cycle progression *73*

5.2.2. Inhibition of hormone signalling and dysregulation of global metabolism ... *77*

5.2.3. Virus intercellular movement and systemic spread *79*

5.2.4. Suppression of DNA methylation and RNA silencing *80*

5.3. DIFFERENTIAL EXPRESSION OF HORMONE ASSOCIATED GENES AND THE PRODUCTION OF PHYTOHORMONES HIGHLIGHTS THE CONTRASTING RESPONSES OF T200 AND TME3 AGAINST SACMV ... 82

5.3.1. Dynamics of gene expression and hormone production during early infection *82*

5.3.2. Establishment of systemic acquired resistance during systemic infection *84*

5.3.3. Recovery from CMD and tolerance through induced systemic resistance *85*

CHAPTER 6: CONCLUSIONS 87

6.1. KEY FINDINGS OF THE STUDY 87

6.2. IMPLICATIONS OF THE STUDY 88

6.3. LIMITATIONS 88

6.4. FUTURE WORK 89

REFERENCES 90

LIST OF FIGURES

***Figure 1**: Cassava leaves (**a** and **b**) (captured in 2022) alongside the tuber roots (**c**) (Parmar et al., 2017). 10*

***Figure 2**: A representation of the annual production (in million tons) of cassava in 2023, based on FAO data (Ritchie et al., 2023). 12*

***Figure 3**: Comparison of the symptoms that occur in cassava during cassava bacterial blight (CBB) (**a**), cassava brown streak disease (CBSD) (**b** and **c**), and cassava mosaic disease (CMD) (**d** and **e**) 13*

***Figure 4:** The genome organisation of bipartite begomoviruses (Rey & Vanderschuren, 2017). 15*

***Figure 5:** The salicylic acid biosynthesis pathways, directed by either Isochorismate Synthase (ICS) or phenylalanine ammonia-lyase (PAL), with chorismic acid acting as a precursor in both pathways (Lefevere et al., 2020) 22*

***Figure 6:** The jasmonic acid biosynthesis pathway (Sasaki et al., 2001) 24*

***Figure 7:** The ethylene biosynthesis pathway, with the S-adenosyl-$_L$-methionine (SAM) as a precursor (Pattyn et al., 2021) 26*

***Figure 8:** The abscisic acid biosynthesis pathway (Wasilewska et al., 2008) 28*

***Figure 9:** The indole-3-acetic acid (IAA) biosynthesis pathway (Zhao, 2012) 30*

***Figure 10:** Workflow outlining the approach of the research 32*

***Figure 11:** Agarose gel, of 3% (w/v), showing PCR products from Colony PCR of A. tumefaciens C58C1 clones 53*

***Figure 12:** Agarose gels, of 1% (w/v), showing intact DNA extracted from cassava leaves and the outcome post-purification 54*

Figure 13: *Agarose gels, of 2% (w/v), showing intact RNA extracted from cassava leaves....55*

Figure 14: *Agarose gel, of 3% (w/v), showing qPCR products generated from the amplification of South African cassava mosaic virus genes of interest.....56*

Figure 15: *Melt curve peaks for oligonucleotide pairs used to target the selected South African cassava mosaic virus genes.....57*

Figure 16: *Agarose gel, of 3% (w/v), showing qPCR products generated from the amplification of cassava genes of interest.....58*

Figure 17: *Melt curve peaks for oligonucleotide pairs used to target the selected salicylic acid-related genes.....59*

Figure 18: *Melt curve peaks for oligonucleotide pairs used to target the selected jasmonic acid-, abscisic acid-, and auxin-related genes.....60*

Figure 19: *Melt curve peaks for oligonucleotide pairs used to target the selected ethylene-, brassinosteroid-, and cytokinin-related genes.....61*

Figure 20: *Symptom development in South African cassava mosaic virus-infected T200 and TME3 at 12-, 32-, and 67-dpi.....62*

Figure 21: *Agarose gel, of 2% (w/v), showing PCR products generated from the amplification of AV1 and BC1.....63*

Figure 22: *Quantification of DNA-A viral copies in cassava during South African cassava mosaic virus infection.....64*

Figure 23: *Differential expression of South African cassava mosaic virus genes in cassava during cassava mosaic disease.....65*

Figure 24: *Differential expression of hormone biosynthesis genes in cassava during cassava mosaic disease.....66*

Figure 25: *Differential expression of hormone response genes in cassava during cassava mosaic disease 68*

Figure 26: *Perturbations in hormone biosynthesis in South African cassava mosaic virus-infected T200 and TME3 .....69*

Figure 27: *Hormone production influences the response of cassava to South African cassava mosaic virus infection.....70*

LIST OF TABLES

Table 1: *Gene specific polymerase chain reaction primer sequences for targeted genes.....34*

Table 2: *Components of a single colony polymerase chain reaction reaction.....34*

Table 3: *Cycling conditions for the polymerase chain reaction 34*

Table 4: *Gene specific qPCR primer sequences for targeted SACMV genes.....38*

Table 5: *Gene specific qPCR primer sequences for selected cassava genes 39*

Table 6: *Components of a single qPCR reaction 43*

Table 7: *Cycling conditions for the qPCR.....43*

Table 8: *Components of a single qPCR reaction 45*

Table 9: *Cycling conditions for the qPCR.....45*

Table 10: *Components of a single DNAse treatment reaction.....48*

Table 11: *Gene specific PCR primer sequences for selected housekeeping genes.....48*

Table 12: *Components of a single qPCR reaction 49*

Table 13: *Cycling conditions for the qPCR.....49*

ABBREVIATIONS

AAO	Aldehyde oxidase
ABA	Abscisic acid
ABF	ABA-responsive element binding factor
ABI5	Abscisic acid insensitive 5
ABRE	ABA-responsive element
AC1	Replication initiation protein (Rep)
AC2	Transcription activator protein (TrAP)
AC3	Replication enhancer protein (Ren)
AC4	Silencing suppressor protein
AC5	Silencing suppressor protein
ACC	1-aminocycloproane-1-carboxylic acid
ACMV	*African cassava mosaic virus*
ACN	Acrylonitrile
ACO	ACC oxidase
ACS	ACC synthase
ACX	Acyl-CoA oxidase
ADK	Adenosine kinase
AGO1	ARGONAUTE 1
AGO5	ARGONAUTE 5
AGO18	ARGONAUTE 18
AOC	Allene oxide cyclase
AOS	Allene oxide synthase
ARF	Auxin Response Factor
Aux	Auxin
AV1	Capsid protein
AV2	Putative protein kinase
avr	Avirulence
BA	Benzoic acid
BC1	Nuclear shuttle protein (NSP)

b-CHI	Basic chitinase
bHLH	Basic helix-loop-helix
BR	Brassinosteroid
BV1	Movement protein (MP)
bZIP	Basic leucine zipper
CA2+	Calcium ion
Carb	Carbenicillin
CBB	Cassava Bacterial Blight
CBSD	Cassava Brown Streak Disease
CBSV	*Cassava Brown Streak Virus*
cDNA	Complementary DNA
CGs	Cyanogen Glucosides
CIRP	Ca^{2+}-induced ROS production
CK	Cytokinins
CM	Chorismate mutase
CMD	Cassava Mosaic Disease
CMG	Cassava Mosaic Geminivirus
CO2	Carbon dioxide
COI1	Coronatine-insensitive 1
CP	Capsid protein
CR	Common region
CTAB	hexadecyltrimethylammonium bromide
CTR1	Constitutive triple response 1
CuLCvV	*Cucurbit leaf crumple virus*
$CuSO_4$	Copper (II) Sulphate
CW	Cell wall
DAMP	Damage-associated molecular pattern
DEPC	Diethyl pyrocarbonate
dH2O	Distilled water
DNA	Deoxyribonucleic acid
DNase	Deoxyribonuclease

dpi	days post-infection
dsDNA	Double-stranded DNA
dsRNA	Double stranded RNA
EACMV	*East African cassava mosaic virus*
ECM	Extracellular matrix
EDS5	Enhanced Disease Susceptibility 5
EDTA	Ethylenediaminetetraacetic Acid
EIN2	Ethylene Insensitive 2
EIN3	Ethylene Insensitive 3
EPS1	Enhanced Pseudomonas Susceptibility 1
ET	Ethylene
ETI	Effector-triggered immunity
ETR1	Ethylene Receptor 1
FAO	Food and Agriculture Organization of the United Nations
GA	Gibberellic acid
GDP	Gross Domestic Product
GMV	Geminivirus
GO	Gene ontology
h	Hour(s)
HCl	Hydrogen chloride
HR	Hypersensitive response
IAA	Indole-3-acetic acid
IC	Isochorismate
ICS	Isochorismate synthase
IPA	Indole-3-pyruvate
ISR	Induced systemic resistance
JA	Jasmonic acid
JA-Ile	Jasmonoyl-isoleucine
JMT	JA carboxyl methyltransferase
Kan	Kanamycin
Kb	Kilobase

LiCl	Lithium Chloride
LOX	Lipoxygenase
LRR	Leucine-rich repeat
MAMP	Microbe-associated molecular pattern
MAPK	Mitogen activated protein kinases
MeJA	Methyl jasmonate
MeOH	Methanol
MFP	Multifunctional protein
min	Minute(s)
miRNA	micro-RNA
MP	Movement protein
mRNA	Messenger RNA
MS	Murashige and Skoog
MTA	5'-methylthioadenosine
N	Nitrogen
NaCl	Sodium chloride
NaOH	Sodium hydroxide
NB-LRR	Nucleotide-binding leucine-rich repeat
NO	Nitric oxide
NPR1	Non-expressor of pathogenesis-related 1
NSP	Nuclear Shuttle Protein
nt	Nucleotide
OD600	Optical density at 600 nm
OPR3	12-oxo-phytodienoic acid reductase
ORF	Open reading frame
PAL	Phenylalanine ammonia-lyase
PAMP	Pathogen-associated molecular pattern
pBINSA-A	pBIN19-SACMV-DNA-A clone
pBINSA-B	pBIN19-SACMV-DNA-B clone
PBS3	avrPphB Susceptible 3
PCR	Polymerase chain reaction

PD	Plasmodesmata
PDF1.2	Plant defensin 1.2
PepGMV	*Pepper golden mosaic virus*
Phe	Phenylalanine
PKC	Putative protein kinase
ppb	parts per billion
ppm	Parts per million
PPV	*Plum pox virus*
PR	Pathogenesis-related
PRR	Pattern recognition receptor
PTGS	Posttranscriptional gene silencing
PTI	PAMP triggered immunity
PVP-40	Polyvinylpyrolidone Av. Mol. Wt. 40,000
PYR1	Pyrabactin resistance 1-like 1
RCR	Rolling circle replication
RdDM	RNA-directed DNA methylation
RDR	Replication-dependent recombination
RDV	*Rice dwarf virus*
REn	Replication enhancer protein
Rep	Replication initiation protein
RFs	Replicative forms
RICR	ROS-induced Ca2+-release
RNA	Ribonucleic acid
RNAi	Interfering RNA
RNase	Ribonuclease-free
ROS	Reactive oxygen species
rRNA	Ribosomal RNA
RSV	*Rice stripe virus*
RT-qPCR	Reverse transcription quantitative polymerase chain reaction
SA	Salicylic acid
SACMV	*South African cassava mosaic virus*

SAM	*S*-adenosyl-L-methionine
SAR	Systemic Acquired Resistance
sec	Second(s)
siRNAs	Short interfering RNAs
SLCMV	*Sri Lankan cassava mosaic virus*
SnRK1	Sucrose non-fermenting-related kinase 1
SnRK2	Sucrose nonfermenting 1 related protein kinase 2
ssDNA	Single-stranded DNA
TAE	Tris-Acetate-EDTA
TBE	Tris-Borate-EDTA
t-CA	Trans-cinnamic acid
TF	Transcription factor
TGS	Transcriptional gene silencing
TMV	*Tobacco mosaic virus*
TrAP	Transcriptional activator protein
Tris	Tris(hydroxymethyl)-aminomethane
Trp	Tryptophan
TYLCV	*Tomato yellow leaf curl virus*
UHPLC-MS	Ultra-high performance liquid chromatography mass spectrophotometry
VSR	Viral suppressor of RNA silencing
YEP	Yeast Extract Peptone media
YUC	YUCCA flavin monooxygenase

RESEARCH OUTPUTS

Oboikanyo Mokoka, Bulelani Sizani, and Marie E.C. Rey, 2023. Cassava Mosaic Disease recovery is associated with phytohormones, *South African cassava mosaic virus* titre, and viral effector-proteins. Poster presentation at the Molecular Biosciences Research Thrust (MBRT), 7 December 2023

Oboikanyo Mokoka, Bulelani Sizani, and Marie E.C. Rey, 2024. Cassava Mosaic Disease recovery is associated with phytohormones, *South African cassava mosaic virus* titre, and viral effector-proteins. Oral presentation at the Regional Plant Biotechnology Forum (under the African Centre for Gene Technologies), 6 September 2024

Oboikanyo Mokoka, Bulelani Sizani, and Marie E.C. Rey, 2024. Cassava Mosaic Disease recovery is associated with phytohormones, *South African cassava mosaic virus* titre, and viral effector-proteins. Poster presentation at Metabolomics South Africa (under the African Centre for Gene Technologies), 17 September 2024

Oboikanyo Mokoka, Bulelani Sizani, and Marie E.C. Rey, 2024. Cassava Mosaic Disease recovery is associated with phytohormones, *South African cassava mosaic virus* titre, and viral effector-proteins. Oral presentation at the Molecular Biosciences Research Thrust (MBRT), 5 December 2024

Sizani, B.L., Krinsky, K., Mokoka, O.A., Rey, M.E.C, 2025. Comparative Analysis of Pattern-Triggered and Effector-Triggered Immunity Gene Expression in Susceptible and Tolerant Cassava Genotypes Following Begomovirus Infection. *PLOS ONE* 20, e0318442. https://doi.org/10.1371/journal.pone.0318442

Chapter 1: Introduction

1.1. General Introduction of Cassava and Cassava Mosaic Disease

Manihot esculenta Crantz, commonly referred to as cassava, is a perennial tuber crop of the *Euphorbiaceae* family (Ceballos & de la Cruz, 2012). While its tubers are starch-rich, cassava leaves contain micronutrients such as vitamins and minerals, allowing for their consumption throughout any year due to the perennial nature of cassava (Uchechukwu-Agua *et al.*, 2015; Parmar *et al.*, 2017). Despite its moderate tolerance to drought, or nutrient-poor soil with unbalanced pH or poor water drainage (Anikwe & Ikenganyia, 2018; Kawaye & Hutchinson, 2021), cassava is susceptible to cassava mosaic disease (CMD). This disease is caused by whitefly-transmitted (*Bemisia tabaci* Gennadius) cassava mosaic geminiviruses (CMGs), which are prevalent in cassava-producing regions across African countries as well as the southeast Asian countries of India and Sri Lanka (Legg & Fauquet, 2004; Patil & Fauquet, 2009). Symptoms of CMD are characterized by leaf curling, mottling and chlorosis, as well as mosaic patterning of leaves, resulting in agricultural and economic losses (Lozano, 1986; Legg & Fauquet, 2004; Maruthi *et al.*, 2005; Zhang *et al.*, 2005).

Overall, there are eleven species of CMGs, which have their own strains and variants (Rey & Vanderschuren, 2017). The species are namely: *African cassava mosaic virus* (ACMV), *East African cassava mosaic virus* (EACMV), *East African cassava mosaic Kenya virus*, *East African cassava mosaic Malawi virus*, *East African cassava mosaic Zanzibar virus*, *Cassava mosaic Madagascar virus*, *South African cassava mosaic virus*, *East African cassava mosaic virus* Cameroon [Cameroon-1998], *African cassava mosaic virus* Burkina Faso, *Indian cassava mosaic virus*, and *Sri Lankan cassava mosaic virus* (Rey & Vanderschuren, 2017). *South African cassava mosaic virus*, a bipartite CMG, whose genome consists of two comparts, is one of the causative agents of CMD in South Africa, and was first noted in fields in Mpumalanga and Swaziland in the 1980s (Berrie *et al*., 1998). Its genome consists of DNA-A and DNA-B, which contain several open reading frames (ORFs), namely *AC1*, *AC2*, *AC3*, *AC4*, *AC5*, *AV1*, and *AV2*, as well as *BC1* and *BV1* (Zerbini *et al*., 2017). These ORFs encode for multifunctional pathogenicity determinants that are involved in viral replication, regulation

of viral and host gene expression, countering host defence mechanisms, encapsulation of the viral genome, and cell-to-cell movement (Briddon et al., 2010).

1.2. Problem Statement

Despite lacking in protein and lipid content, being starch-rich makes cassava a food security and sustenance crop for more than 800 million people globally (Parmar *et al.*, 2017). In addition being a food crop, cassava is also used as animal feed and has industrial application in the production of alcoholic beverages, textile products, biofuels, and plywood (Uchechukwu-Agua & Opara, 2015; Nuwamanya *et al.*, 2017; Parmar *et al.*, 2017). The global production of cassava occurs in countries situated in tropical regions and it is preferred due to its capability to adapt to environmental stresses (Parmar *et al.*, 2017; Anikwe & Ikenganyia, 2018; Ritchie & Roser, 2020). As of 2023 and per data published by the Food and Agriculture Organization of the United Nations (FAO), more than 333 million tons of cassava tubers produced in 2023 and Africa accounted for 63% of all global production (Ritchie et al., 2023).

These characteristics of environmental stress tolerance have allowed for cassava to be considered as a crop that would be least affected by climate change compared to others such as maize and potato (Jarvis *et al.*, 2012; Anikwe & Ikenganyia, 2018). However, cassava production across sub-Saharan Africa and Asia is negatively impacted by CMD, due to the prevalence of whitefly-transmitted CMGs in these cassava-producing regions (Reynolds et al., 2015). Historically, CMGs have caused several CMD outbreaks in cassava producing regions in Africa and southeast Asia, affecting tuber yields and cassava production (Combala *et al*., 2024; Malichan *et al*., 2023). In southeast Asia, recent outbreaks of *Sri Lankan cassava mosaic virus* caused CMD outbreaks that affected cassava growing regions in Cambodia, Vietnam, Thailand, and Laos, significantly impacting cassava production (Malichan *et al*., 2023). In West Africa alone, uncontrolled outbreaks of CMD causes up to 90% yield losses, significantly affecting food security (Combala *et al*., 2024). Furthermore, in the 1990s, Uganda faced a famine crisis driven by the emergence of *East African cassava mosaic virus-Uganda*, which devastated cassava plantations (Legg *et al*., 2006)

However, plants have adapted various mechanisms such as structural and chemical defences, transcriptional and posttranscriptional gene silencing, protein modification and/or degradation, and autophagy, which can all be fine-tuned to specific pathogens, such as viruses. (Garcia-Ruiz, 2019; Zhao & Li, 2021). Phytohormones, which are involved in plant growth and development, play a critical role in plant defence and immunity, as they lead to the production of defence/response proteins and the activation of genes involved in defence pathways (Zhu *et al*., 2022). These phytohormones include salicylic acid (SA), jasmonic acid (JA), ethylene (ET), abscisic acid (ABA), auxins (Aux), gibberellic acids (GAs), cytokinins (CKs), and brassinosteroids (BRs) (Zhao & Li, 2021). Plant defence against pathogens is primarily coordinated by SA, JA, and ET whilst ABA, Aux, CKs, BRs, and GAs are involved in modulating the plant immune responses and defence (Müllender *et al*., 2021). The interactions between viruses and their host plants often lead to rapid changes in hormone homeostasis and signalling (Müllender *et al*., 2021). As such, considering the role of phytohormones in plant immunity and disease response, there is interest to assess how phytohormones would play a role in the response of cassava to infection with SACMV.

1.3. Rationale of the study

With climate change already posing a negative effect on global crop yields, food security, particularly in developing countries, is under threat (Ray *et al*., 2019). Cassava crop is of interest, particularly because of its ability to withstand ever changing environmental conditions and for its delayable annual food production (Parmar *et al.*, 2017; Anikwe & Ikenganyia, 2018). Despite being a versatile and durable crop, cassava is considered as only being a food security crop and it is also used to supplement other forms of high calorie foods, while not having global popularity (Parmar *et al.*, 2017). However, this is changing across many countries in sub-Saharan Africa, including South Africa (Amelework et al., 2021; Nuwamanya et al., 2017). Recently, the potential use of cassava as a starch source and in biofuel production has further driven cassava popularity (Amelework et al., 2021; Nuwamanya et al., 2017). However, in sub-Saharan Africa, cassava is threatened by whitefly-transmitted CMGs, which cause CMD, resulting in stunted growth and great yield loss (Amelework et al., 2021; Nuwamanya et al., 2017). Due to the potential of cassava, further research is necessary to realise the potential of this crop in South Africa, and one of the

yield and quality constraints, namely CMD, needs to be examined further. Understanding the molecular mechanisms contributing to CMD resistance or tolerance is paramount.

Cassava TME3 has the CMD2 resistance locus and it displays tolerance to CMD, with *CMD2* being dominant, unlike the recessive *CMD1*, wherein CMD1 resistance is mediated in a polygenic manner (Akano *et al*., 2002). The T200 landrace, contrastingly, displays susceptibility to CMD (Allie *et al*., 2014). Working with the CMD-tolerant TME3 and CMD-susceptible T200, Allie *et al.*, 2014 found that both landraces remain asymptomatic at 12 days post-infection (dpi), only for symptoms to develop uniformly over time. At 32 dpi, both landraces were showing moderate symptoms and were fully symptomatic at 67 dpi. However, while TME3 had already recovered at this point and shown attenuation of symptoms, T200 symptoms remained severe at 67 dpi, and it never recovered. The appearance and attenuation of symptoms correlated with SACMV loads in both landraces. At 12 dpi, T200 had a low DNA-A levels while TME3 had significantly lower than those of T200. At 32 dpi and 67 dpi, however, T200 had 10-fold higher levels of viral DNA than TME3 at the same time points, suggesting that viral load suppression can explain the CMD recovery in TME3. Moreover, global gene expression profiling showed that over the 67-day dpi period, SACMV-infected TME3 had fewer differentially expressed genes than the SACMV-infected T200, suggesting that TME3 was no longer under the same stress level.

Virus suppression in TME3 correlates with high levels of SA, which has been shown to lower viral load by acting on SACMV *AC* genes responsible for replication. In addition, analysis of messenger RNA (mRNA) has shown that at 32 dpi, in T200 and TME3, there is an upregulation of genes that are involved in hormone biosynthesis and signalling of JA, ET, and ABA. At 67 dpi, cassava genes involved in SA signal transduction and SAR were also observed to be differentially expressed. Overall, TME3 effectively downregulates several genes associated with SA, JA, ABA, and ET at 12 dpi while there is no change in expression of these genes in T200. At 32 dpi, TME3 and T200 upregulate genes associated with those hormones, with T200 upregulating a higher number of genes. Lastly, at 67 dpi, T200 maintains that upregulation of hormone-related genes while TME3 represses the expression. This project

sought to determine the levels of cassava phytohormones at early, active, and late stages of SACMV infection, and relate that to symptom development, susceptibility, tolerance, and recovery. It also sought investigate the effect of viral *AC2* expression on phytohormone expression.

The work done by Allie *et al.*, 2014 is a foundation for this project. Transcriptomic studies conducted in cassava by Allie *et al.*, 2014 show *South African cassava mosaic virus* infection causes significant differential expression of genes in CMD-susceptible T200 and CMD-tolerant TME3 and that symptom severity and disease progression were associated with SACMV load at 12 dpi, 32 dpi, and 67 dpi. While TME3 showed decreased viral load and attenuated symptoms at 67 dpi, T200 remained symptomatic (Allie *et al*., 2014). Gene ontology (GO) assessments between the CMD-susceptible T200 and CMD-tolerant TME3 revealed that there was varying gene expression across the three stages of infections for genes transcribing for cellular components, molecular functions, and biological processes. Based on the GO profiles of the two landraces, transcriptomics analyses were performed for the three time points. The data showed that during SACMV infection in T200 and TME3, SACMV-responsive genes are transcriptionally activated or repressed. These genes are seemingly involved in plant resistance, defence, phytohormone signalling, as well plant structures including the CW and PD. TME3 had higher expression of genes involved in defence compared to T200, while T200 had higher expression of plant genes involved in CW degradation, protein degradation, and cell cycle progression.

Another foundation for this project is the work done by Freeborough *et al*., 2021, which assessed how cassava WRKY TFs contribute to either CMD tolerance or susceptibility. Working with the CMD-tolerant TME3 and CMD-susceptible T200, Freeborough *et al*., 2021 found that across the three time points, there was differential expression of 9 *MeWRKY* TFs in T200 and 4 *MeWRKY* TFs in TME3, with differential expression of one of them being common in both landraces at the same time point. While T200 showed differential expression across all time points, TME3 showed significant fold change in expression during the 32 dpi, i.e., the symptomatic stage of infection. At 12 dpi, TME3 downregulates response genes such as those involved in nitric oxide (NO) signalling, localisation of cell

death, and wounding responses. These genes are later upregulated in TME3 at 32 dpi but not at 67 dpi.

1.4. Novelty of the study

Perturbations in the production of SA, JA, ABA, and ET due SACMV infection in cassava, in-tandem the assessment of the expression of SACMV and cassava hormone-related is yet to be attempted. A number of previous studies have assessed hormone production and gene expression in response to GMV *AC2* transgene expression, assessed metabolite profiles in response to *Sri Lankan cassava mosaic virus* infection in tolerant and susceptible cassava, or assessed the influence of virus insect vectors on host metabolomics (Chaowongdee *et al*., 2023; Lozano-Durán *et al*., 2011; Luan *et al*., 2013; Malichan *et al*., 2023; Rosas-Díaz *et al*., 2016). The novelty of this study is that it focuses on assessing the accumulation of multiple cassava hormones, alongside assessing viral and host gene expression, all in response to infection with SACMV.

1.5. Hypothesis

As a result of SACMV infection in T200 and TME3, phytohormones will be produced and the quantities will change as CMD progress. Due to TME3 both recovering from and becoming tolerant to CMD, the key defence hormones SA and JA will play a role in this outcome.

1.6. Research questions

- Given the role of phytohormones and gene expression in plant defence response and immunity, what will be the distinction between T200 and TME3 across the three stages of SACMV infection and/or CMD progression?
- Are phytohormone production and the expression of hormone-related genes underlying mechanisms by which cassava TME3 can recover from CMD and tolerate the SACMV?

- How does the expression of SACMV genes promote the progression of CMD in T200 and TME3?

1.7. Aims and Objectives

Aim

The main aim of this research project was to quantify the phytohormone levels of salicylic acid (SA), jasmonic acid (JA), abscisic acid (ABA), and ethylene (ET) in the CMD-susceptible T200 and CMD-tolerant TME3 across the three stages of *South African cassava mosaic virus* infection to determine if these phytohormones contribute to either susceptibility or recovery.

Specific objectives

1. Quantify the endogenous phytohormone levels of SA, JA, ABA, and ET at 12-, 32-, and 67-dpi in mock-infected and SACMV-infected using Ultra-High Pressure Liquid Chromatography-Mass Spectrometry.
2. Determine the expression of hormone biosynthesis and response genes in T200 and TME3 in response to SACMV infection at 12-, 32-, and 67-dpi.
3. Determine the expression of SACMV AC2 (transcriptional activator protein; TrAP) in T200 and TME3 to determine its role in either tolerance or susceptibility to cassava mosaic disease. The Geminivirus TrAP protein is a pathogenicity determinant that has shown to interfere with phytohormone signalling and regulatory pathways.

1.8. Structure of the dissertation

Chapter 1 of the thesis present background information on cassava and CMD, problem statement, rationale, novelty of the study, hypothesis , and research question. Chapter 2 present an extensive literature review of food security, cassava, CMGs, plant defence mechanisms, and the role of molecular signalling in plant defence. Chapter 3 presents the materials and methods for SACMV infection trials, nucleic acid extractions, viral

load determination, gene expression studies, and phytohormone extraction and quantification. Chapter 4 presents the results of the infection trials, viral load determination, gene expression studies, and phytohormone quantification. Chapter 5 is the discussion, focused on elucidating the mechanisms through which TME3 recover from CMD while T200 remains severely symptomatic. Lastly, Chapter 6 is the conclusions section, addressing the key findings and implication of the study while highlighting limitations and suggesting future work.

Chapter 2: Literature Review

2.1 Overview of food security

2.1.1 Food security in Africa

Food security refers to when people have access to sufficient and nutritious food that can maintain their livelihoods and health (McCarthy *et al*., 2018). Food insecurity is an issue that predominantly affects developing countries, particularly on the African continent, wherein an interaction of environmental, social, economic, and political factors further exacerbate it (Denny *et al*., 2018; Gustavsson, 2011). Lack of access to food leads to undernourishment and prolonged hunger, affecting a number of countries across sub-Saharan Africa such as Kenya, Somalia, and Madagascar (Sasson, 2012). Other countries, such as South Africa, while having a high food production food import capacity and being food secure, still have a proportion of the country's population being food insecure, as confirmed by statistics published in 2019 (du Toit *et al*., 2011; Statistics South Africa, 2019).

2.1.2 The threat posed by climate change

Concerningly, global warming and climate change pose a threat to global crop production, as has been witnessed with its negative impact on crop production in Europe, sub-Saharan Africa, and Oceania (Ray *et al*., 2019; Sasson, 2012). Furthermore, it may detrimentally impact developing countries more considering statistical projections that with increasing population growth over time in developing countries, only high Gross Domestic Product (GDP) nations will be able to address increased crop demands (McCarthy *et al*., 2018; Tilman *et al*., 2011). Considering these food insecurity concerns for developing nations and the impact of climate change on food production, developing food security is a priority.

2.2 *Manihot esculenta* Crantz

2.2.1 Brief overview of cassava and its uses

Manihot esculenta Crantz, commonly referred to as cassava, is a perennial tuber crop of the *Euphorbiaceae* family (Ceballos & de la Cruz, 2012). Cassava leaves, shown in **Figure 1a** and **Figure 1b**, are usually large and lobed, spiralling along the stem of the plant. The leaves offer nutrition in the forms of micronutrients such as vitamins and minerals, allowing for their consumption throughout any year due to the perennial nature of cassava (Uchechukwu-Agua *et al.*, 2015; Parmar *et al.*, 2017). Cassava tubers, shown in **Figure 1c**, are thick due to the deposition of starch as the tubers develop over time, with the colouration of the tubers giving an indication of either calcium and ascorbic acid accumulation (white-fleshed tubers), or carotenoid accumulation (yellow-fleshed tubers) (Parmar *et al.*, 2017). While lacking in protein and lipid content, being starch-rich makes cassava a food security and sustenance crop for more than 800 million people globally (Parmar *et al.*, 2017). In addition being a food crop, cassava is also used as animal feed and has industrial application in the production of alcoholic beverages, textile products, biofuels, and plywood (Uchechukwu-Agua & Opara, 2015; Nuwamanya *et al.*, 2017; Parmar *et al.*, 2017).

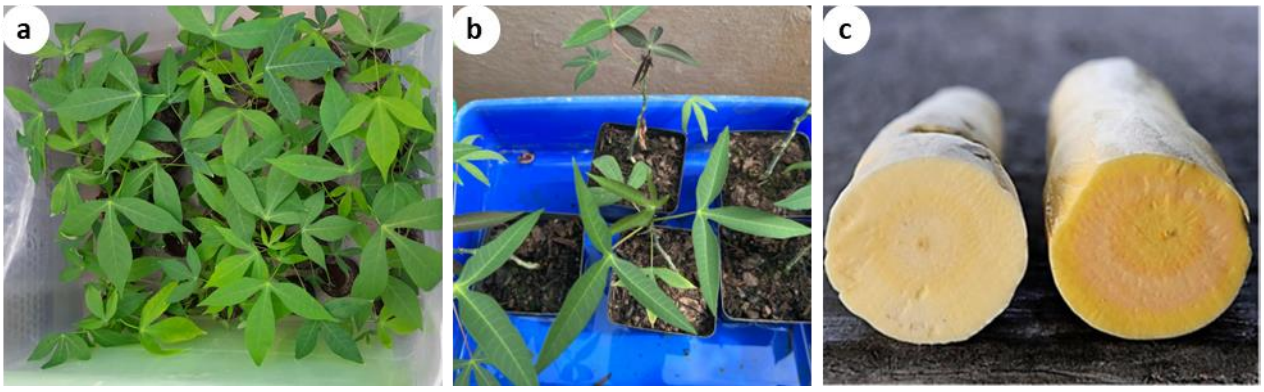


Figure 1: Cassava leaves (**a** and **b**) (captured in 2022) alongside the tuber roots (**c**) (Parmar *et al.*, 2017).

2.2.2 General characteristics

A moderately-drought tolerant crop, cassava grows optimally in humid, tropical conditions at temperatures between 24°C and 30°C, with moderate light exposure (Kawaye & Hutchinson, 2021). Soil conditions should be optimal as well, with the pH being slightly neutral or alkaline and having good drainage of water, as poor drainage can lead to tuber rot (Anikwe & Ikenganyia, 2018). However, even in soil with high acidity and low nutrient

content, cassava is able to have very high yield as compared to other crops such as maize (Anikwe & Ikenganyia, 2018; Kawaye & Hutchinson, 2021).

These characteristics of tolerating drought and low soil fertility conditions have allowed for cassava to be considered as a crop that would be least affected by climate change compared to others such as maize and potato (Jarvis *et al.*, 2012; Anikwe & Ikenganyia, 2018). The same study by Ray *et al.*, 2019 found that while the production and yield of some cereals and legumes have been negatively affected by climate change in recent years, cassava yields actually increased overall in sub-Saharan Africa due to it being more heat and drought tolerant. The tolerance of cassava against environmental stress, coupled with it being a C3-C4 intermediate plant, make it a viable food security crop in the age of climate change (El-Sharkawy & Cock, 1987; Taylor *et al.*, 2012). When exposed to 580 ppm of carbon dioxide (CO_2), which is the predicted level of atmospheric CO_2 in 2050, cassava performed well compared to C4 plants, such as maize, corn, and sorghum (Taylor *et al.*, 2012; Sage, 2016). Due to having lower levels of photorespiration and CO_2 release compared to other C3 plants and a high rate of photosynthetic activity, cassava is considered a C3-C4 intermediate plant (El-Sharkawy & Cock, 1987; Zang *et al.*, 2024).

2.2.3 Global production

The global production of cassava occurs in countries situated in tropical regions, such as Brazil, Nigeria, Ghana, as well as Thailand and Indonesia (Parmar *et al.*, 2017; Ritchie & Roser, 2020). It is preferred in these tropical regions as it can adapt to stresses, poor soil conditions, and inconsistent irrigation, which would adversely affect the yields of other crops (Anikwe & Ikenganyia, 2018). As of 2023 and per data published by the Food and Agriculture Organization of the United Nations (FAO) (**Figure 2**), Nigeria is the leading global producer of cassava tubers, with an output of 62 million metric tons while Africa is the global continental leader of cassava tuber production, with an output of 213 million tons, followed by Asia with 92 million tons (Ritchie *et al*., 2023). Of the more than 333 million tons of cassava tubers produced in 2023, Africa accounted for 63% of all global production, highlighting its commercial and social importance (Ritchie *et al*., 2023).

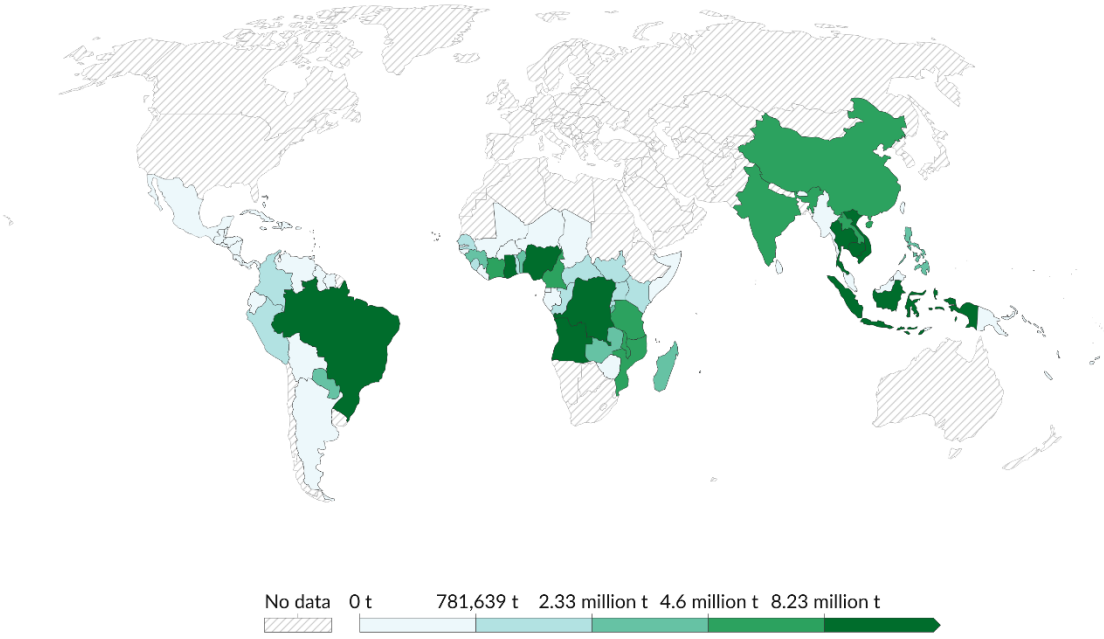


Figure 2: A representation of the annual production (in million tons) of cassava in 2023, based on FAO data (Ritchie *et al*., 2023).

2.2.4 Devastating impact of plant diseases in cassava

Despite its ability to tolerate harsh environmental conditions detrimental to other commercially and agriculturally important crops, cassava is susceptible to various pests and pathogens including mites, mealybugs, whiteflies, parasitic nematodes, fungi, viruses, and bacteria (Lebot, 2009). The insect pests can additionally act as vectors for plant viruses, with these pests and microorganisms diseases that affect the leaves, stems, and/or roots of infected/affected plants (Lebot, 2009). To this end, cassava produces cyanogen glycosides (CGs), which are toxic to humans with prolonged consumption, but function as anti-herbivory and insecticidal chemical defence compounds (Parmar *et al.*, 2017; Anikwe & Ikenganyia, 2018).

Cassava production across sub-Saharan Africa and Asia is negatively impacted by three notable diseases: cassava bacterial blight (CBB), cassava brown streak disease (CBSD), and cassava mosaic disease (CMD) (Reynolds *et al*., 2015). Firstly, CBB is caused by *Xanthomonas axonopodis* pv. *Manihotis*, which can be found in cassava-producing regions across South

America, sub-Saharan Africa, and Asia, and is spread by rainwater over short distances or over long distances by vectors such as sap-sucking insects (Lozano, 1986; Boher & Verdier, 1994). Secondly, CBSD is caused by viruses of the genus *Ipomovirus*, which are widespread across sub-Saharan Africa, particularly in countries in east Africa, and are vectored by insects such as white flies, *Bemisia tabaci* (Lebot, 2009; Maruthi *et al*., 2005). Lastly, CMD, which is caused by cassava mosaic geminiviruses (CMGs), is prevalent in cassava-producing regions across African countries as well as the southeast Asian countries of India and Sri Lanka (Patil & Fauquet, 2009). Notably, CMGs are transmitted by the whitefly vector, *Bemisia tabaci* Gennadius, which is prevalent in these cassava producing regions (Legg & Fauquet, 2004).

While the symptoms of CBB infection usually manifest on the leaves and stems of the cassava as spots and blight (**Figure 3a**), CBSD is characterized by the occurrence of yellow necrotic lesions, mottling of leaves, and chlorosis along the veins of the leaves (**Figure 3b** and **Figure 3c**, respectively), and CMD symptoms are characterized by leaf curling, mottling and chlorosis, as well as mosaic patterning of leaves (**Figure 3d and Figure 3e**) (Lozano, 1986; Legg & Fauquet, 2004; Maruthi *et al.*, 2005; Zhang *et al.*, 2005).

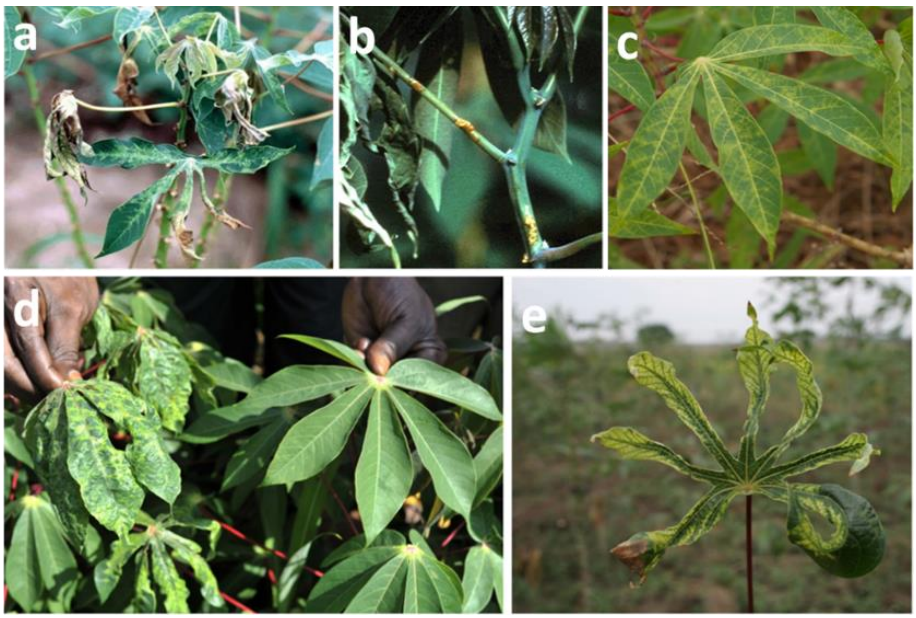


Figure 3: Comparison of the symptoms that occur in cassava during cassava bacterial blight (CBB) (**a**), cassava brown streak disease (CBSD) (**b** and **c**), and cassava mosaic disease (CMD) (**d** and **e**)

2.3 Cassava mosaic geminiviruses

2.3.1 General overview

Cassava mosaic geminiviruses (CMGs) are plant viruses classified in the genus *Begomovirus*, in the family *Geminiviridae* (Zerbini *et al*., 2017). *Geminiviridae* is characterized by viruses whose covalently-closed, circular single-stranded deoxyribonucleic acid (ssDNA) genomes are encapsulated in twinned, isometric capsids (Briddon *et al.*, 2010; Rey & Vanderschuren, 2017). *Geminiviridae*, which consists of viruses that cause significant yield losses of agriculturally and economically important crops, now consists of 14 genera: *Becurtovirus*, *Curtovrius*, *Mastrevirus*, *Topovirus*, *Gablovirus*, *Capulavirus*, *Turncurtovirus*, *Eragrovirus*, *Opunvirus, Mulcrilevirus, Citlodavirus,*, *Topilevirus,* and *Maldovirus* (Roumagnac *et al*., 2022; Zerbini *et al*., 2017). Genus *Begomovirus* is the largest of all *Germiniviridae* genera, consisting of monopartite and bipartite geminiviruses (GMVs) across more than 320 species (Rodríguez-Negrete *et al*., 2013; Zerbini *et al*., 2017).

2.3.2 Genome organisation of begomoviruses and their pathogenicity determinants

The genome of a bipartite begomovirus consists of two ssDNA components, DNA-A and DNA-B, each being 2.5-2.6 kilobases (kb) in length (Zerbini *et al*., 2017). These two ssDNA components contain several open reading frames (ORFs), namely *AC1*, *AC2*, *AC3*, *AC4*, and *AC5*, as well as *AV1* and *AV2* (**Figure 4**). Additionally, DNA-B encodes for *BC1* and *BV1* (**Figure 4**).

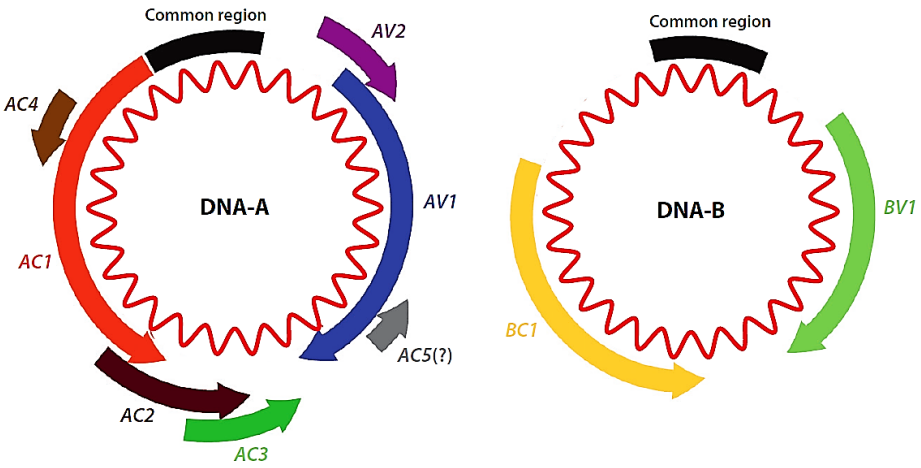


Figure 4: The genome organisation of bipartite begomoviruses (Rey & Vanderschuren, 2017).

The ORFs of DNA-A encode for proteins involved in viral replication, regulation of gene expression, countering host defence mechanisms as well as encapsulation of the viral genome (Briddon *et al*., 2010). The gene *AV1* encodes for the capsid protein (CP) and *AV2* encodes for the precoat protein/putative protein kinase (PKC) (Rey & Vanderschuren, 2017). Furthermore, *AC1* encodes for the replication initiation protein (Rep), *AC2* encodes for the transcription activator protein (TrAP), *AC3* encodes for the replication enhancer protein (REn), *AC4* encodes for the silencing suppressor protein, and *AC5*, which may encode a silencing suppressor protein (Rey & Vanderschuren, 2017). On DNA-B, *BC1* encodes for the movement protein (MP) and *BV1* encodes for the nuclear shuttle protein (NSP) (Rey & Vanderschuren, 2017).

The only sequence similarity that exists between the two DNA components is the common region (CR), a 200 nucleotide region wherein 85% sequence identity is shared (Briddon *et al*., 2010). The CR, an absolutely conserved region in GMVs, is a hairpin structure that contains the nonanucleotide sequence, TAATATTAC, where rolling circle replication is initiated in either the circular DNA-A or DNA-B (Briddon *et al*., 2010). The CR plays a critical role in maintaining the integrity of the bipartite begomovirus genome because it ensures that the replication of both DNA-A and DNA-B can be initiated by Rep, which recognises and cleaves the nonanucleotide sequence (Briddon *et al*., 2010; Zerbini *et al*., 2017). While the

CR maintains the integrity of the DNA-A and DNA-B components, pseudo-recombination has been reported to occur between the two components (Briddon *et al*., 2010).

Following successful GMV infection of a host, viral genome replication relies on rolling-circle replication (RCR) in the nucleus, wherein the ssDNA genome is replicated in a semi-conservative manner to form double stranded deoxyribonucleic acid (dsDNA) replicative forms (RFs) (Rodríguez-Negrete *et al*., 2013). These dsDNA RFs then associate with histone proteins, forming viral minichromosomes from which replication and transcription of the viral genome can be initiated (Rodríguez-Negrete *et al*., 2013). Furthermore, the dsDNA RFs will then serve as templates for recombination-dependent replication (RDR), wherein homologous recombination enable for the *de novo* synthesis of new viral DNA copies (Rodríguez-Negrete *et al*., 2013). However, for viral replication to be successful, GMVs need to reprogramme their host (Maio *et al*., 2020). Geminiviruses specifically target terminally differentiated cells and induce the expression of or enhance the activity of various host factors to reprogramme the host and facilitate DNA replication and transcription (Kong *et al*., 2000).

2.3.3 Prevalence of Cassava Mosaic Geminiviruses (CMGs)

Overall, there are eleven species of CMGs, which have their own strains and variants (Rey & Vanderschuren, 2017). The species are namely: *African cassava mosaic virus* (ACMV), *East African cassava mosaic virus* (EACMV), *East African cassava mosaic Kenya virus*, *East African cassava mosaic Malawi virus*, *East African cassava mosaic Zanzibar virus*, *Cassava mosaic Madagascar virus*, *South African cassava mosaic virus*, *East African cassava mosaic virus* Cameroon [Cameroon-1998], *African cassava mosaic virus* Burkina Faso, *Indian cassava mosaic virus*, and *Sri Lankan cassava mosaic virus* (Rey & Vanderschuren, 2017). While ACMV evolved first in west Africa having been introduced to the region in the 16th century, EACMV seems to be the centre of CMG diversity (Rey & Vanderschuren, 2017). This is because the East African EACMV seems to have a higher degree of genetic diversity, in terms of variants, as compared to the sub-Saharan ACMV (Rey & Vanderschuren, 2017). Overall, the occurrence of CMGs across cassava-producing regions likely began as the result

of cassava being introduced to these regions while not being endemic to them (Rey & Vanderschuren, 2017). Due to lacking the natural capabilities of recognising and countering begomovirus infection likely present in the indigenous and wild plants present, whitefly vectors could have transmitted the begomoviruses from these indigenous plants to the exotic cassava (Rey & Vanderschuren, 2017). This, coupled with recombination due to mixed infection and the transplantation of infected cassava across different regions, could have laid the foundation for the emergence of the various species and variants that exist across sub-Saharan Africa and east Africa (Rey & Vanderschuren, 2017).

Cassava mosaic geminiviruses (CMGs) have caused several CMD outbreaks in cassava producing regions in Africa and southeast Asia, affecting tuber yields and cassava production (Combala *et al*., 2024; Malichan *et al*., 2023). In southeast Asia, recent outbreaks of *Sri Lankan cassava mosaic virus* caused CMD outbreaks that affected cassava growing regions in Cambodia, Vietnam, Thailand, and Laos, significantly impacting cassava production (Malichan *et al*., 2023). In West Africa alone, uncontrolled outbreaks of CMD causes up to 90% yield losses, significantly affecting food security (Combala *et al*., 2024). Furthermore, in the 1990s, Uganda faced a famine crisis driven by the emergence of *East African cassava mosaic virus-Uganda*, which devastated cassava plantations (Legg *et al*., 2006). Interestingly, EACMV-Ug is a recombination product of African cassava mosaic virus and *East African cassava mosaic virus*, the latter of which shares 85% sequence identity with *South African cassava mosaic virus*, via the DNA-A component (Berrie *et al.*, 2001; Combala *et al.*, 2024). The DNA-A components of the CMGs contain several multiple open reading frames (ORFs) that encode for multifunctional proteins that aid viral replication, regulation of gene expression, countering host defence mechanisms as well as encapsulation of the viral genome (Briddon *et al*., 2010), while the DNA-B components in begomoviruses contain ORFs that encode for viral movement proteins (Noueiry *et al.*, 1994).

2.3.4 *South African cassava mosaic virus*

South African cassava mosaic virus is a bipartite species of CMGs that is one of the causative agents of CMD in South Africa, which was first noted in fields in Mpumalanga and

Swaziland in the 1980s (Berrie *et al*., 1998). The causative agent of this CMD was later identified as a new species of CMGs, *South African cassava mosaic virus* (Berrie *et al*., 1998)., With 85% sequence identity in DNA-A and 90% sequence identity in DNA-B, SACMV is closely related to EACMV (Berrie & Rey, 2001). However, considering that the sequence identity for DNA-A was less than 90%, SACMV was classified as a novel species (Berrie & Rey, 2001). *South African cassava mosaic virus* also has high sequence identity with a monopartite begomovirus, *Tomato yellow leaf curl virus* (TYLCV) (Berrie *et al*., 1998). As with other CMGs, SACMV is transmitted by *Bemisia tabaci* Gennadius (Briddon *et al*., 2004).

2.4 Plant defence and immunity mechanisms

Due to being sessile and growing in a single area through their entire life, plants constantly encounter a plethora of pathogens and insects, and have had to develop an array of defence mechanisms to counteract infection and infestation (Zhao & Li, 2021). These mechanisms involve structural and chemical defences, transcriptional and posttranscriptional gene silencing, protein modification and/or degradation, and autophagy, which can all be fine-tuned to specific pathogens, such as viruses. (Garcia-Ruiz, 2019; Zhao & Li, 2021).

2.4.1. Basal Immunity

Basal/innate immunity is regulated by structural and chemical mechanisms that prevent or limit the occurrence of pathogenic infection (Doughari, 2015). Structural barriers include the leaf wax layer and cuticle, the extracellular matrix, as well as the cell wall itself (Doughari, 2015). To supplement these barriers, there is the production of antimicrobial compounds, antitoxins, and phytoanticipins which are constitutively accumulated to deter and counteract potential pathogens (Doughari, 2015).

2.4.2. PAMP-Triggered Immunity (PTI) and Effector-Triggered Immunity (ETI)

Should pathogens overcome the mechanisms of innate immunity and invade a localised area of cells, pathogen-associated molecular pattern (PAMP) triggered immunity

(PTI) will be activated (Doughari, 2015). Using plasma-membrane bound pattern recognition receptors (PRRs), which are leucine-rich repeat (LRR) proteins, plants are able to recognise microbe-associated molecular patterns (MAMPs) such as chitin, flagellin, and ergosterol, and activate downstream signalling pathways to counteract infection (Doughari, 2015; Shamrai, 2014). The downstream signalling results in the production of antimicrobial secondary metabolites as well as plant defence proteins such as basic chitinase (b-CHI) and plant defensin (PDF1.2) (Cheng *et al*., 2013; Doughari, 2015).Plants are also able to recognise damage-associated molecular patterns (DAMPs), which act as endogenous elicitors of PTI while MAMPs act as exogenous elicitors (Doughari, 2015). Viral double stranded ribonucleic acid (dsRNA) has also been shown to be an elicitor of PTI (Bigeard *et al.*, 2015; Huang, 2021).

If the pathogens manage to overcome PTI and deliver their avirulence/effector proteins across the cell wall into the cytoplasm, this will activate effector triggered immunity (ETI) (Doughari, 2015). In the case of viruses, avirulence (avr) factors interfere with host regulation of transcriptional machinery and genome replication, promoting conditions that are optimal for viral replication (Doughari, 2015). However, host resistance genes produce nucleotide-binding leucine-rich repeat (NB-LRR) proteins, which intracellularly recognise avr factors and activate the downstream expression of pathogenesis-related (PR) genes in the infected cell and the surrounding cells (Doughari, 2015; Irigoyen *et al*., 2020). These *PR* genes encode for PR proteins involved in the biosynthesis of phytohormones, the production of antimicrobial compounds, callose deposition to strengthen the cell wall (CW), as well as lignification of the vascular networks (Doughari, 2015). *PR* genes arise from *PR* families, which consist of proteins of varying function and activities such as proteases, defensins, chitinases, and glucanases (Irigoyen *et al*., 2020). During the downstream responses of ETI, salicylic acid (SA) will accumulate in the infected areas and bind to the NPR3 receptor of the PR genes, triggering localised cell death (Doughari, 2015). This accumulation of SA during ETI results in the development of the hypersensitive response (Doughari, 2015).

2.4.3. Hypersensitive Response

The hypersensitive response (HR) is localised programmed cell death that restricts fungi, bacteria, and viruses to one particular region and prevents systemic spread (Doughari, 2015). The mechanism is highly regulated, relying on transcriptional reprogramming, calcium ion (Ca^{2+}) influx, production of reactive oxygen species (ROS) and nitric oxide species (NO), and the activation of mitogen activated protein kinase (MAPK) signalling (Doughari, 2015). In both *Nicotiana benthamiana* and *Arabidopsis thaliana*, ROS bursts, followed by NO bursts, are pivotal in inducing HR (Frederickson Matika & Loake, 2014). Furthermore, a lack of NO bursts only induces a weakened or ineffective HR while NO-bursts in the absence of ROS production does not lead to HR development (Frederickson Matika & Loake, 2014).

2.4.4. Systemic Acquired Resistance (SAR) and Induced Systemic Resistance (ISR)

Induced systemic resistance (ISR) and systemic acquired resistance (SAR) are both forms of induced resistance, a state of increased defensive readiness, but they differ significantly (Vallad & Goodman, 2004). Systemic acquired resistance is a conserved mechanism across all plants and has high efficiency against biotic elicitors originating from pathogenic bacteria, fungi, and viruses, in addition to environmental stresses as well (Vallad & Goodman, 2004). The SA signalling pathway plays an important role in the activation and regulation of SAR as both SA and PRs accumulate extensively during SAR, heightening a state of resistance within the plant to ready it against potential future stresses (Vallad & Goodman, 2004; Doughari, 2015; Zhu *et al.*, 2022). Conversely, ISR is restricted to particular species and genotypes and is highly effective in the countering of disease-causing bacteria, fungi, and viruses, responding principally against biotic elicitors (Vallad & Goodman, 2004). Furthermore, ISR is mainly activated and regulated by ET and JA (Vallad & Goodman, 2004).

2.4.5. Transcriptional and Posttranscriptional Gene Silencing

Transcriptional gene silencing (TGS) and posttranscriptional gene silencing (PTGS) are two key antiviral mechanisms that target either viral DNA or viral RNA, respectively, and mediate their inactivation or degradation (Doughari, 2015). Plants assemble complexes that degrade foreign nuclear material but also retain portions of these genomic and genetic

fragments for recognition of the same pathogen during future infections (Doughari, 2015). In terms of TGS, which involves DNA methylation, plants can epigenetically modify, through methylation, viral DNA genomes, resisting replication and transcription, facilitating plant recovery (Wang *et al*., 2019). Conversely, PTGS leads to RNA silencing of viral transcripts, preventing the accumulation of viral proteins that may act as pathogenicity determinants (Wang *et al*., 2019). As such, viruses have evolved to counteract TGS by targeting and interfering with the pathways involved in regulating plant global methylation, as well as counteracting PTGS by expressing viral suppressors of RNA silencing (VSRs), which target RNA silencing pathways.

2.5 Molecular signalling and regulation of defence pathways

2.5.1. Phytohormones

Phytohormones play a crucial role in plant defence and immunity, as they lead to the production of PR proteins and the activation of transcription factors (TFs) involved in defence pathways (Zhu *et al*., 2022). These phytohormones include SA, jasmonic acid JA, ET, ABA, Aux, GAs, CKs, and BRs (Zhao & Li, 2021). Plant defence against pathogens is primarily coordinated by SA, JA, and ET whilst ABA, Aux, CKs, BRs, and GAs are involved in modulating the plant immune responses and defence (Müllender *et al*., 2021). The interactions between viruses and their host plants often lead to rapid changes in hormone homeostasis and signalling (Müllender *et al*., 2021).

Salicylic Acid

Salicylic acid (SA) is a phytohormone that regulates plant growth and development directly and indirectly, regulates thermogenesis as well as mediating responses to biotic and abiotic stresses (Dempsey & Klessig, 2017). The production of SA occurs in PTI following the accumulation of ROS and in ETI after PR proteins recognise virus effectors (Doughari, 2015). The accumulation of SA in infected host cells will result in the initiation of localised cell death, leading to the hypersensitive response (Gupta *et al.*, 2022). The biosynthesis of SA can occur via to two pathways, the isochorismate synthase (ICS) pathway and the

phenylalanine ammonia-lyase (PAL) pathway, both of which require chorismic acid as a starting point (**Figure 5**) (Dempsey & Klessig, 2017).

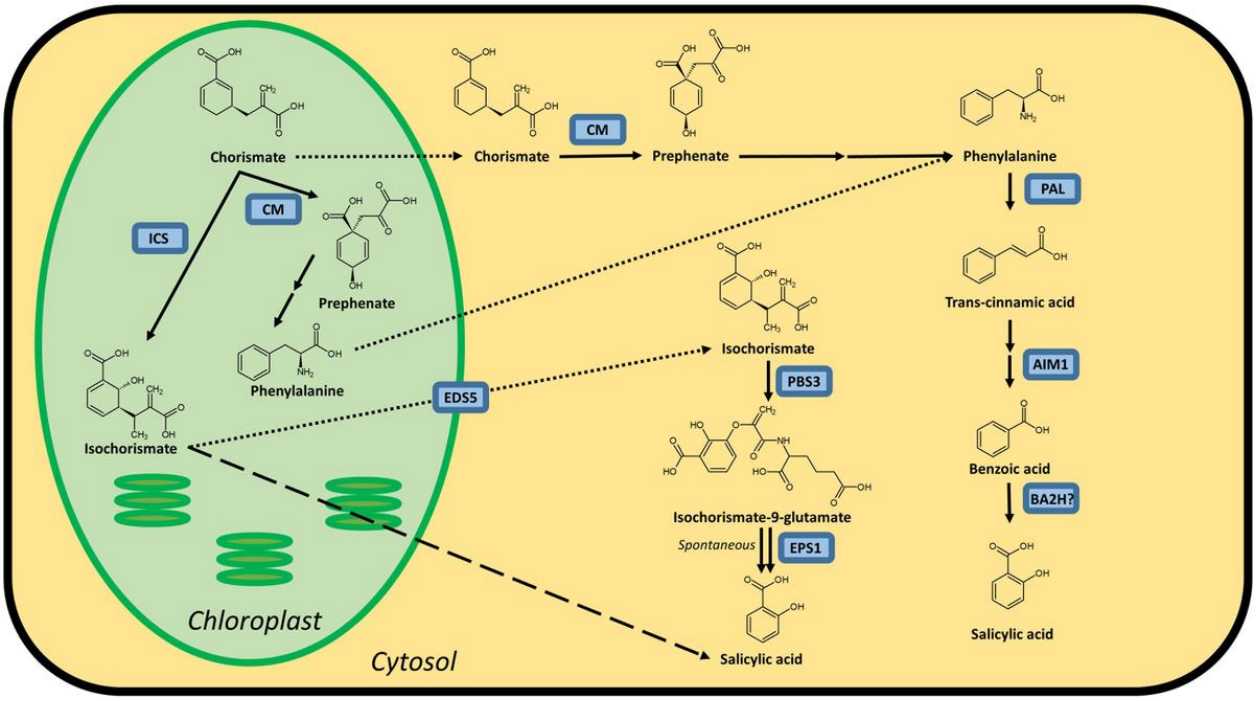


Figure 5: The salicylic acid biosynthesis pathways, directed by either Isochorismate Synthase (ICS) or phenylalanine ammonia-lyase (PAL), with chorismic acid acting as a precursor in both pathways (Lefevere *et al.*, 2020)

For SA biosynthesis, the IC pathway or the PAL pathway can be used. In the IC pathway, chorismate is catalysed into isochorismic (IC) acid by Isochorismate Synthase (ICS) (Lefevere *et al.*, 2020). The IC will then be exported into the cytoplasm by Enhanced Disease Susceptibility 5 (EDS5), a MATE transporter, where avrPphB Susceptible 3 (PBS3) will conjugate IC to glutamate, forming isochorismate-9-glutamate (Lefevere *et al.*, 2020). Enhanced Pseudomonas Susceptibility 1 (EPS1) will then catalyse the conversion of isochorismate-9-glutamate into salicylic acid, which can also occur spontaneously without EPS1 (Lefevere *et al.*, 2020). Conversely, the PAL pathway involves chorismate export into the cytoplasm, wherein chorismate mutase (CM) will catalyses the conversion of chorismate into prephenic acid, with prephenic acid being catalysed into phenylalanine (Phe) (Dempsey & Klessig, 2017; Lefevere *et al.* 2020). Phenylalanine will then be catalysed into trans-

cinnamic acid (*t*-CA) by PAL (Lefevere *et al.*, 2020). Depending on the plant species, *t*-CA will be converted into either benzaldehyde or *ortho*-coumaric acid (benzoic acid) (Dempsey & Klessig, 2017). The *ortho*-coumaric acid will be spontaneously converted into salicylic acid while aldehyde oxidase (AAO) will convert the benzaldehyde into benzoic acid (BA). At this point, the BA will be converted into SA by an unidentified plant gene (Dempsey & Klessig, 2017).

Salicylic acid signalling is mediated via redox-regulated TFs such as the basic leucine zipper (bZIP) TGA1 and the transcriptional coactivator Non-expressor of pathogenesis-related 1 (NPR1) (Li & Loake, 2016). The accumulation of SA can be triggered in response to a virus eliciting ETI and HR (Gupta *et al.*, 2022). These high levels of SA will alter the cellular redox state, which will reduce NPR1 oligomers into monomers (Gupta *et al.*, 2022). These NPR1 monomers will translocate into the nucleus and interact with the TGA TFs that regulate SA-associated defence genes, leading to their expression, resulting in systemic acquired resistance (Gupta *et al.*, 2022). In *Nicotiana benthamiana*, it was shown that infection with either *Sri Lankan cassava mosaic virus* and *Cabbage leaf curl virus* led to increased expression of SA-associated PR-genes such as *PR1*, *PR2*, and *PR5* (Gupta *et al.*, 2022). There was also an increased expression of SA biosynthesis and response genes. In another instance, such as infection with *Tomato yellow leaf curl Sardinia virus*, there was a downregulation of the SA biosynthesis genes in *Arabidopsis thaliana* (Gupta *et al.*, 2022). The accumulation of SA during ETI results in the development of the HR and is crucial for the establishment of systemic acquired resistance (Doughari, 2015). During viral infection, SA can interfere with viral cell-to-cell movement, systemic infection, as well as viral replication, in addition to inducing HR, SAR, *PR* gene expression and triggering the accumulation of ROS (Zhao & Li, 2021). Furthermore, SA is involved in modulating the interfering RNA (RNAi) pathway, which is part of the RNA silencing defence mechanism of plants against viruses (Doughari, 2015; Zhao & Li, 2021).

Jasmonic Acid

Jasmonic acid (JA) is a phytohormone that regulates physiological processes such as flowering and senescence, as well as mediating defence responses and regulating the

expression of various genes in plants (Sasaki *et al*., 2001). Jasmonic acid is crucial in plant defence hormone as it regulates and modulates processes that target both the virus and its vector (Ghosh & Chakraborty, 2021). Jasmonic acid production may occur in basal immunity due to biotic stresses triggering the production of terpenes and glucosinolates, which JA regulates (Ghosh & Chakraborty, 2021). Jasmonic acid also coordinates RNAi-based defences against the viruses as well as ISR (Ghosh & Chakraborty, 2021). Increases in JA levels can, however, have a positive or negative effect on defence against plant viruses, depending on the stage of infection and the virus in question (Zhao & Li, 2021). The biosynthesis of JA is a six-step reaction that is catalysed by five enzymes in total, as shown in (**Figure 6**) (Sasaki *et al*., 2001).

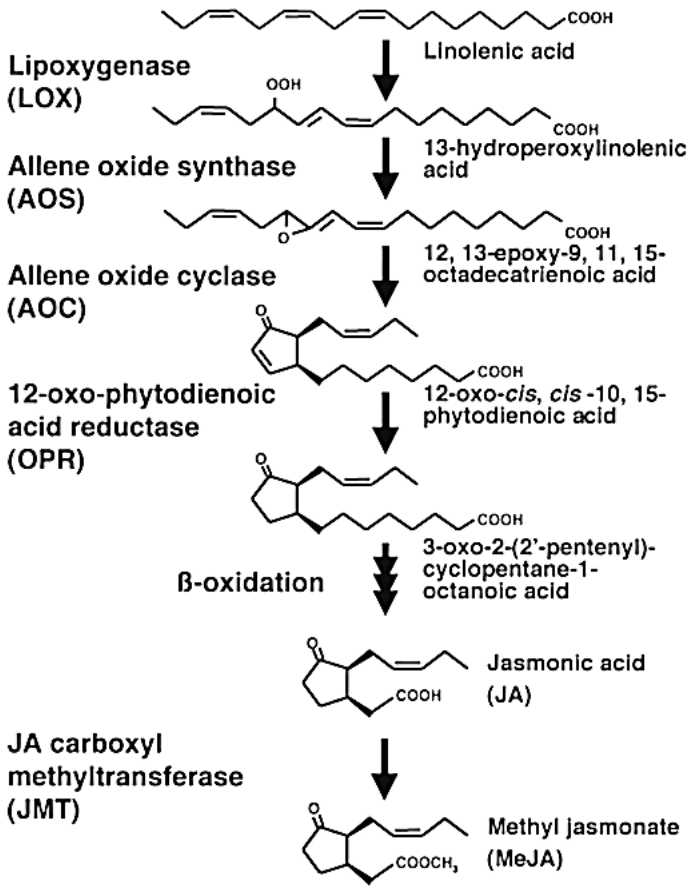


Figure 6: The jasmonic acid biosynthesis pathway (Sasaki *et al*., 2001)

As detailed by Schaller & Stintzi, 2009, The conversion of linolenic acid is catalysed into 13-hydroperoxy linolenic acid by Lipoxygenase (LOX). Allene oxide synthase (AOS) catalyses the conversion of 13-hydroperoxy linolenic acid into 12, 12-epoxy-9, 11, 15-octadecatrienoic acid. The conversion of 12, 12-epoxy-9, 11, 15-octadecatrienoic acid into 12-oxo-*cis*, *cis*-10,

15-oc phytodienoic acid is catalysed by allene oxide cyclase (AOC). 12-oxo- phytodienoic acid reductase (OPR3) then catalyses the conversion of 12-oxo-*cis*, *cis*-10, 15-oc phytodienoic acid into 3-oxo-2-(2'-pentenyl)-cyclopentane-1-octanoic acid. This acid undergoes oxidation to form JA. Lastly, JA is converted into methyl jasmonate (MeJA), a reaction that is catalysed by JA carboxyl methyltransferase (JMT) (Sasaki *et al*., 2001) .

Jasmonic acid signalling is mediated by TFs, such as the basic helix-loop-helix (bHLH) MYC2, which are involved in the production of the chemical defences that are used in basal immunity such as terpenoids and glucosinolates (Gautam *et al*., 2021; Gupta *et al*., 2022). However, in *Nicotiana tabacum* infected with *tomato yellow leaf curl China virus*, there is suppression of these chemical production pathways, allowing for whitefly colonisation of the leaves of the plant (Gupta *et al.*, 2022). This shows that the virus manipulates and alters basal immunity mechanisms to the benefit of its vector (Gupta *et al.* , 2022). During a viral infection, there are increases in the levels of jasmonoyl-isoleucine (JA-Ile), the highly active form of JA, and ethylene to initiate systemic acquired resistance (Gupta *et al.*, 2022). However, in *A. thaliana* infected with *cabbage leaf curl virus*, there is downregulation of the JAR1 protein, which converts JA to JA-Ile, repressing the JA signalling via the MYC2 pathway. It has been shown that geminiviruses actively target JA signalling cascades to weaken the plant's overall defensive capacity (Gupta *et al.*, 2022). Geminiviruses such as *tomato yellow leaf curl virus* make use of the AC2/C2 protein to interfere with JA signalling (Gupta *et al.*, 2022). The production of JA has been shown to decrease viral DNA titre during geminivirus infection, particularly *Beet curly top virus* (Zhao & Li, 2021). JA has also been shown to promote RNA silencing by the use of micro-RNAs (miRNAs), as well as promoting ARGONAUTE 18 (AGO18) activity by upregulating its TFs (Zhao & Li, 2021). Given the similarity of the roles that SA and JA play, the crosstalk between the two hormones has been shown to be important in plant-virus interactions, as JA regulates ISR alongside ET (Zhao & Li, 2021).

Ethylene

Ethylene (ET) is a gaseous phytohormone that regulates many developmental and physiological processes in plants (Pattyn *et al*., 2021). As a volatile compound, it can be

rapidly disseminated throughout the plant from the site of production to achieve a systemic effect (Pattyn *et al*., 2021). The common biosynthesis pathway for ET, as depicted in **Figure 7**, is a two-step SAM-dependent pathway, wherein *S*-adenosyl-$_L$-methionine (SAM) is converted into 1-aminocyclopropane-1-carboxylic acid (ACC), which is further catalysed to ethylene (Pattyn *et al*., 2021). The conversion of SAM into ACC is catalysed by ACC Synthase (ACS), with the conversion of ACC into ET being catalysed by ACC oxidase (ACO) (Pattyn *et al*., 2021).

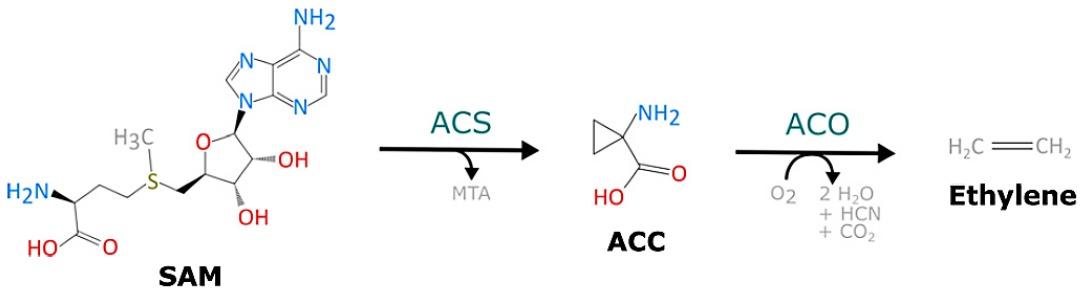


Figure 7: The ethylene biosynthesis pathway, with the *S*-adenosyl-$_L$-methionine (SAM) as a precursor (Pattyn *et al*., 2021)

The reactions are catalysed by ACS and ACO, with 5'-methylthioadenosine (MTA), water (H_2O), hydrogen cyanide (HCN), and carbon dioxide (CO_2) being the by-products.

The ethylene-responsive signalling cascade is negatively regulated by Ethylene Receptor 1 (ETR1), a kinase that is part of a phosphorelay cascade that inactivates and localises Ethylene Insensitive 2 (EIN2) to the endoplasmic reticulum (Mur *et al*., 2013). Following the binding of ET to ETR1, there is loss of EIN2 phosphorylation, and EIN2 translocates into the nucleus, where it activates the ET-responsive transcription factor Ethylene Insensitive 3 (EIN3). EIN3 regulates the expression of other response regulating transcription factors such as *ERF1* and *ORA59* (Mur *et al*., 2013; Solano *et al*., 1998). The production of ET is initially induced during PTI and ETI, until ISR occurs (Vallad & Goodman, 2004). The increase in ET levels arises from the activation of signalling cascades in PTI and ETI that lead to its production (Gupta *et al.*, 2022). However, the high ET levels have also been shown to be due to higher levels *ACO* transcripts, which is used as a plant measure to counteract miRNA-based viral repression of *ACS* transcripts (Gupta *et al.*, 2022). The build-up of ET in response to viral infection is for it

to act as a systemic signal and to also set the foundation for induced systemic resistance, which it regulates alongside JA (Vallad & Goodman, 2004; Pattyn *et al.*, 2021). The production of ET in PTI can result due to the detection of viral pathogens that have breached the basal immunity mechanisms (Gupta *et al.*, 2022). The ET-associated transcription factor, EIN3, was found to be upregulated in *Arabidopsis thaliana* infected with *cabbage leaf curl virus* (Gupta *et al.*, 2022). Another instance of upregulation is of *Nicotiana tabacum* expressing the *African cassava mosaic virus* AC2 protein (Gupta *et al.*, 2022). It was found that there were higher levels of both ACO and *ERF1* transcripts present, indicating that the AC2/C2 protein may contribute to elevated levels of ET within the plant (Gupta *et al.*, 2022). Lastly, in *Nicotiana benthamiana* infected with *tomato yellow leaf curl virus*, the expression of *ERF* genes in the resistant cultivar was four to sixfold higher than in the susceptible cultivar (Gupta *et al.*, 2022). It has thus been shown that ET plays an important role in the defence responses of plants during viral infection, as it either improves defence response or increases susceptibility (Zhu *et al*., 2022).

Abscisic Acid

Abscisic acid (ABA) is a phytohormone that regulates plant growth and development processes such as seed maturation and dormancy, while also playing a role in the adaptation of plants to environmental stresses (Seo *et al*., 2000). It also functions in plant defence by modulating the antiviral RNA silencing mechanism alongside JA, and regulating callose deposition during ETI (Doughari, 2015; Zhao & Li, 2021). The ABA signalling pathway is activated in conjunction with the SA signalling pathway, resulting in an increase in ABA levels during ETI, although both pathways are antagonistic to each other (Ghosh & Chakraborty, 2021; Zhao & Li, 2021). The biosynthesis of ABA begins in the chloroplast and reaches completion in the cytoplasm, as shown in **Figure 8** (Seo *et al*., 2000).

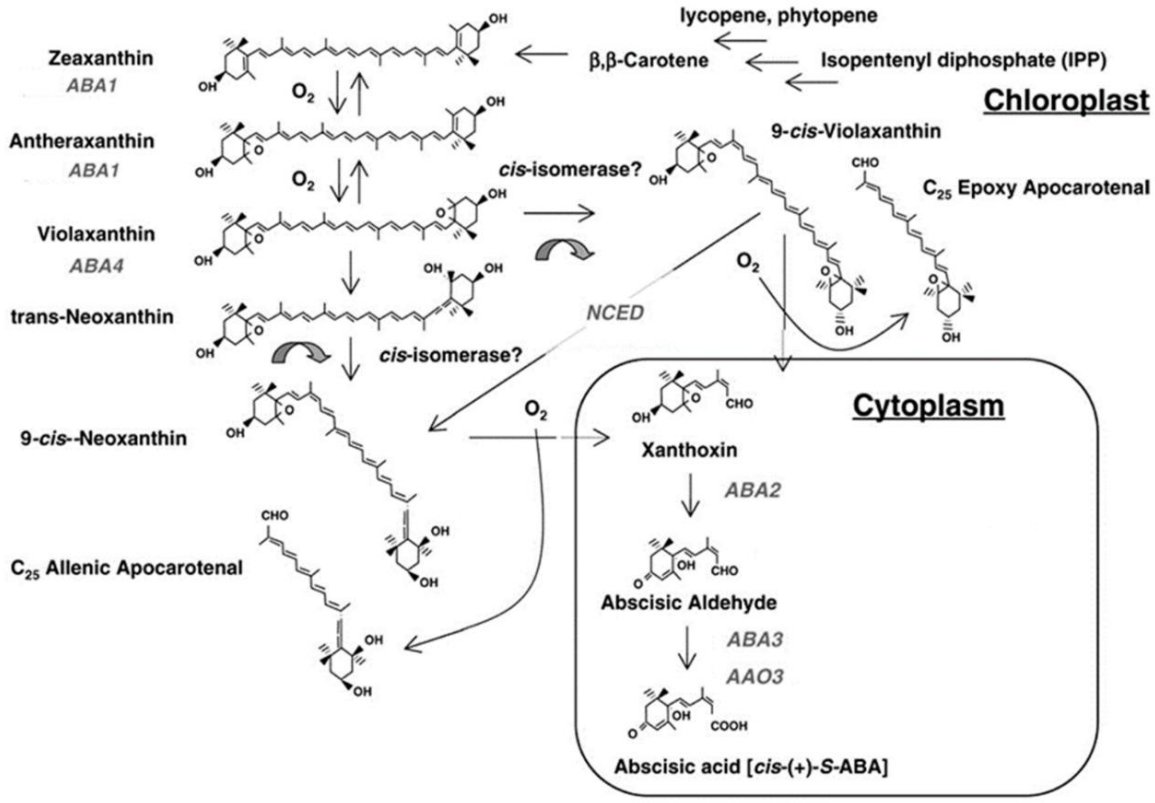


Figure 8: The abscisic acid biosynthesis pathway (Wasilewska *et al*., 2008)

As detailed by Wasilewska *et al*., 2008*,* the pathway begins in the chloroplast, with the production of β-carotene from isopentenyl diphosphate. β-carotene hydroxylase catalyses hydroxylation reactions that form zeaxanthin. The epoxidase ABA1 catalyses the conversion of zeaxanthin into antheraxanthin, and the conversion of antheraxanthin into violaxanthin. Neoxanthin synthase (ABA4) catalyses the conversion of violaxanthin into trans-neoxanthin. This product is converted into 9-*cis*-neoxanthin by an unelucidated reaction. 9-*cis*-neoxanthin is translocated into the cytoplasm where NCED, 9-*cis*-neoxanthin dioxygenase, catalyses the cleavage of 9-*cis*-neoxanthin dioxygenase into xanthoxin. Xanthoxin dehydrogenase (ABA2) reduces xanthoxin into abscisic aldehyde. Molybdenum cofactor sulfurase (ABA3) is required for the activity of AAO3, an aldehyde oxidase, with both ABA3 and AAO3 promoting the production of ABA.

Abscisic acid signalling is mediated by ABA-responsive Sucrose Non-Fermenting-Related Kinase 2 (SnRK2) proteins such as Pyrabactin Resistant-like 1 (PYR1), which phosphorylate the bZIP TFs ABA-responsive element binding factors (ABF), leading to the transcription of ABA-responsive genes (Ng *et al*., 2014). PYR1 also phosphorylates both the signalling

proteins and the negative regulators of ABA signalling, activating the former and suppressing the latter, promoting ABA signalling (Ng *et al*., 2014). Both ABA and ET play specific or synergistic roles in basal resistance, ETI, and regulation of defence gene expression (Zhao & Li, 2021). Importantly, ABA has been found to influence plant-virus interactions by modulating both callose deposition in the plasmodesmata (PD) and the RNAi pathway (Zhao & Li, 2021). The levels of ABA have been reported to be upregulated during viral infection but downregulated in some instances, depending on the particular virus-host pair (Zhao & Li, 2021). Furthermore, exogenous treatment of plants with ABA has been shown to increase host resistance viruses, thus indicating that ABA could have antiviral activity (Zhao & Li, 2021). This antiviral activity occurs by ABA preventing the expression of callose-degrading β-1,3-glucanases, enabling for callose deposition in the PD (Zhao & Li, 2021). Moreover, ABA levels have been shown to modulate *ARGONAUTE 1* (*AGO1*) expression, in so doing regulating the RNAi pathway (Zhao & Li, 2021).

Auxins

Auxins (Aux) are phytohormones that play a role in most of the major aspects of plant growth and development (Zhao, 2012). Auxins are predominantly targeted by many viruses such as *Tobacco mosaic virus* or *Rice dwarf virus*, leading to disease development in infected plants (Zhao & Li, 2021). Auxins ensure that cell growth is well-regulated in plants and for this reason, auxin signalling pathways are targeted by viral effectors to increase auxin levels in the plant (Ghosh & Chakraborty, 2021). The main naturally occurring Aux, indole-3-acetic acid (IAA), is produced in a two-step biosynthesis pathway, as shown in **Figure 9** (Zhao, 2012). As described by Zhao, 2012, TAA, an amino transferase, catalyses the conversion of tryptophan (Trp) into indole-3-pyruvate (IPA), transferring the Trp amino group to pyruvate. YUCCA flavin monooxygenase (YUC) catalyses the formation of IAA in an oxygen and NADPH-dependent reaction.

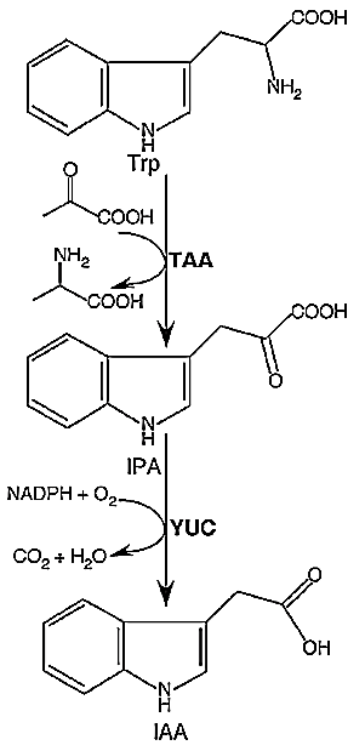


Figure 9: The indole-3-acetic acid (IAA) biosynthesis pathway (Zhao, 2012)

Alterations in plant aux metabolism have also been shown to be important for the modulation of plant defence responses, to the point that plant viruses have evolved their multifunctional proteins to manipulate aux signalling in plant hosts (Müllender *et al*., 2021). Auxin signalling cascades play important roles in plant-virus interaction as their virus-mediated disruption results in dysregulated aux-mediated gene expression and leads to disease development (Zhao & Li, 2021). Viruses specifically target Auxin Response Factors (ARFs) such as ARF12 and ARF16, which have diversified antiviral functions, to ensure that they are able to replicate without difficulty (Zhao & Li, 2021).

2.5.2. Reactive Oxygen Species and Nitric Oxide

Reactive oxygen species (ROS) have antimicrobial properties but are also important in the biosynthesis of SA, playing a crucial role in SAR (Doughari, 2015). Furthermore, these bursts of ROS during the early stages of infection are often crucial for the initiation of the HR (Balint-Kurti, 2019). The activity of the SA transcriptional coactivator, NPR1, is regulated by both SA binding and redox changes, as the latter allows for the reduction of cysteine

residues in oligomeric NPR1, forming monomeric NPR1 (Seyfferth & Tsuda, 2014). Furthermore, binding of SA triggers the conformational changes required for NPR1 to be able to promote the expression of SA-responsive genes (Seyfferth & Tsuda, 2014). The initial production of ROS during PTI creates bursts and waves of ROS and Ca^{2+} ions, respectively (Gilroy *et al*., 2014). ROS-induced Ca^{2+}-release (RICR) and Ca^{2+}-induced ROS production (CIRP) regulate each other, the former occurring in the extracellular matrix (ECM) and the latter within the cytoplasm (Gilroy *et al*., 2014). Lastly, excessive ROS production and accumulation can trigger programmed cell death, facilitating the hypersensitive response (Jalmi & Sinha, 2015).

Conversely, nitric oxide (NO) species regulate protein activity through the posttranslational modification of S-nitrosylation, targeted to cysteine residues (Vidhyasekaran, 2014). Through nitration of proteins such as PYR1, as well as TGAs and NPR1, NO can negatively regulate the signalling of ABA and SA, respectively, by enhancing their homo-oligomerisation (León & Costa-Broseta, 2020). Additionally, NO can also promote or repress phytohormone biosynthesis. Through S-nitrosylation of MAT1, an ET biosynthesis protein, NO prevents the formation of SAM, an ET precursor (Mur *et al*., 2013). This lack of ET accumulation represses EIN3 signalling, which can inhibit *ICS1* transcription (Mur *et al*., 2013). Jasmonate production is positively regulated through NO-driven upregulating the expression of *LOX3*, and *OPR1/2/3*. However, NO can then also inhibit the activity of AOC over time, perhaps through S-nitrosylation (Mur *et al*., 2013). Lastly, by inducing the expression of *ACS*, NO promotes ET production, and also represses it through MAT1 S-nitrosylation (Mur *et al*., 2013).

Chapter 3: Materials and Methods

3.1. Methodology Flow Chart

The flowchart illustrates the work performed to address the specific objectives of the research project, in a time course experiment manner. Tissue culture maintenance of T200 and TME3, coupled with nodal micro-propagation and SACMV infection trials, ensured that SACMV-infected plants and mock-infected plants could be generated for downstream applications, such as viral load determination, gene expression studies of SACMV and cassava genes, and the quantification of hormones across 67 days post-infection (dpi).

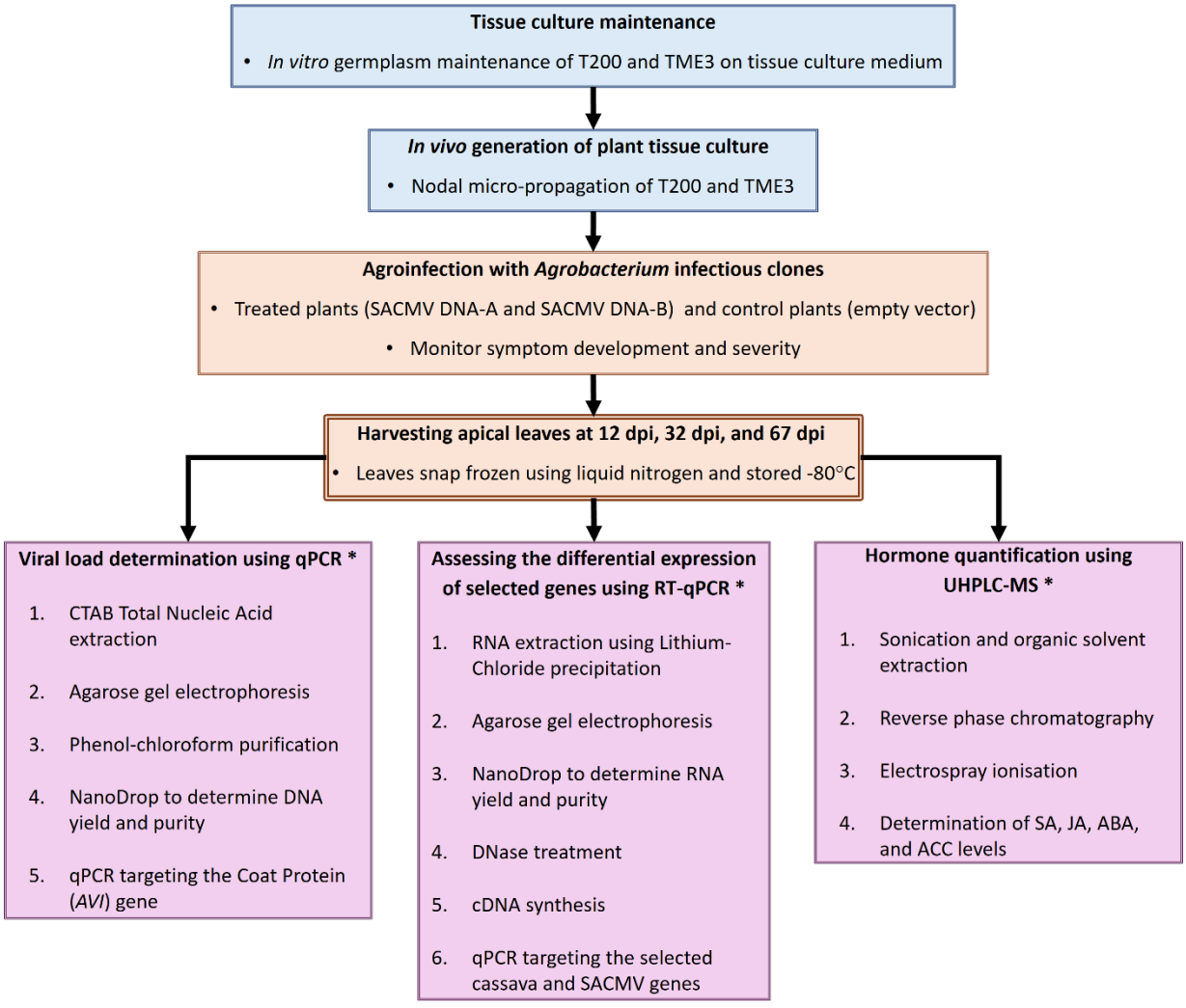


Figure 10: Workflow outlining the approach of the research

For viral load determination, gene expression studies, and the quantification of plant hormones, there were three biological replicates with three technical replicates per biological, as denoted by the asterisk (*).

3.2. Reagents and Materials

Reagents and materials for nucleic acid (DNA and RNA) extractions were sourced from Sigma-Aldrich (Burlington, Massachusetts, United States), Honeywell (Offenbach, Germany) Sisco Research Laboratories Pvt. Ltd. (SRL Chem) (Maharashtra, India), Merck (Darmstadt, Germany), and Bio-Rad Laboratories (Hercules, California, United States). Reagents and materials for plant tissue culture maintenance and propagation were sourced from Sigma-Aldrich (Burlington, Massachusetts, United States), Duchefa Biochemie (Haarlem, The Netherlands), Merck (Darmstadt, Germany), and Jiffy Products International B.V (Zwijindrecht, The Netherlands). Reagents for complementary DNA (cDNA) synthesis were sourced from New England Biolabs (Ipswich, Massachusetts, USA) and Thermo Fisher Scientific (Waltham, Massachusetts, United States). Reagents for polymerase chain reaction (PCR) and reverse transcription quantitative PCR (RT-qPCR) were sourced from Thermo Fisher Scientific (Waltham, Massachusetts, United States) and New England Biolabs (Ipswich, Massachusetts, USA). Lastly, reagents for plant hormone extraction and quantification were sourced from Sigma-Aldrich (Burlington, Massachusetts, United States), Romil Pure Chemistry (Cambridge, United Kingdom), and Merck (Darmstadt, Germany).

3.3. *Agrobacterium tumefaciens* C58C1 infectious clone stocks

Infection of cassava with SACMV was achieved using *Agrobacterium tumefaciens* C58C1 clones that harbour pBIN19 head-to-tail clones of the SACMV DNA-A component and the SACMV DNA-B component (Berrie *et al.* 2001). Prior to commencement of SACMV infection trials in cassava, existing stocks of infectious clones were assessed via colony Polymerase Chain Reaction to isolate and proliferate clones containing either pBIN19-SACMV-DNA-A (pBINSA-A) or pBIN19-SACMV-DNA-B (pBINSA-B), as well as clones containing the empty pBIN19 vector (*Agl*-1). *Agl*-1 clones were used for mock-infections, which serve as a control for either genotype.

For detection of pBINSA-A, the core coat protein gene, *AV1*, was targeted, whereas in the case of pBINSA-B, the cell-to-cell movement protein gene, *BC1*, was targeted. The PCR primer sequences are listed below:

Table 1: Gene specific polymerase chain reaction primer sequences for targeted genes

Gene	Accession Number	Forward Primer (5' – 3')	Reverse Primer (5' – 3')	Annealing temperature	Product size (bp)
AV1	NC_003803	GCACAAACAAGCGTCGARP	CTGCCAGTATGCTTAACGTCA	63.8°C	550
BC1	NC_003804	CGAGCAGTTGGAGTGGGATT	ACATCAACAGCAAACGCACC	58.1°C	538

The PCR reactions were set up as follows, using reagents from Thermo Fisher Scientific:

Table 2: Components of a single colony polymerase chain reaction reaction

Component	**Volume in 25 µL reaction**	**Final concentration**
10X DreamTaq Green Buffer	2.5 µL	1X
10 mM dNTP Mix	0.5 µL	0.2 mM
10 µM Forward Primer	1.25 µL	0.5 µM
10 µM Reverse Primer	1.25 µL	0.5 µM
DreamTaq DNA Polymerase	0.25 µL	1.25 U
Nuclease-free water	18.25 µL	-
Bacterial aliquot	1 µL	-

The cycling conditions, carried out on the Bio-Rad T100^{TM} Thermal Cycler, were as follows:

Table 3: Cycling conditions for the polymerase chain reaction

Step	**Temperature**	**Time**	**Cycle(s)**
Initial denaturation / DreamTaq activation	95°C	3 min	1
Denaturation	95°C	30 sec	35
Annealing	*AV1*: 58.8°C *BC1*: 53.1°C	30 sec	
Extension	72°C	1 min	
Final extension	72°C	15 min	1

Agarose gel electrophoresis was performed with a 3% agarose gel prepared with 1X Tris-Acetate-EDTA (TAE) buffer working solution and 0.2 µg/mL Ethidium Bromide (SRL Chem). The working solution was prepared using 50X TAE Buffer (Bio-Rad Laboratories), by mixing 20 mL 50X TAE in 1:20 (v/v) with dH_2O up to 1 L. The molecular weight marker used was the E-Gel™ 1 Kb Plus DNA Ladder (Thermo Fisher Scientific). The electrophoresis was run at 100V for 90 min, prior to the gel being visualised using a Bio-Rad ChemiDoc™ Imaging System. Following identification of reliable SACMV DNA-containing *Agrobacterium* clones and *Agl*-1 clones, 1 mL glycerol stocks of pBINSA-A, pBINSA-B, and *Agl*-1 clones were separately prepared with 50% glycerol in 1:1 (v/v) and stored at -80°C.

3.4. Plant tissue culture maintenance and propagation

In vitro germplasm maintenance of the cassava T200 and TME3 genotypes was achieved using tissue culture medium, as developed by Murashige and Skoog (MS) (Murashige & Skoog, 1962). Nodal cuttings, of two nodes per cut, were propagated onto MS20 plant growth medium, consisting of 4.4 g/L MS Basal Medium (Sigma-Aldrich), 20 g/L Sucrose (Sigma-Aldrich), 2 µM $CuSO_4$ (Copper (II) Sulphate) (Merck), and 7.8 g/L plant agar (Duchefa Biochemie), at pH 5.8. Incubation conditions for the nodal cuttings were 25°C under a light intensity of 150 $\mu Em^{-2}.sec^{-1}$ during a 16-hour (h) photoperiod, followed by 8 h of darkness. Progression of development from nodal cuttings into plantlets was monitored across 6-8 weeks, and once fully developed plants were attained *in vitro*, nodal cutting propagation onto fresh mediums would be undertaken again. Through this approach, bulking up of germplasm was achieved.

3.5. In vivo generation of plant tissue culture

Nodal cuttings, of one node per cut, were propagated onto petri dish-contained MS20 plant growth medium, consisting of 4.4 g/L MS Basal Medium, 20 g/L Sucrose, 2 µM $CuSO_4$, and 6.8 g/L plant agar, at pH 5.8. Incubation conditions were similar to those for tissue culture maintenance, coupled with 4-5 weeks of monitoring. Once substantial root density had developed, the plantlets were transferred onto Jiffy® 7C Starter Pellets (Jiffy Products International B.V) and placed into deep plastic trays, which were covered with cling

wrap film to maintain humidity. The plantlets were incubated in a walk-in growth chamber at 28°C under a light intensity of 150 $\mu Em^{-2}.sec^{-1}$ during a 16-h photoperiod, followed by 8 h of darkness. Over the course of 4 weeks, the developing plantlets would be gradually acclimatised to the growth chamber, through cutting of holes into cling wrap film, until plants had developed to the 4-6 leaf stage.

3.6. Cassava T200 and TME3 infection trials

3.6.1. Preparation of infectious clones

Yeast Extract Peptone (YEP) media was prepared, consisting of 10 g/L Yeast Extract (Sigma), 5 g/L NaCl (Sodium Chloride) (SRL Chem), and 10 g/L Tryptone (SRL Chem), at pH 7.2 ((Chilton *et al*., 1974)). Starter cultures of pBINSA-A, pBINSA-B, and *Agl*-1 *Agrobacterium* clones were prepared in 5 mL YEP media, in 1:10 (v/v), using glycerol stocks. For selectivity, 100 µg/µL of kanamycin (Kan) (Sigma) and 10 µg/µL of carbenicillin (Carb) (Sigma) were added to the pBINSA-A and pBINSA-B cultures, while the *Agl*-1 culture only contained 10 µg/µL of carbenicillin. The cultures were incubated overnight at 28°C and 250 rpm. The starter cultures were sub-inoculated, in 1:30 (v/v), into 30 mL fresh YEP media (containing 10 µg/µL of Kan and 10 µg/µL of Carb for both pBINSA-A and pBINSA-B cultures, or 10 µg/µL of carb for *Agl*-1 culture). These cultures were further incubated at 28°C and 250 rpm, with monitoring of cell density at 600 nm. Once OD_{600} of 1.6 was reached, cultures were centrifuged at 4200 rpm for 15 min. The resulting pellets were washed once, via resuspension in 25 mL autoclaved dH_2O and centrifugation at 4200 rpm for 15 min. The washed pellets were resuspended in 10 mL YEP media, containing both 50 µg/µL of Kan and 50 µg/µL of Carb for pBINSA-A and pBINSA-B cultures and 50 µg/µL of Carb only for *Agl*-1 culture. The pBINSA-A and pBINSA-B cultures were mixed into a single culture, with this mixed culture being incubated alongside the *Agl*-1 culture at 28°C and 250 rpm for 20 min.

3.6.2. Agroinfection of T200 and TME3

Cassava T200 and TME3 plants at the 4-6 leaf stage were selected and each was pressure-infiltrated along the stem and apex, with either the pBINSA-A/pBINSA-B mixed

culture (SACMV-infected plants) or the *Agl*-1 culture (mock-infected plants). Following agroinfection, plants were pooled according to treatment per genotype and placed into deep plastic trays, which were covered with cling wrap film to maintain humidity. The plantlets were incubated in the walk-in growth chamber at 28°C under a light intensity of 150 $\mu Em^{-2}.sec^{-1}$ during a 16-h photoperiod, followed by 8 h of darkness. The infected plants were re-acclimated to the growth chamber by gradually cutting holes into the cling wrap until they had fully readjusted.

3.7. Sample harvesting and storage

Symptom development was monitored over the course of 67 days post-infection (dpi) and the first leaves at the apex of each plant were pooled, per treatment per genotype, and snap frozen with liquid nitrogen at 12-, 32-, and 67-dpi. These samples were homogenised using cell lysis beads and the Qiagen TissueLyser II, at a frequency of 25.0 shakes per second (sec) for 60 sec. The powder was weighed out to 100 mg in 2 mL Eppendorf Safe-Lock microcentrifuge tubes (Sigma-Aldrich) and stored at -80C for downstream application

3.8. Primer design and optimisation

3.8.1. Primer design for SACMV-specific ORFs

Primer design for SACMV gene-specific primers was conducted on NCBI Primer Blast (Ye *et al*., 2012). Primer specificity was verified using the NCBI Basic Local Alignment Search Tool to blast the primers against both the *Manihot esculenta* Crantz genome and the *A. tumefaciens* genome, to assess for any potential off-target bindings. The qPCR primer sequences are listed below:

Table 4: Gene specific qPCR primer sequences for targeted SACMV genes

Gene	Accession Number	Forward Primer (5' – 3')	Reverse Primer (5' – 3')	Product size (bp)
AV1		CAGGCTTGGTGGGAGATT	AGCGTAGCATACACTGGATTAG	75
AV2		AGGTGATGGGGCCTACCATA	ACGTGGCGCCTCTTATATCC	91
AC1	NC_0038	TGGGGCTAGTTCCCGGATTA	CAATGACGCTTACGCCAAGG	76
AC2	03	GTCGTGGTTGGTGATGTCGA	TCGACTGCATCAACCATGGA	120
AC3		AGAAAAGACCAGTCGGAGGC	ACATCAGGAAGGCATTGGGG	84
AC4		CTTGGCGTAAGCGTCATTGG	CCAATGGGGCGAGTTTCAGA	76
BC1	NC_0038	ATAACCGACCCAGTTGCGTT	CAGGCTACCATGCGACTCAA	98
BV1	04	CTTTCGTTCCAGAGGGGGTC	AACCTAGGCATGCCGTACAC	85

3.8.2. Primer design for cassava hormone biosynthesis and response genes

Primer design for hormone-related genes was conducted on NCBI Primer Blast (Ye *et al.*, 2012). Primer specificity was verified using the NCBI Basic Local Alignment Search Tool to blast the primers against both the *Manihot esculenta* Crantz genome and the *A. tumefaciens* genome, to assess for any potential off-target bindings. The qPCR primer sequences are listed below:

Table 5: Gene specific qPCR primer sequences for selected cassava genes

Hormone	Function	Gene	Gene Name	Manes ID	Primers		Product size (bp)
Jasmonic acid	Biosynthesis	*AOS*	Allene oxide synthase,	Manes.05G166301	**F**	AAGAACCCACCATCCACACC	120
					R	CCATCTTCTCAGCCTCGTCA	
		AOC1	Allene oxide cyclase 1	Manes.14G098200	**F**	TGCCCTTCACCAACAAGCTT	120
					R	ATGTAGCCTCGTATCTGTCGC	
	Response	*OPR3*	12-oxophytodienoate reductase 3	Manes.18G120601	**F**	CTTTGGGACTTCACATGGCTG	120
					R	TGGGCTGAAGACTCTCTGGA	
		JAR1	Jasmonic acid-amido synthetase	Manes.01G248400	**F**	CCGCAGTCCACACTACAAAA	120
					R	AACCCGCATAAGAGATGGCA	
		JMT	Jasmonic acid carboxyl methyltransferase	Manes.05G156400	**F**	GCGGCCGTATGGTATTGTCA	89
					R	TTTTGCAAGCAGCTCCCACT	
Ethylene	Biosynthesis	*ACS4*	1-Aminocyclopropane-1-carboxylate synthase 4-related	Manes.12G118500	**F**	CACGTGCAACACTCATGGC	120
					R	TTCTCAGCGAGACCCATCTG	
		ACO10	1-Aminocyclopropane-1-carboxylate oxidase homolog 10-related	Manes.15G037800	**F**	TGCTATCACAGGCTTTGGGG	119
					R	GCCCATGGTGAACTCTGGTT	
	Response	*ERF1*	Ethylene-responsive transcription factor 1	Manes.13G033200	**F**	ACGCCGCCGAGATTAGAGA	120

					R	TCGAACCCCGCATGGAAAAT	
		ETR1	Ethylene receptor (ETR1, ERS2-related)	Manes.09G149700	**F**	AAGCCAGATTCAGCACTTGG	120
					R	TAGTTCAGGTGTGCCTCCCT	
		EIN3	Ethylene-insensitive protein 3-like 4 protein-related	Manes.13G092960	**F**	CGGCTCGTTACGCAATCAAA	118
					R	TGAGGCATTTCTGCGTGAGT	
		ERF096	Ethylene-responsive transcription factor 096	Manes.13G033000	**F**	TAGAGGTGTAAGACGGCGGC	86
					R	TCCCCAGCCATATCCTAGCTC	
Abscisic acid	Biosynthesis	*NCED*	9-cis-epoxycarotenoid dioxygenase	Manes.13G114801	**F**	TATGGCCTTGGATGCTGTGG	81
					R	ACAGCTGGGTCAGCAGTTTT	
		AAO3	Abscisic-aldehyde oxidase	Manes.04G051100	**F**	GGCCCCTTGGAAATGCTTTG	120
					R	TGCCAAAACCACCAAAAGCC	
	Response	*PYR1*	Pyrabactin resistance-like 1-related	Manes.17G013400	**F**	CTGCCACCAGTACAGAGAGG	120
					R	AGCCATGCACAGTGGTTACC	
Salicylic acid	Biosynthesis	*ICS1*	Isochorismate synthase 1	Manes.14G075200	**F**	AAGCCGAAGAAAGGACGACG	117
					R	TGCCTAAAGGTAACCGCAGA	
		EPS1	Enhanced Pseudomonas Susceptibility 1	Manes.13G121400	**F**	GCCTCCATTGCCTGAAGAGT	103
					R	CAAAGCAGCGAAGCCTAACC	
	Response	*PR7f5*	Pathogenesis-related protein 7f5	(Malichan *et al*., 2023)	**F**	CAGTCCCCAAGAAATGGAGA	145
					R	TCCTGAACGGTGTTTGATGA	
		PR9e	Pathogenesis-related protein 9		**F**	GGAGGCCATGCTTACTGATC	144

					R	CTCCATAGTAGGAGTAGTGTC	
		MeHSP 90.9	Heat shock protein 90.9		**F**	CGCTATATATGCTCCGCAAA	151
					R	TGAGATGAGAGATAAAAGGCACA	
		MeSRS 1	SHI-related sequence 1		**F**	CCACCAACTGAAATCCCACA	317
					R	CTCCTGCAACAAGTCCTACACC	
		MeHsf8	Heat Shock Factor 8		**F**	TGAAGAAAATTCATAGACGGAAGC	63
					R	CGTGGATATTTTCATTTTGCAC	
		MeSYP 121	Syntaxin-related Protein 1/ Syntaxin of Plants 121		**F**	ATCCAGATGTCAGAGATGCC	244
					R	GAGCCTCCAAACGAACCTTA	
Auxin	Response	*ARF19*	Auxin Response Factor 19	Manes.03G043900	**F**	TTCCCACCCATGCTTCCTTC	101
					R	CTTGGTACAGACAGGCCAGG	
Cytokinins	Response	*ARR15*	Two-component Arabidopsis Response Factor 15	Manes.14G071300	**F**	TCTCAGTTGCCTTCTTCCGAT	72
					R	GTACAAGGTGGATGTTTGTGTCG	
Brassinosteroids	Biosynthesis	*BRD1*	Brassinosteroid C-6 Oxidase	Manes.02G093100	**F**	TTGGGGAGCCAACAATAGTCT	93
					R	TTCTCGGGTAGCTGCATTCAAA	
	Response	*BAK1*	Brassinosteroid Insensitive 1 (BIN1/BRI1)-Associated Kinase 1	Manes. 04G061700	**F**	TCAAGAATCGCAACCCCCAC	81
					R	TGCAAATAAGCCAGACCTCGT	

3.8.3. Primer efficiency

DNA extraction was performed following a modified CTAB/Chloroform-Isoamyl Alcohol DNA Extraction Protocol (Doyle & Dickson, 1987; Doyle & Doyle, 1987; Cullings, 1992). The CTAB buffer consisted of 100 mM Tris(hydroxymethyl)-aminomethane (Tris)-HCl (pH 8.0), 1.4 M sodium chloride (NaCl), 20 g/L hexadecyltrimethylammonium bromide (CTAB), 20 mM Ethylenediaminetetraacetic Acid (EDTA) (pH 8.0) in 1L of distilled dH_2O. Prior to extraction, the CTAB buffer was supplemented with 2-mercaptoethanol at a concentration of 0.2% (v/v) and Polyvinylpyrolidone Av. Mol. Wt. 40,000 (PVP-40) at a concentration of 2% (v/v). Crushed leaf samples (100 mg) were resuspended in preheated (65°C) 1 mL CTAB extraction buffer in 1:10 (w/v) and briefly vortexed. The resulting mixture was incubated for 60 minutes (min) at 65°C, with inversion every 15 min. Following incubation, equal volume of chloroform: isoamyl alcohol (24:1) (Sigma Aldrich) was added to each sample, followed by brief vortexing and centrifugation for 10 min at 13 000xg and 4°C. The resulting aqueous phase was transferred to a new microcentrifuge tube and mixed with an equal volume of chloroform: isoamyl alcohol (24:1), followed by vortexing and centrifugation for 10 min at 13 000xg and 4°C. This was repeated once more. The resulting aqueous phase was transferred into a new microcentrifuge tube, followed by the addition of 0.08 volumes of 7.5 M ammonium acetate and 0.54 volumes of cold 2-propanol (Honeywell) to precipitate the DNA. The solution was vortexed and incubated at -20°C for 60 min, followed by centrifugation for 10 min at 13 000xg and 4°C. The resulting supernatant was discarded, followed by centrifugation of the pellet with cold 70% molecular grade ethanol at 13 000xg and 4°C. This wash step was repeated. The resulting pellet was vacuum dried for 5 min in an Eppendorf Concentrator Plus and resuspended with 50 µL pre-heated (65°C) nuclease-free water. All DNA samples were stored at -20°C.

Agarose gel electrophoresis was performed with a 1% agarose gel prepared with 1X TAE buffer working solution and 0.2 µg/mL ethidium bromide, to assess overall DNA quality. The DNA samples, from infected T200 at 32 dpi, were prepared for electrophoresis by mixing with 6X Purple Gel Loading Dye (New England Biolabs) in 1:6 (v/v) prior to loading on the agarose gel. The molecular weight marker was the E-Gel™ 1 Kb Plus DNA Ladder (Thermo Fisher Scientific). The electrophoresis was run at 100V for 90 min, prior to the gel being

visualised using a Bio-Rad ChemiDoc™ Imaging System. To assess DNA purity and concentration, the NanoDrop One (Thermo Fisher Scientific) system was used. Samples with 260/280 ratios greater than 1.8 and 260/230 ratios greater than 2.0 were selected. The 260/280 ratio assesses samples for protein contamination whilst the 260/230 assesses samples for phenol or salt contamination, with these contaminants acting as possible interference in downstream applications.

Selected DNA samples were used for the preparation of triplicate dilution series, with each replicate having concentrations of 500 ng/uL, 50 ng/uL, 5 ng/uL, 0.5 ng/uL, 0.05 ng/uL, and 0.005 ng/µL in its series. Real Time quantitative PCR reactions with each primer pair were prepared in triplicate, per the dilution series.

The RT-qPCR reactions were set up as follows, using reagents from New England Biolabs:

Table 6: Components of a single qPCR reaction

Component	Volume in 10 µL reaction	Final concentration
2X Luna® Universal qPCR Master Mix	5 µL	1X
10 µM Forward Primer	0.25 µL	0.25 µM
10 µM Reverse Primer	0.25 µL	0.25 µM
Nuclease-free water	3.5 µL	-

The cycling conditions, carried out on the Bio-Rad C1000 Touch™ Thermal Cycler, were as follows:

Table 7: Cycling conditions for the qPCR

Step	Temperature	Time	Cycle
Initial denaturation	95°C	60 sec	1
Denaturation	95°C	30 sec	40 (39X)
Extension (Plate Read)	72°C	60 sec	
Melt Curve	60-95°C	-	1

Melt curve analysis was performed using the Bio-Rad CFX Maestro software. The Quantification Cq data was analysed in Microsoft Excel, with the graphing of Log Concentration vs Cq standard curves used to determine the equations of the standard curves per the data of each primer pair. The gradient values of each standard curve were used in the PCR efficiency formula:

$$Primer\ Efficiency = \left(10^{\left(-\frac{1}{slope}\right)} - 1\right) \times 100$$

Primer pairs with an efficiency value between 90 and 110% (1.9 and 2.1) were selected.

3.9. Detection (conventional) PCR of SACMV-infected cassava

Following DNA extraction from mock-infected and SACMV-infected cassava T200 and TME3 at 32- dpi, convention PCR was performed, targeting the *AV1* gene (DNA-A) and the *BV1* gene (DNA-B). Primer details and cycling conditions detailed in **Section 2.3**. Subsequently, agarose electrophoresis was performed on a 3% agarose gel prepared with 1X TAE buffer working solution and 0.2 µg/mL ethidium bromide at 100V for 60 min. The molecular weight marker was the E-Gel™ 1 Kb Plus DNA Ladder. The electrophoresis was run at 100V for 60 min, prior to the gel being visualised using a Bio-Rad ChemiDoc™ Imaging System.

3.10. Viral load determination

Using both the standard curve data for the *AV1* qPCR primers and guidelines from the Bio-Rad Real-Time PCR Applications Guide, the equation for absolute quantification of SACMV copies was determined. Using the Absolute Quantification equation below:

$$Quantity = 10^{\left(\frac{C_t - constant}{gradient}\right)}$$

The equation for viral load quantification in infected T200 and TME3 was determined to be:

$$SACMV\ viral\ load = 10^{\left(\frac{C_t - 34{,}258}{-3{,}5107}\right)}$$

Following DNA extraction from the T200 and TME3 samples harvested from the SACMV infection trials, dilutions of 100 ng/µL were prepared. The *AV1* qPCR primers were used for quantification of viral load in SACMV-infected T200 and TME3 at 32- and 67-dpi from three biological replicates, with three technical replicates per biological.

The RT-qPCR reactions were set up as follows, using reagents from New England Biolabs:

Table 8: Components of a single qPCR reaction

Component	**Volume in 10 µL reaction**	**Final concentration**
2X Luna® Universal qPCR Master Mix	5 µL	1X
10 µM Forward Primer	0.25 µL	0.25 µM
10 µM Reverse Primer	0.25 µL	0.25 µM
Nuclease-free water	3.5 µL	-

The cycling conditions, carried out on the Bio-Rad C1000 Touch™ Thermal Cycler, were as follows:

Table 9: Cycling conditions for the qPCR

Step	**Temperature**	**Time**	**Cycle**
Initial denaturation	95°C	60 sec	1
Denaturation	95°C	30 sec	40 (39X)
Extension (Plate Read)	72°C	60 sec	
Melt Curve	60-95°C	-	1

The Quantification Cq data was analysed in Microsoft Excel, with the SACMV load equation being used to determine viral load in 100 ng/µL of extracted DNA per treatment per genotype of cassava.

3.11. cDNA synthesis

3.11.1. RNA extraction

RNA extraction was performed following a modified Lithium Chloride/Phenol-Chloroform-Isoamyl Alcohol DNA Extraction Protocol ((Behnam *et al*., 2019)). The RNA extraction buffer consisted of 100 mM Tris-HCl (pH 7.5), 100 mM NaCl, 1% (w/v) Sodium Dodecyl Sulphate (SDS) (Merck), 25 mM EDTA (pH 8.0), and 2% (w/v) PVP-40, 2% (v/v) 2-mercaptoethanol per 1L of autoclaved dH_2O treated with 0.1% (v/v) Diethyl pyrocarbonate (DEPC) (SRL Chem). This buffer was freshly prepared each time. Crushed leaf samples (100 mg) were resuspended in 1:7 (w/v) of RNA extraction buffer and briefly vortexed prior to incubation at 65°C for 60 sec. This was followed by incubation at room temperature for 60 sec, and the addition of an equal volume of chloroform. The mixture was briefly vortexed and then centrifuged at 15 000xg for 20 min at 4°C. The resulting aqueous phase was transferred to a new microcentrifuge tube and an equal volume of chloroform was added, with the mixture being inverted by hand briefly before undergoing centrifugation at 15 000xg for 20 min at 4°C. This was repeated once more. The resulting aqueous phase was transferred into a new microcentrifuge tube and 0.33 volumes of 8M Lithium Chloride (LiCl, prepared with 0.1% DEPC-treated water) were added and the solutions were incubated overnight at 4°C.

The solutions were centrifuged at 15 000xg for 10 min at 4°C, with the supernatants being discarded and the pellets being resuspended in 500 µL 0.1% DEPC-treated water. Acidic phenol (pH 4.3) was used to prepare phenol: chloroform: isoamyl alcohol (25:24:1) and this was mixed in equal volumes with the resuspended pellets. The resulting mixture was briefly vortexed, and the resulting emulsion was centrifuged at 15 000xg for 10 min at 4°C. The resulting aqueous phase was transferred to a new microcentrifuge tube and an equal volume of chloroform: isoamyl alcohol (24:1) was added, with the solution being centrifuged at 15 000xg for 10 min at 4°C. The aqueous phase was transferred to a new microcentrifuge tube and 0.25 volumes of 5M NaCl and 2.5 volumes of cold absolute ethanol were added, with the solutions being incubated for 30 min at -80°C. The solutions were then centrifuged at 15 000xg for 10 min at 4°C, with the supernatants being discarded. The pellets were

washed with cold 70% molecular grade ethanol at 15 000xg for 10 min at 4°C, with the supernatants being discarded thereafter. The pellets were air dried for 10 min at room temperature and then resuspended in 30 µL 0.1% DEPC-treated water. All RNA samples were stored at -80°C.

Agarose gel electrophoresis was performed with a 2% agarose gel prepared with 1X Tris-Borate-EDTA (TBE) buffer working solution and 0.2 µg/mL ethidium bromide, to assess overall RNA quality. The working solution was prepared using 10X TBE Buffer (Bio-Rad Laboratories), by mixing 100 mL 10X TBE in 1:10 (v/v) with dH_2O up to 1 L. The RNA samples were prepared for electrophoresis by mixing with 2X RNA Loading Dye (New England Biolabs) in 1:1 (v/v) and heating at 70°C for 10 min to denature the RNA, followed by incubation on ice for 2 min. The molecular weight marker, RiboRuler High Range RNA Ladder (Thermo Fisher Scientific), was prepared in a similar manner to a volume of 4 µL. The electrophoresis was run at 100V for 45 min, prior to the gel being visualised using a Bio-Rad ChemiDoc™ Imaging System. To assess RNA purity and concentration, the NanoDrop One system was used. Samples with 260/280 ratios greater than 1.8 and 260/230 ratios greater than 2.0 were selected.

3.11.2. Deoxyribonuclease (DNase) treatment

DNase treatment was performed using ribonuclease-free (RNase-free) DNase I (New England Biolabs). Briefly, 1000 ng of RNA was added to 1 µL DNase I reaction buffer (10X), 0.5 µL DNase I, and the volume was made up to 10 µL with DEPC-treated water. The reaction was incubated at 37°C for 10 min, followed by DNase I inactivation through the addition of 1 µL of 50 mM EDTA and subsequent incubation at 75°C for 10 min.

3.11.3. First Strand synthesis

First Strand synthesis was carried out using the RevertAid cDNA Synthesis Kit (Thermo Fisher Scientific). The reactions were set up as follows, in order of components:

Table 10: Components of a single DNAse treatment reaction

Component	Volume in 20 µL reaction
DNase-treated RNA	11 µL
Oligo (dT)18 primer	1 µL
5X Reaction Buffer	4 µL
RiboLock RNase Inhibitor (20 U/µL)	1 µL
10 mM dNTP Mix	2 µL
RevertAid M-MuLV RT (200 U/µL)	1 µL

The reactions were incubated at 42°C for 10 min, followed by denaturation of the RevertAid M-MuLV RT at 72°C for 5 min. All cDNA samples were stored at -20°C.

3.12. Gene expression studies

The expression of SACMV genes, namely, *AV1*, *AV2*, *AC1*, *AC2*, *AC3*, *AC4*, *BC1*, and *BV1*, was assessed across 12-, 32-, and 67-dpi in mock-infected and SACMV-infected T200 and TME3. Additionally, the expression of host hormone biosynthesis and response genes related to JA, ET, ABA, SA, Aux, CK, and BR was also assessed across 12-, 32-, and 67-dpi in mock-infected and SACMV-infected T200 and TME3. RT-qPCR was performed using cDNA prepared from samples harvested from the two cassava genotypes, per treatment. Two housekeeping genes, GTP-binding protein (*GTPb*) and Ubiquitin 10 (*UBQ10*), were used as internal controls for the gene expression studies.

Table 11: Gene specific PCR primer sequences for selected housekeeping genes

Gene name	Accession Number	Forward Primer (5’ – 3’)	Reverse Primer (5’ – 3’)	Product size (bp)
GTPb	110622574	GTTGCCTTCTTTTGCGTTTCT	GCAATTTGATCCGTTTTCCAT	114
UBQ10	110619528	GGTCGGACGCTAGCAGATTA	TCCGAGCTTTCGACTTCCAG	134

The RT-qPCR reactions were set up as follows, using reagents from New England Biolabs, with three biological replicates (three technical replicates per biological) for each SACMV gene:

Table 12: Components of a single qPCR reaction

Component	Volume in 10 µL reaction	Final concentration
2X Luna® Universal qPCR Master Mix	5 µL	1X
10 µM Forward Primer	0.25 µL	0.25 µM
10 µM Reverse Primer	0.25 µL	0.25 µM
Nuclease-free water	3.5 µL	-

The cycling conditions, carried out on the Bio-Rad C1000 Touch™ Thermal Cycler, were as follows:

Table 13: Cycling conditions for the qPCR

Step	Temperature	Time	Cycle
Initial denaturation	95°C	60 sec	1
Denaturation	95°C	30 sec	40 (39X)
Extension (Plate Read)	72°C	60 sec	
Melt Curve	60-95°C	-	1

The Quantification Cq data was analysed in Microsoft Excel and changes in gene expression were determined using the $2^{-\Delta\Delta Ct}$ method. Two-tailed paired student *t*-tests were performed per gene to assess significant differences in gene expression between SACMV-infected T200 and SACMV-infected TME3. A *p-value* < 0.05 was considered significant.

3.13. Quantification of cassava phytohormones during infection by SACMV

3.13.1. Validation of hormone extraction protocol

In all the work involving hormone extractions, ROMIL-SpS^{TM} Super Purity Methanol 215 (Romil Pure Chemistry) and Supelco LiChrosolv Water for Chromatography (LC-MS Grade) (Merck) were used. Authentic standards of salicylic acid (SA), jasmonic acid (JA), abscisic acid (ABA), and the ethylene precursor 1-aminocyclopropane-1-carboxylic acid (ACC), as well as the internal standard p-fluoro-DL-phenylalanine (P-fluoro) were sourced from Sigma-Aldrich.

The standards were used to prepare stock solutions of 1000 parts per million (ppm), each in 1mL 50% Methanol (MeOH). From the 1000 ppm stock solutions, dilution series were prepared in triplicate at nine levels of dilution: 1000 parts per billion (ppb), 250 ppb, 100 ppb, 75 ppb, 50 ppb, 20 ppb, 10 ppb, 5 ppb, and 1 ppb. Each dilution was filtered into chromatography vials using 0.22 µm nylon syringe filters and injected, in triplicates of 2µL, into the Shimadzu Nexera 30AD for reverse phase chromatography via a Shimadzu SHIM-PACK C18, 100 X 2.1 mm, 2µ particle size column. The mobile phase was MeOH:H_2O with 0.1% formic acid. This was coupled with the Shimadzu MALDI-8030 for electrospray ionization (ESI). Following UHPLC-MS, the processed data was analysed in Microsoft Excel, with the graphing of a Concentration (ppb) vs Average Peak Area used to determine the Pearson correlation coefficients (R^2) of the generated standard curves, per each standard.

3.13.2. Percentage Recovery study

Percentage recovery work was undertaken to determine the degree to which the targeted hormones could be recovered by the extraction protocol and subsequently reliably quantified. Mock-infected and SACMV-infected T200 were used for the recovery study. A mix of authentic standards (SA, JA, ABA, ACC and P-fluoro) was prepared using 80% methanol, with each standard having a concentration of 50 ppb, whereas a standalone solution of the internal standard (P-fluoro) was also prepared to a concentration of 50 ppb. Three replicates of the hormone mix underwent the extraction protocol, alongside three replicates each of

mock- and SACMV-infected T200 samples (100 mg) resuspended in cold 80% MeOH (either the authentic standard mix or the internal standard) in 1:10 (w/v). In addition to these, three replicates each of authentic standards mix and the internal standard were also prepared but did not undergo the extraction procedure, to serve as controls. These groups of extracted and unextracted samples were the basis of the recovery study.

Briefly, each sample underwent probe sonication with the QSonica Ultrasonic Q500 Sonicator on ice at 230 V, 60 Hz, and a frequency of 20 kHz for 2 min (30 sec pulses at 30 sec intervals, Total time = 3.5 min). The resulting homogenate was centrifuged at 13 000x g for 15 min at 4°C, with the supernatant being transferred to 5 mL Graduated Centrifuge Tubes and undergoing water bath sonication to break down any remaining particulate matter. The extracts were filtered through 0.22 um nylon syringe filters into chromatography vials and stored at 4°C until UHPLC-MS was performed.

The extracts were injected, in triplicates of 2µL, into the Shimadzu Nexera 30AD for reverse phase chromatography via a Shimadzu SHIM-PACK C18, 100 X 2.1 mm, 2µ particle size column. The mobile phase was MeOH:H_2O with 0.1% formic acid. This was coupled with the Shimadzu MALDI-8030 for electrospray ionization (ESI). Following UHPLC-MS, the processed data was analysed in Microsoft Excel, with average peaks per hormone per extracted/unextracted group being determined. By assessing the loss of p-fluoro-DL-phenylalanine across the groups, the percentage loss of the internal standard was used to accordingly adjust the percentage recoveries of SA, JA, ET, and ABA.

3.13.3. Hormone extraction and quantification

Hormone extraction was performed on 12-, 32-, and 67-dpi samples harvested from mock-, and SACMV-infected T200 and TME3, with three biological replicates and three technical replicates -per biological. Each 100 mg of crushed tissue was resuspended in 80% MeOH at 1:10 (w/v) and vortexed for uniformity. Each sample underwent probe sonication with the QSonica Ultrasonic Q500 Sonicator on ice at 230 V, 60 Hz, and a frequency of 20

kHz for 2 min (30 sec pulses at 30 sec intervals, Total time = 3.5 min). Following sonication, samples were centrifuged at 13 000x g for 15 min at 4°C, with the extracts being transferred to 5 mL Graduated Centrifuge Tubes and undergoing water bath sonication. The extracts were then pressed through 0.22 um nylon syringe filters into chromatography vials and stored at 4°C until UHPLC-MS was performed.

The extracts were injected, in triplicates of 3µL, into the Shimadzu Nexera 30AD for reverse phase chromatography via a Shimadzu SHIM-PACK C18, 100 X 2.1 mm, 2µ particle size column. The mobile phase was MeOH:H_2O with 0.1% formic acid. This was coupled with the Shimadzu MALDI-8030 for electrospray ionization (ESI). Following UHPLC-MS, the processed data was analysed in Microsoft Excel. Using the standard curves for each hormone, the area peaks generated from the MS analysis were used to determine the concentration of each hormone per treatment per cassava genotype. Following this, the volume injected into the system was used to determine the concentration of hormone per 100 mg of cassava leaf sample. For statistical analysis, one-way ANOVA was used and a *p-value* < 0.05 was considered significant.

Chapter 4: Results

4.1. Quality control

4.1.1. Confirmation of *A. tumefaciens* C58C1 clones harbouring either pBIN19-SACMV-DNA-A, pBIN19-SACMV-DNA-B, or empty pBIN19 vector

To confirm that the *Agrobacterium* clones that were to be used to infectivity trials contained the pBIN19-SACMV-DNA-A, pBIN19-SACMV-DNA-B, or empty pBIN19 vector, conventional PCR was performed, targeting the SACMV DNA-A encoded *AV1* gene (550 bp) and the SACMV DNA-B encoded *BC1* (538 bp). Additionally, qPCR-specific primers were also used to target *AC2* (120 bp), *AC4* (76 bp), *BC1* (98 bp), and *BV1* (85bp). The pBIN19-SACMV-DNA-A clone only showed amplification of DNA-A specific genes (AV1, qAV1, and qAC2) (**Figure 10**), and the DNA-B specific clones only showed amplification of the DNA-B specific genes (BV1, qBC1, and qBV1) (**Figure 10**), whereas the *Agl*-1clone did not show any amplification of SACMV genes, due to the empty pBIN19 vector (**Figure 10**).

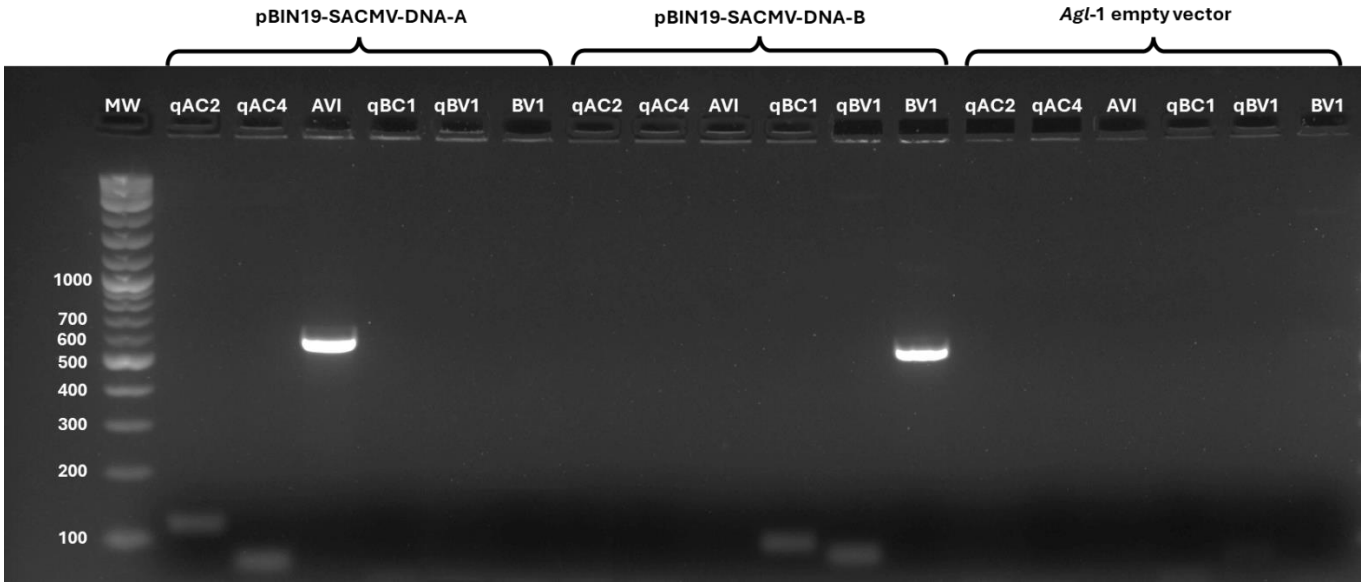


Figure 11: Agarose gel, of 3% (w/v), showing PCR products from Colony PCR of *A. tumefaciens* C58C1 clones

Three PRC products each were amplified for the pBIN19-SACMV-DNA-A clones and pBIN19-SACMV-DNA-B clones, whereas there was no amplification detected with the Agl-1clone.

4.1.2. Nucleic acid extractions

Following DNA and RNA extractions, agarose gel electrophoresis was performed for either nucleic acid type to assess the quality of the extractions. Following DNA extraction, the results showed intact, high molecular weight DNA but it contained phenol contamination (**Figure 12A**). Phenol-chloroform purification was performed, and another gel electrophoresis was conducted, showing a reduction in the contamination (**Figure 12B**). Additionally, most RNA extractions were successful, as 26S, 18S, and 16S ribosomal RNA (rRNA) bands were visible on agarose gels. The optimal samples from both the DNA and RNA extractions, following Nanodrop assessment of purity and concentration, were selected for use downstream.

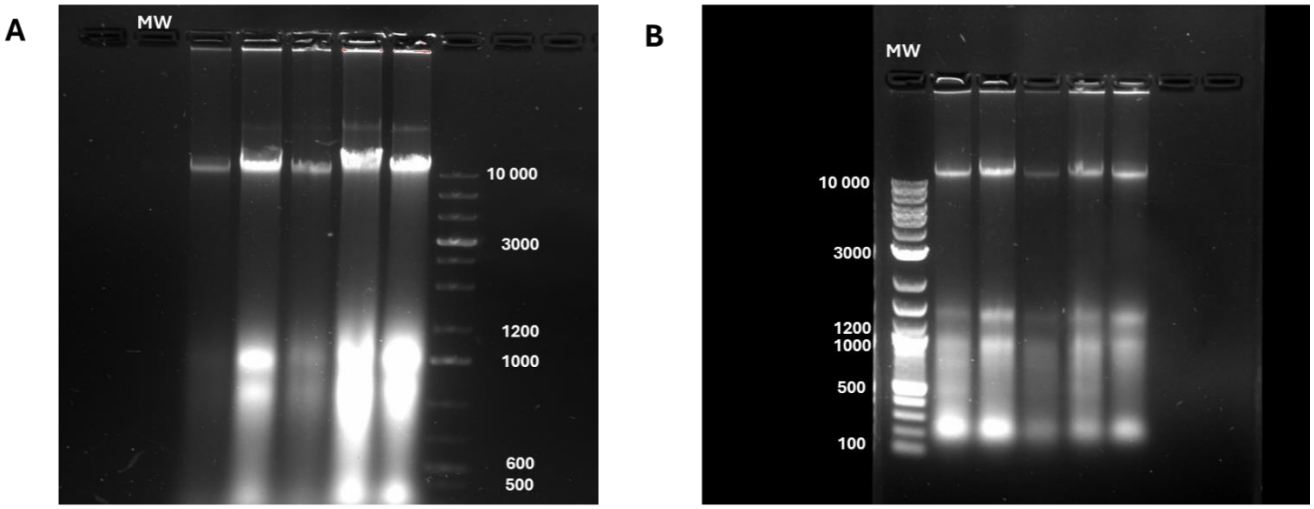


Figure 12: Agarose gels, of 1% (w/v), showing intact DNA extracted from cassava leaves and the outcome post-purification

Successful DNA extractions from cassava leaves that were, however, contaminated with phenol (**Figure 12B**). The result of phenol-chloroform purification of the extracted DNA (**Figure 12B**). The molecular weight marker (MW) was the E-Gel^{TM} 1 Kb Plus DNA Ladder (Thermo Fisher Scientific)

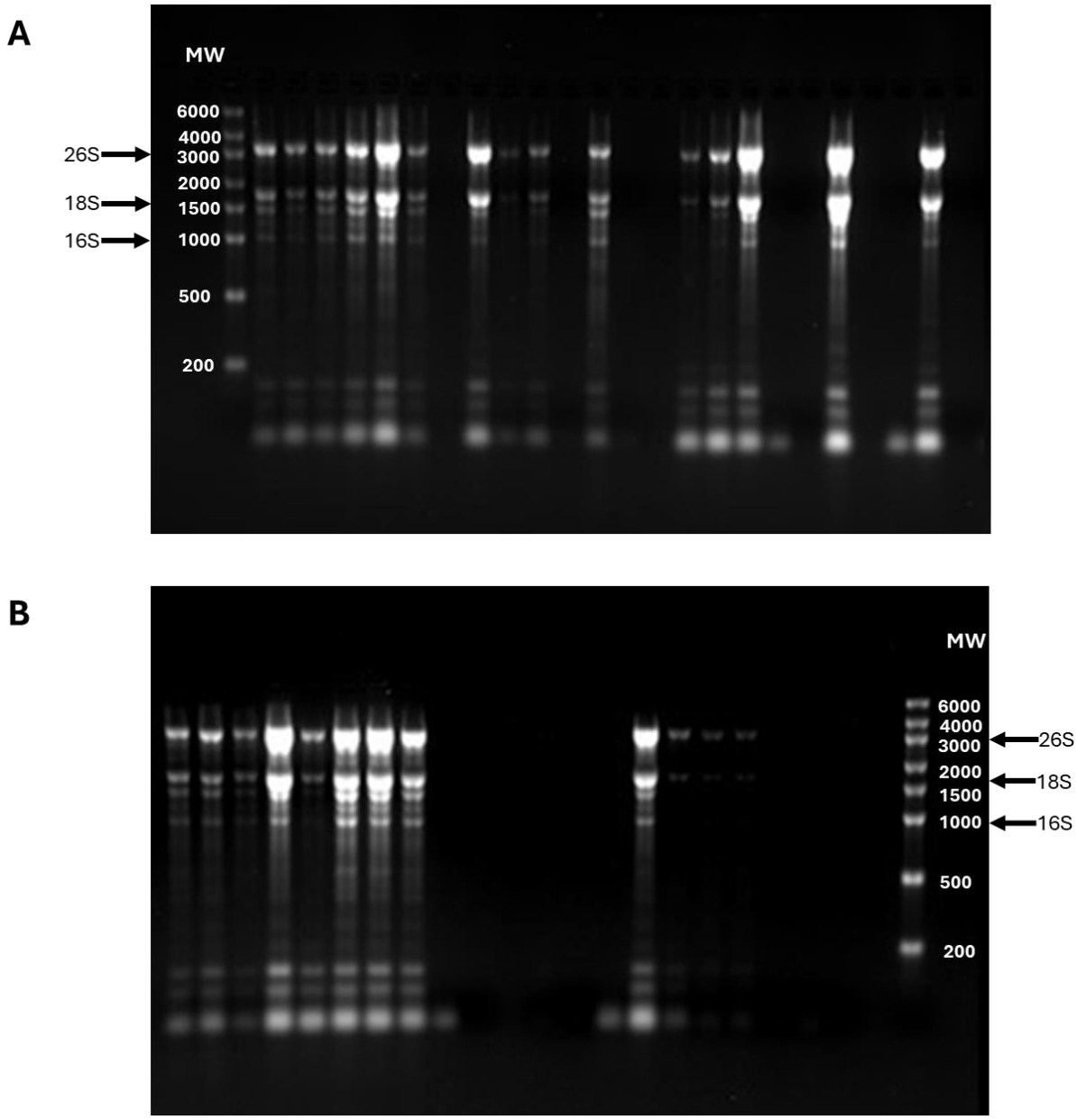


Figure 13: Agarose gels, of 2% (w/v), showing intact RNA extracted from cassava leaves

Successful RNA extractions from cassava leaves harvested from T200 (**Figure 13A**) and TME3 (**Figure 13B**). The molecular weight marker was the RiboRuler High Range RNA Ladder (Thermo Fisher Scientific)

4.1.3. Primer efficiency and specificity for SACMV genes

To assess the specificity of the primers designed to target the SACMV-specific genes, qPCR was performed to enable for melt-curve analysis using Bio-Rad CFX Maestro software. In addition, agarose gel electrophoresis was conducted to assess the qPCR products from each gene-specific run (**Figure 14**). The melt curve analysis showed that for each gene, there was no off-target amplification and that the peaks were all above the threshold. The peaks of one technical replicate per gene are shown (**Figure 15**).

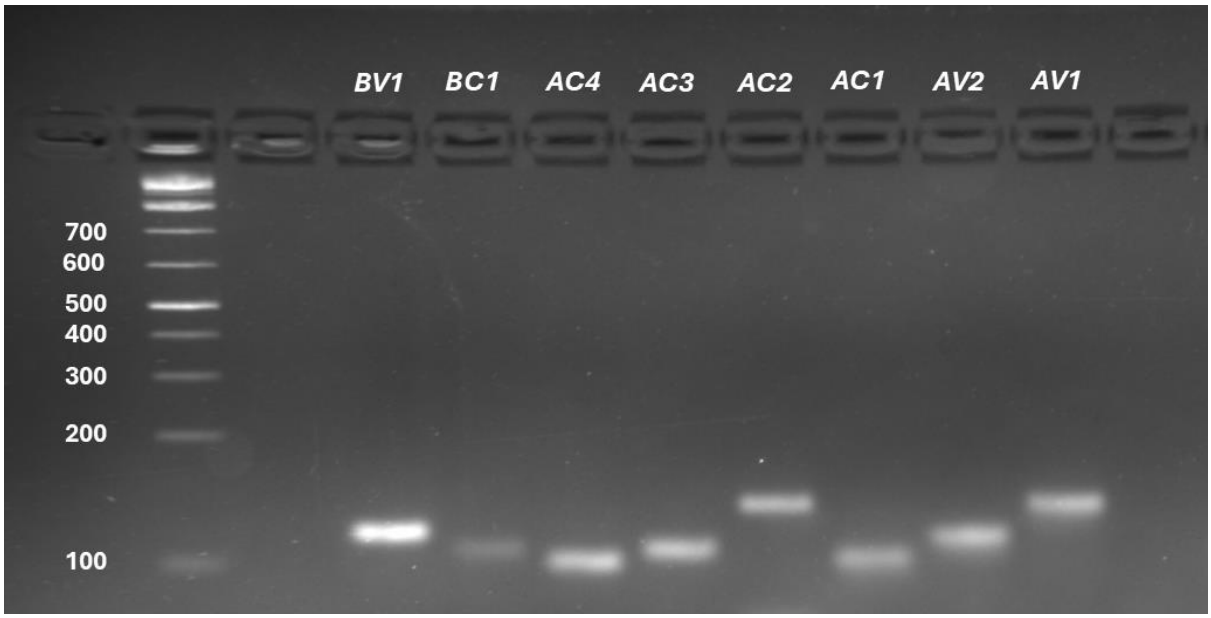


Figure 14: Agarose gel, of 3% (w/v), showing qPCR products generated from the amplification of *South African cassava mosaic virus* genes of interest

Each lane consisted of only one band of expected size for the respective gene. The molecular weight marker (MW) was the E-Gel^{TM} 1 Kb Plus DNA Ladder (Thermo Fisher Scientific)

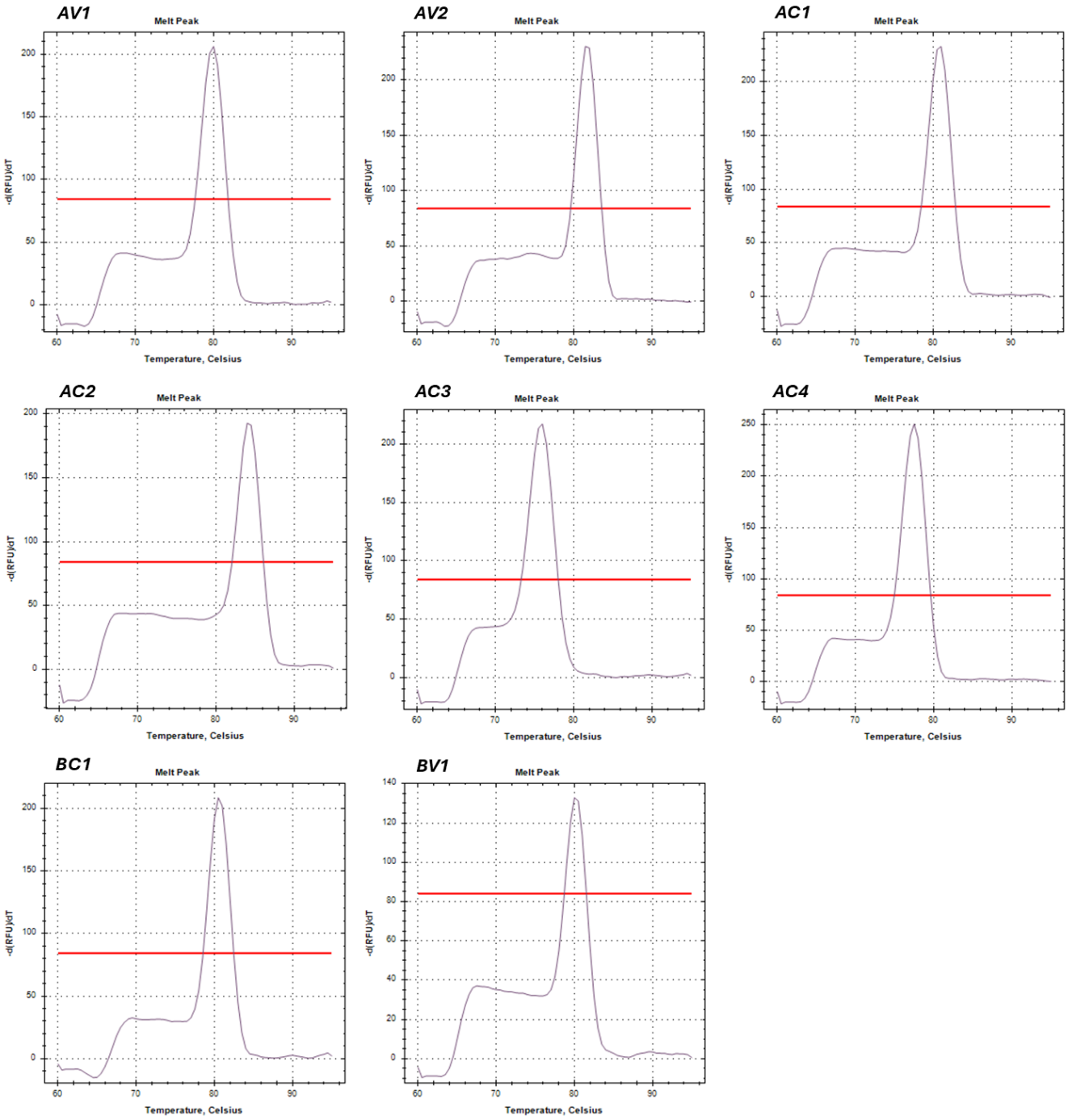


Figure 15: Melt curve peaks for oligonucleotide pairs used to target the selected *South African cassava mosaic virus* genes

Melt curve peaks were used to assess the specificity of the oligonucleotide pairs and each peak for each gene was above the threshold and thus one peak per gene was used for illustration.

4.1.4. Primer efficiency and specificity for selected cassava hormone-related genes

To assess the specificity of the primers designed to target the cassava-specific genes, qPCR was performed to enable for melt-curve analysis using Bio-Rad CFX Maestro software. In addition, agarose gel electrophoresis was conducted to assess the qPCR products from each gene-specific run (**Figure 16**). The melt curve analysis showed that for each gene, there was no off-target amplification and that the peaks were all above the threshold. The peaks of one technical replicate per gene are shown (**Figure 17, Figure 18, Figure 19**).

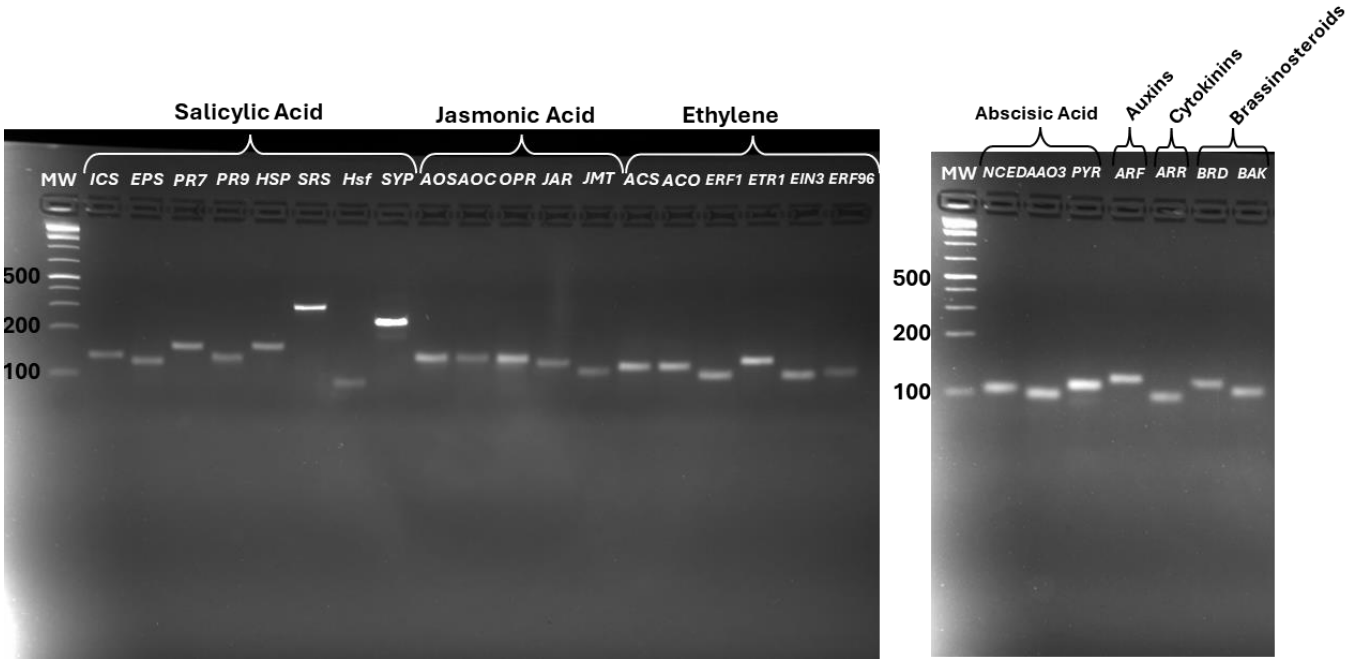


Figure 16: Agarose gel, of 3% (w/v), showing qPCR products generated from the amplification of cassava genes of interest

Each lane consisted of only one band of expected size for the respective gene. The molecular weight marker (MW) was E-Gel^{TM} 1 Kb Plus DNA Ladder (Thermo Fisher Scientific)

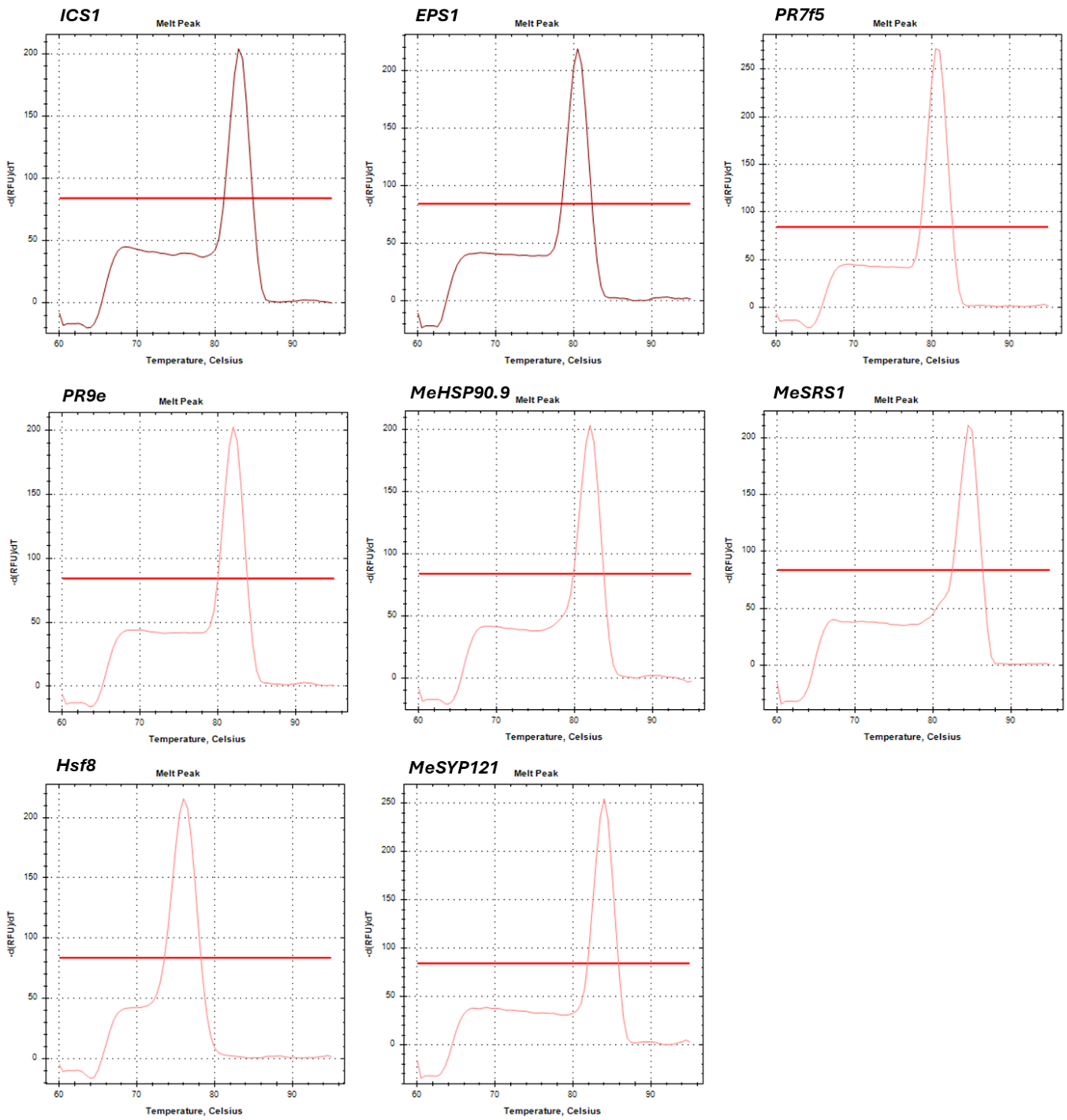


Figure 17: Melt curve peaks for oligonucleotide pairs used to target the selected salicylic acid-related genes

Melt curve peaks were used to assess the specificity of the oligonucleotide pairs and each peak for each gene was above the threshold and thus one peak per gene was used for illustration.

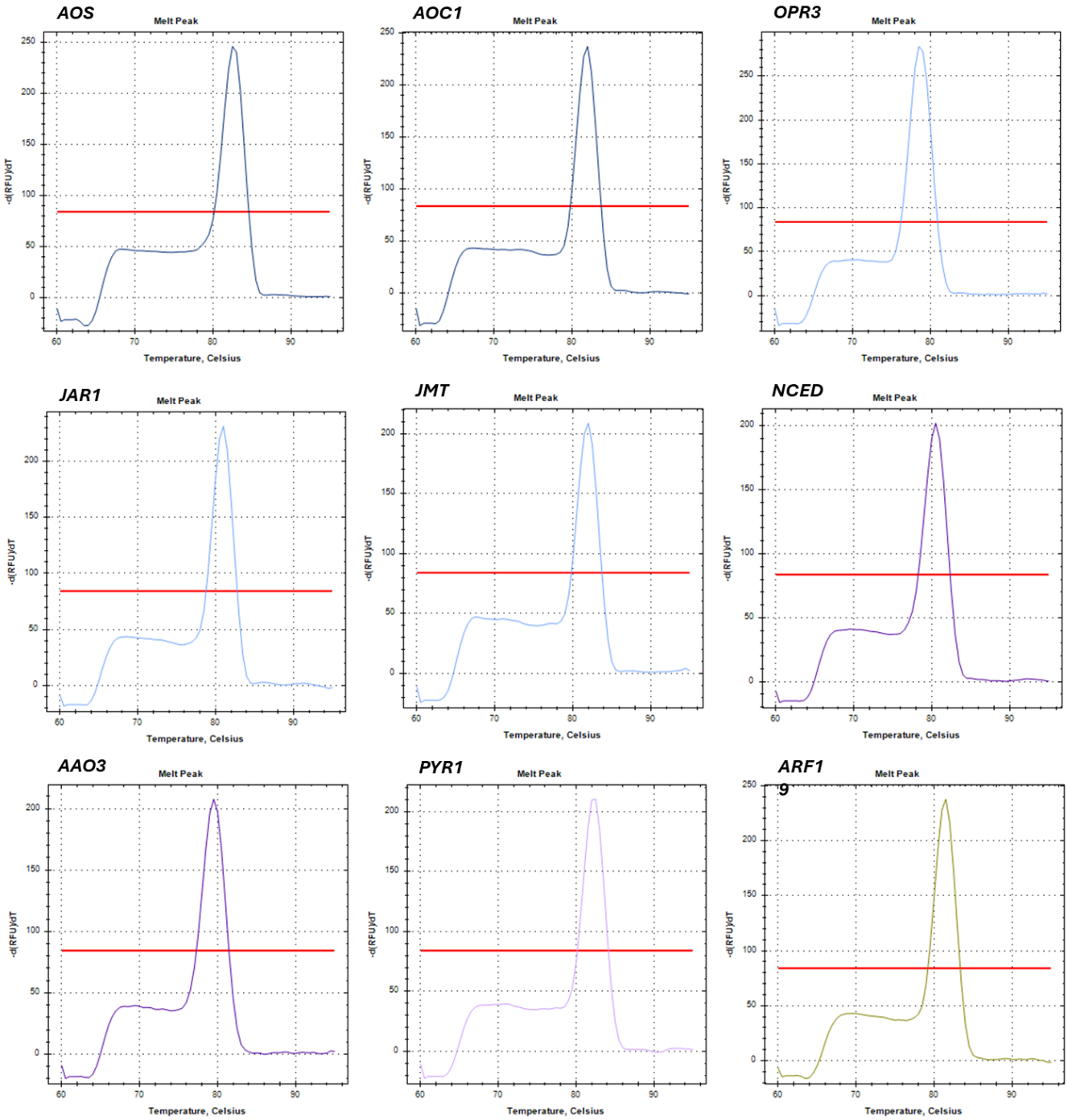


Figure 18: Melt curve peaks for oligonucleotide pairs used to target the selected jasmonic acid-, abscisic acid-, and auxin-related genes

Melt curve peaks were used to assess the specificity of the oligonucleotide pairs and each peak for each gene was above the threshold and thus one peak per gene was used for illustration.

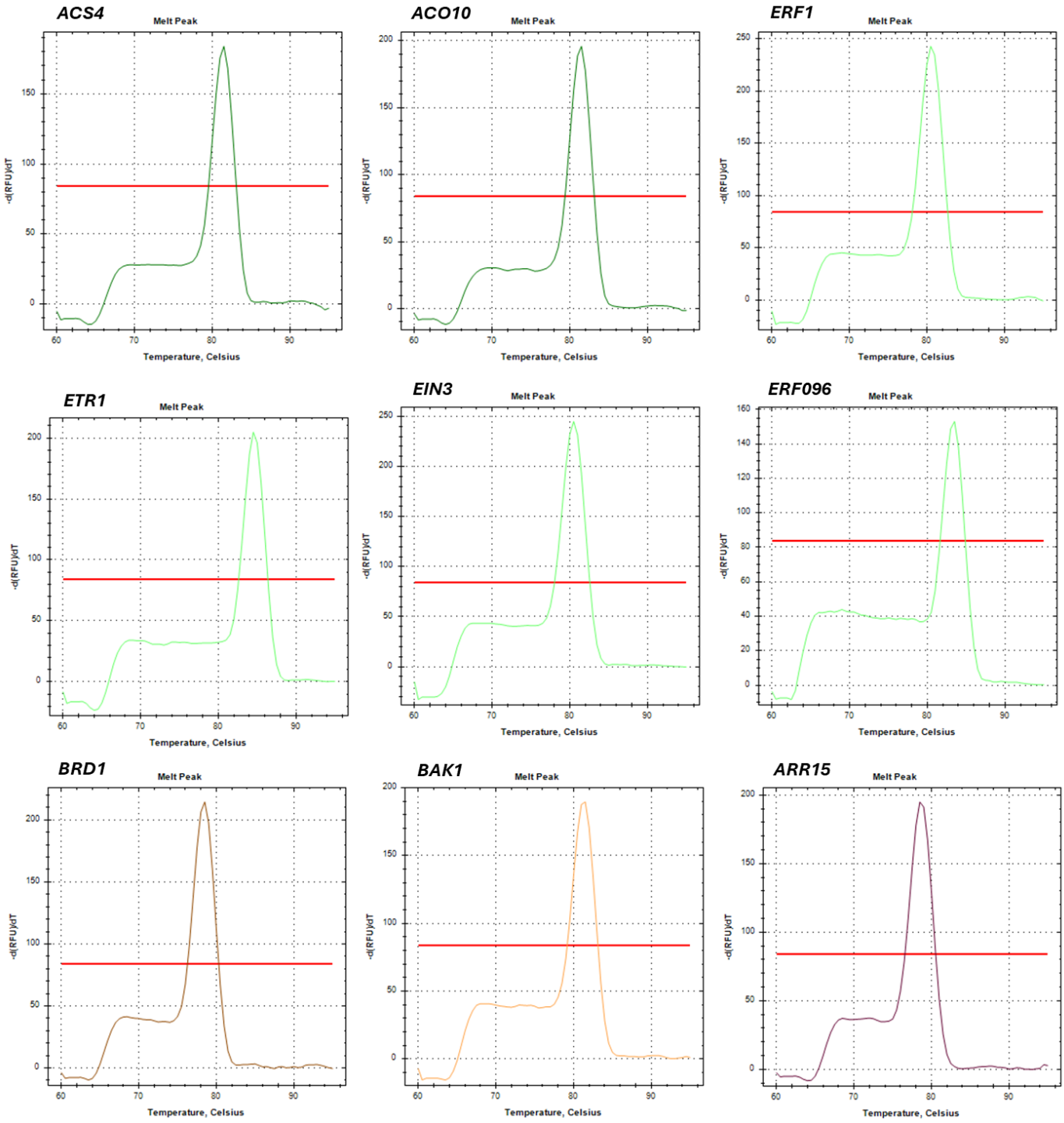


Figure 19: Melt curve peaks for oligonucleotide pairs used to target the selected ethylene-, brassinosteroid-, and cytokinin-related genes

Melt curve peaks were used to assess the specificity of the oligonucleotide pairs and each peak for each gene was above the threshold and thus one peak per gene was used for illustration.

4.2. SACMV infection trials in T200 and TME3

4.2.1. CMD progression and symptom severity in cassava T200 and TME3

To assess and compare CMD progression and symptom severity in T200 and TME3, SACMV-infected T200 and TME3 were observed over the course of 67 days post infection (dpi). Initially, both genotypes showed no observable symptoms at 12 dpi, but symptom severity progressed over the course of the infection trial (**Figure 20**). By 32 dpi, both genotypes showed leaf curling, leaf deformation, reduction in leaf size, as well as mosaic patterning. However, TME3 managed to recover by 67 dpi, as seen by the reduction and/or absence of symptoms in the young leaves, whereas T200 remained severely symptomatic.

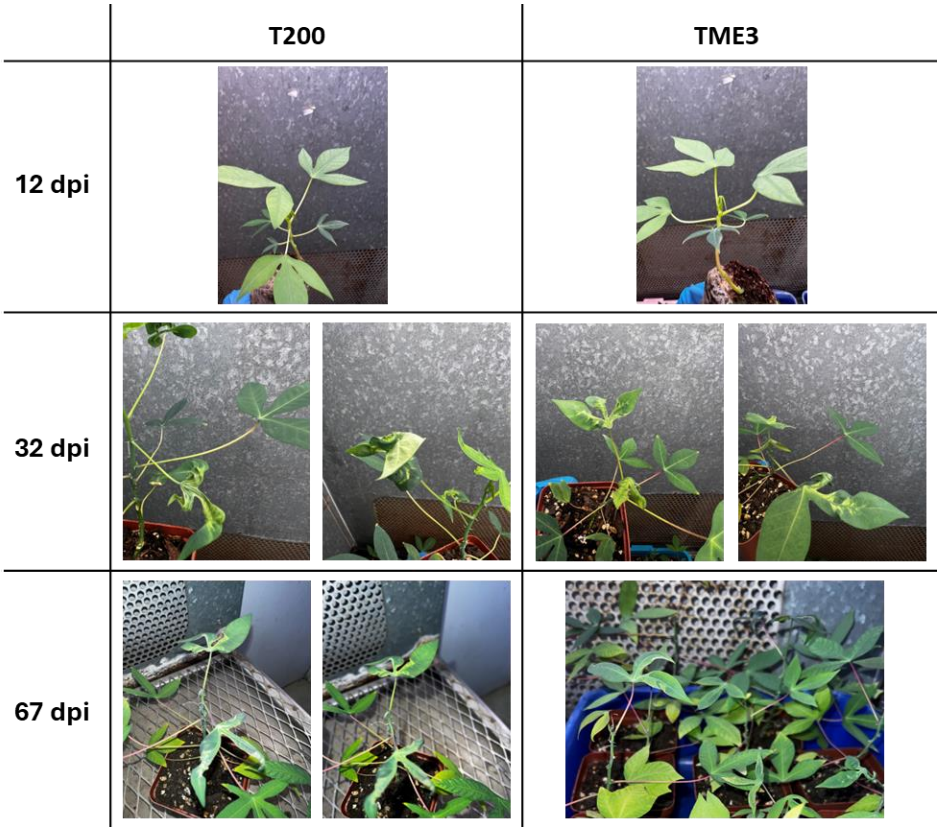


Figure 20: Symptom development in *South African cassava mosaic virus*-infected T200 and TME3 at 12-, 32-, and 67-dpi

At 12 dpi, both T200 and TME3 showed no symptom development and appeared healthy. At 32 dpi, both T200 and TME3 showed symptoms of a similar severity, wherein there was leaf curling, leaf deformation, reduction in leaf size, as well as mosaic patterning. At 67 dpi, T200 still showed the symptoms in its younger leaves, while TME3 no longer showed observable severe symptoms.

4.2.2. Detection PCR for confirmation of SACMV infection in T200 and TME3

Prior to downstream work being undertaken, conventional PCR was performed on DNA extracted from mock-infected and SACMV-infected T200 and TME3, targeting the *AV1* gene of DNA-A and the *BC1* gene of DNA-B in each replicate. In the mock-infected samples for either genotype, there was no amplification, indicating that the mock-infected samples did not harbour SACMV (**Figure 21**). In the infected samples, there was amplification of both *AV1* and *BC1*, confirming that infections were successful (**Figure 21**).

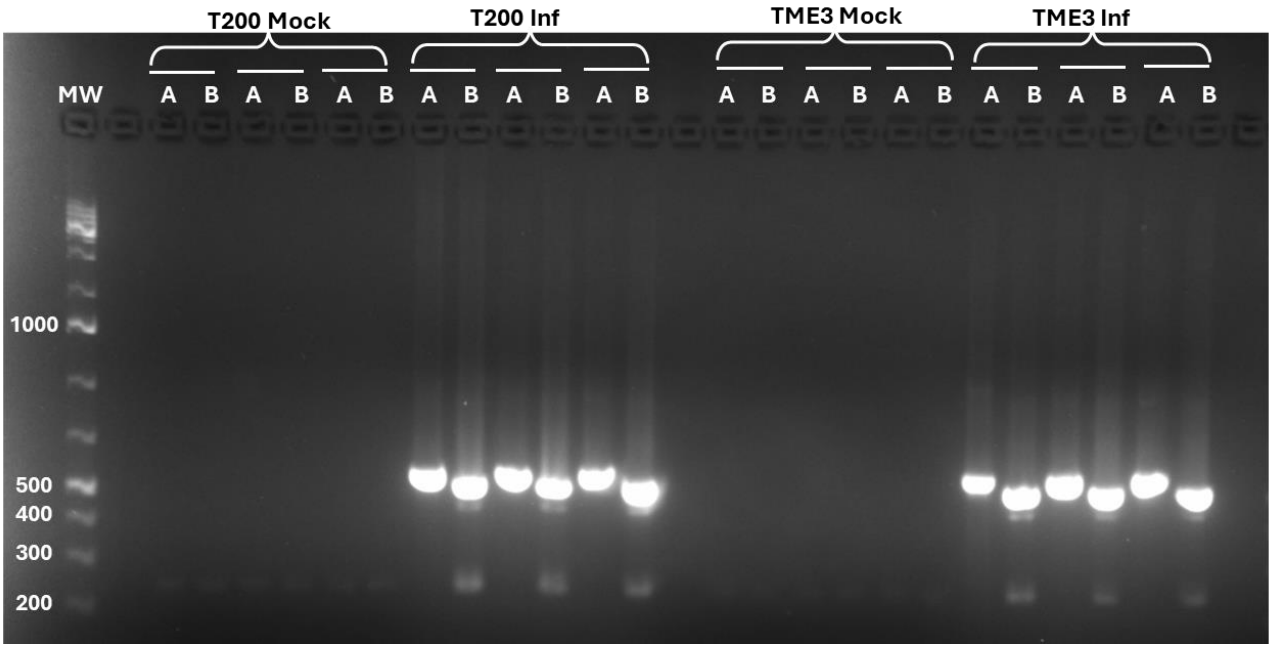


Figure 21: Agarose gel, of 2% (w/v), showing PCR products generated from the amplification of *AV1* and *BC1*

DNA replicates for mock T200 and TME3 samples did not show any bands, with bands only being present for the infected T200 and TME3 samples. . The molecular weight marker (MW) was the E-Gel™ 1 Kb Plus DNA Ladder (Thermo Fisher Scientific)

4.2.3. Viral load quantification in T200 and TME3

Given the lack of any detectable symptoms in T200 and TME3 at 12 dpi, both 32 dpi and 67 dpi were selected as the timepoints for comparison of viral load in SACMV-infected T200 and TME3. While both T200 and TME3 had high accumulation of DNA-A copies during the time course study, with the highest levels recorded at 32 dpi for both genotypes, T200 had significantly higher copies of DNA-A at both timepoints, relative to TME3 (**Figure 22**).

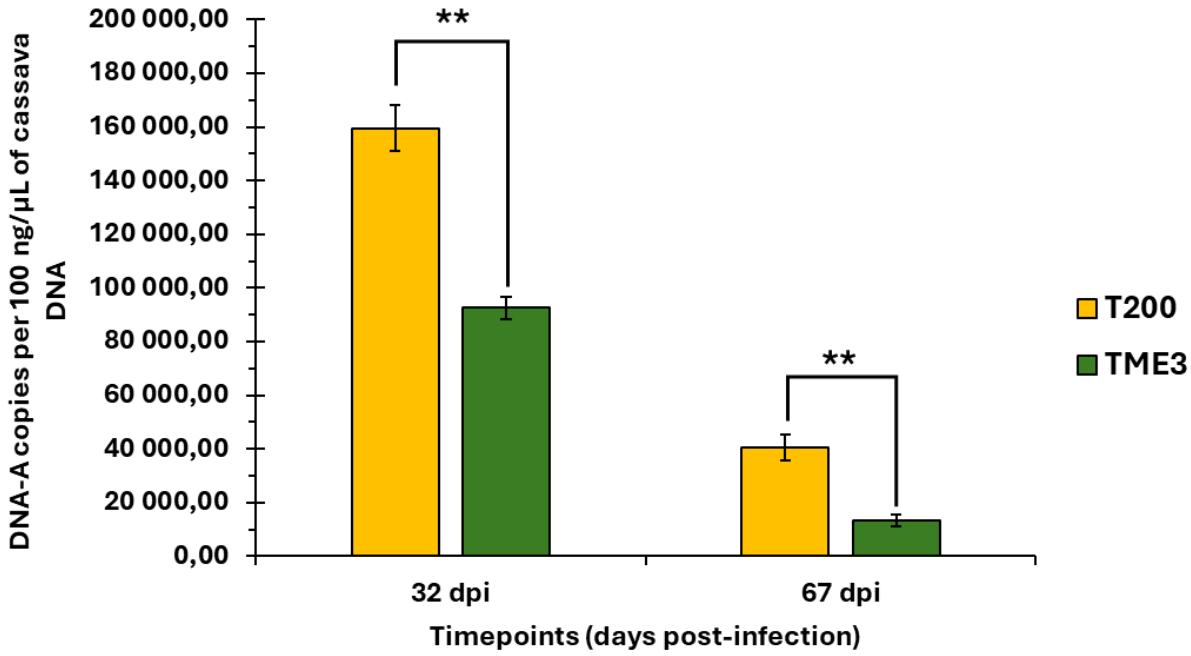


Figure 22: Quantification of DNA-A viral copies in cassava during *South African cassava mosaic virus* infection

At 32 dpi, both T200 and TME3 had a high accumulation of viral DNA per 100 ng/µL of extracted DNA, with T200 accumulating approximately 160 000 copies of DNA-A and TME3 accumulated approximately 90 000 copies of DNA-A. At 67 dpi, T200 had approximately 40 000 copies of DNA-A while TME3 had 10 000 copies. Student's t-tests were performed for statistical analysis and significance was denoted with asterisks: * *p-value* < 0.05, ** *p-value* < 0.01, and *** *p-value* < 0.001. Error bars represent standard deviation of mean (n=3)

4.3. Differential expression of viral ORFs at 12-, 32-, and 67-dpi in SACMV-infected T200 and TME3

As CMD consists of three stages, the early stage (12 dpi), active infection stage (32 dpi) and late stage (67 dpi), the differential expression of the selected SACMV genes (*AV1*, *AV2*, *AC1*, *AC2*, *AC3*, *AC4*, *BC1*, and *BV1*) was assessed at the three time points in SACMV-infected T200 and TME3 to determine the role(s) that SACMV pathogenicity determinants may be contributing to CMD development. At all the time points, T200 showed significantly higher expression of all the selected genes, except for *AC4*, *BC1*, and *BV1* 32 dpi (**Figure 23**).

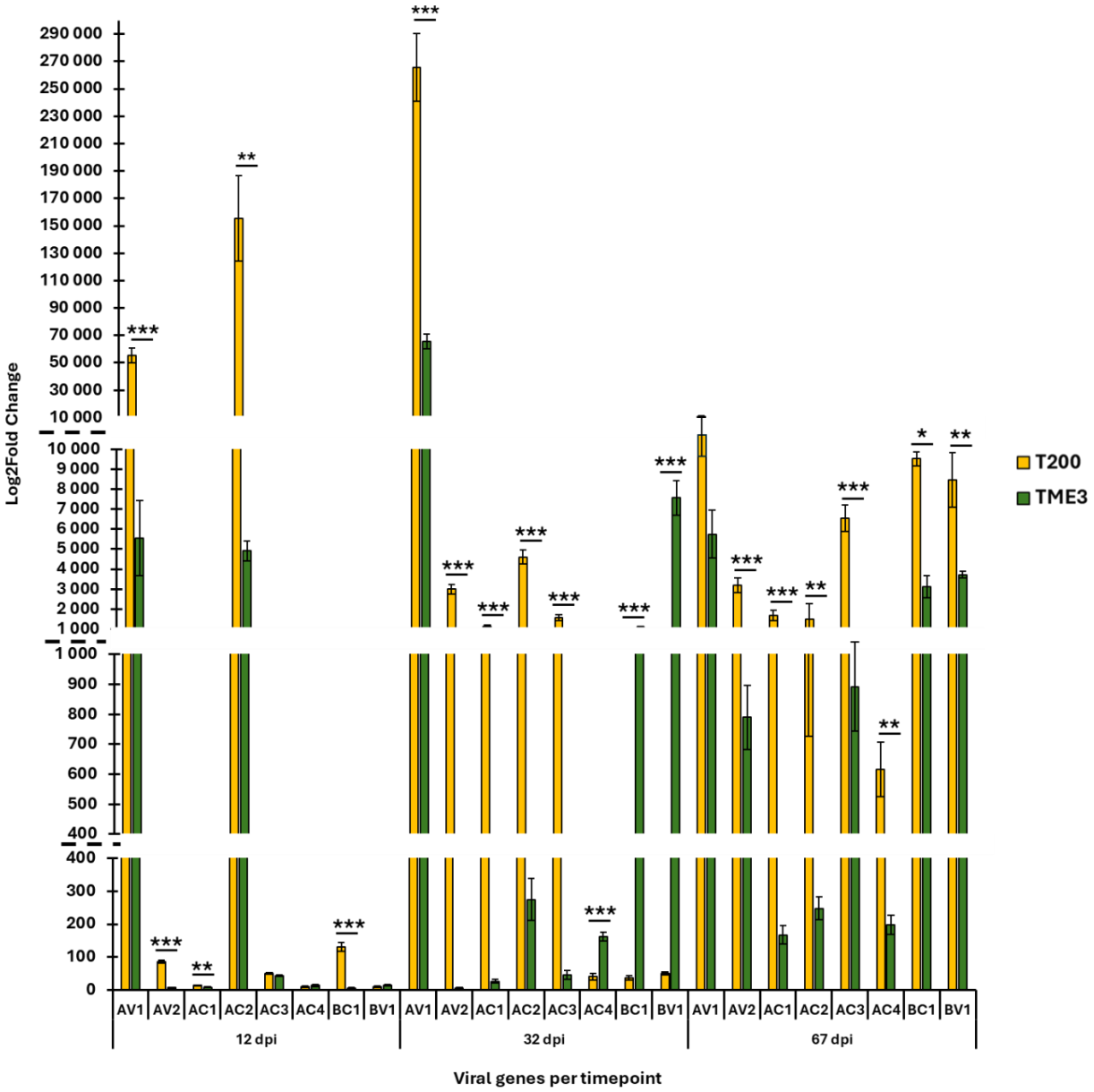


Figure 23: Differential expression of *South African cassava mosaic virus* genes in cassava during cassava mosaic disease

At 12 dpi, T200 showed significantly higher expression of 5 SACMV genes relative to TME3, with there being no significant difference in the expression of *AC3*, *AC4*, and *BV1*. At 32 dpi, while T200 showed significantly higher expression of *AV1*, *AV2*, *AC1*, *AC2*, and *AC3*, TME3 showed significantly higher expression of *AC4*, *BC1*, and *BV1*. At 67 dpi, T200 significantly higher expression of all genes, except for *AV1*, which showed no significant difference. Student's t-tests were performed for statistical analysis and significance was denoted with asterisks: * *p-value* < 0.05, ** *p-value* < 0.01, and *** *p-value* < 0.001. Error bars represent standard deviation of mean (n=3)

4.4. Differential expression of hormone biosynthesis and response genes at 12-, 32-, and 67-dpi in SACMV-infected T200 and TME3

The differential expression of the selected hormone biosynthesis genes (ET, JA, ABA, SA, and BR) and response genes (ET, JA, ABA, SA, Aux, BR and CK) was assessed at the three time points in SACMV-infected T200 and TME3 to assess if the expression of these hormone-related genes contributes to the response of cassava to CMD. Across 12- and 32-dpi, T200 showed significantly higher expression of its upregulated genes, relative to TME3, which showed an attenuated response (**Figure 24, Figure 25**).

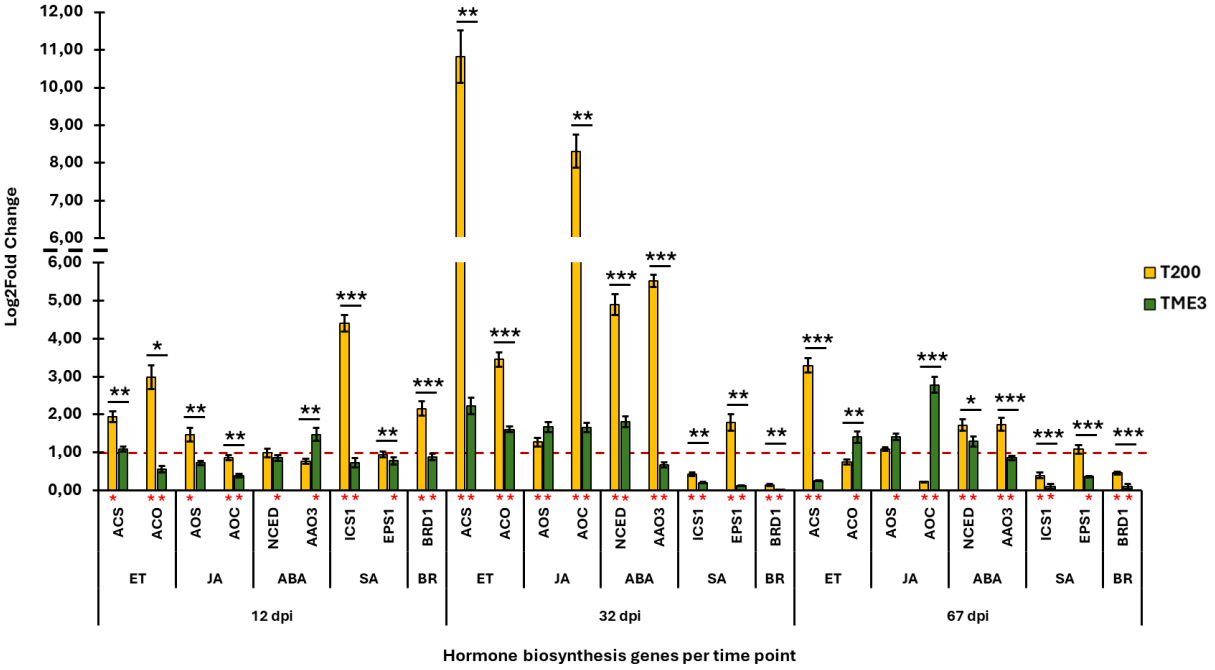


Figure 24: Differential expression of hormone biosynthesis genes in cassava during cassava mosaic disease

Both T200 and TME3 had significant up- and downregulation of hormone biosynthesis genes per genotype per time point. T200 had more biosynthesis genes that were expressed significantly higher than in TME3. Student's t-tests were performed for statistical analysis and significance was denoted with asterisks: * *p-value* < 0.05, ** *p-value* < 0.01, and *** *p-value* < 0.001 for comparison between genotypes (T200 and TME3); * p value < 0.05 for comparison between mock and infected treatment within genotypes. Error bars represent standard deviation of mean (n=3)

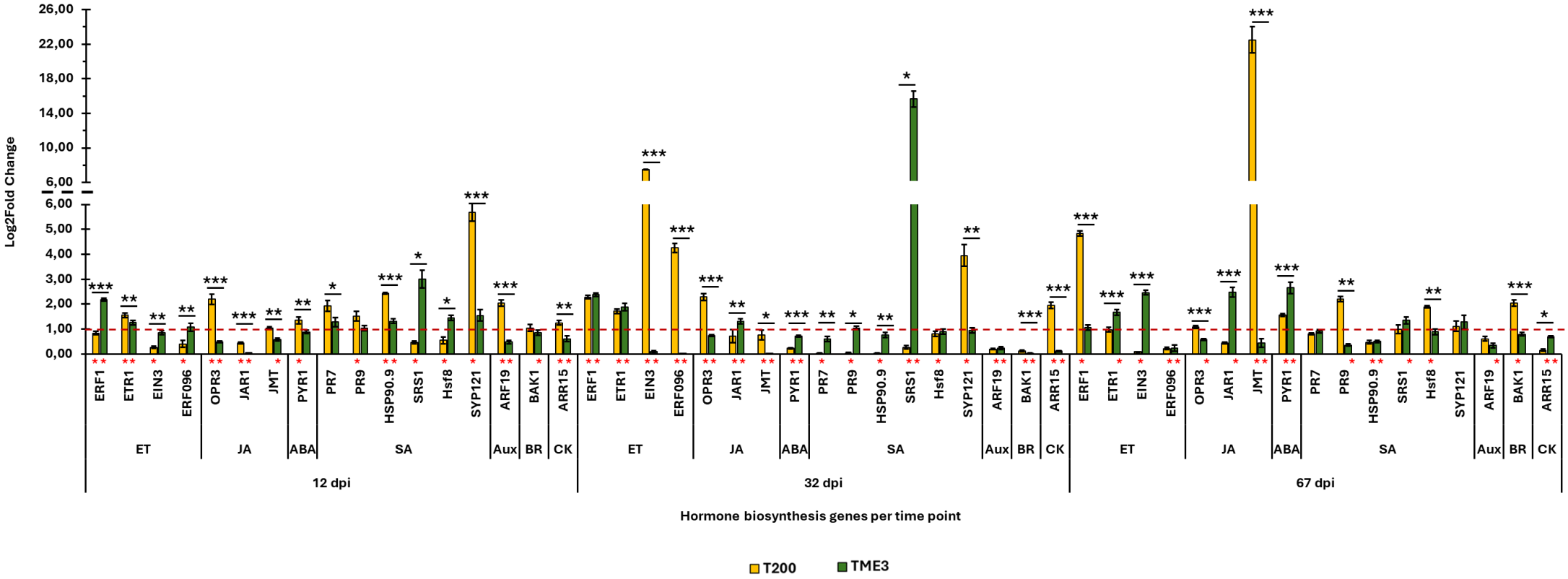


Figure 25: Differential expression of hormone response genes in cassava during cassava mosaic disease

For hormone response genes, both T200 and TME3 had significant up- and downregulation of hormone biosynthesis genes per genotype per time point. T200 had more genes that were expressed significantly higher than in TME3. However, the response of TME3 was more attenuated and well regulated, compared to T200. Student's t-tests were performed for statistical analysis and significance was denoted with asterisks: * *p-value* < 0.05, ** *p-value* < 0.01, and *** *p-value* < 0.001 for comparison between genotypes (T200 and TME3); * p value < 0.05 for comparison between mock and infected treatment within genotypes. Error bars represent standard deviation of mean (n=3)

4.5. Hormone quantification at 12- and 32-dpi in SACMV-infected T200 and TME3

4.5.1. Quantification of hormone production in T200 and TME3 at 12- and 32-dpi during SACMV-infection

The production ABA, ACC, JA, and SA in both mock-infected and SACMV-infected T200 and TME3 was assessed, focusing the early stage (12 dpi) and systemic infection stage (32 dpi) of CMD.

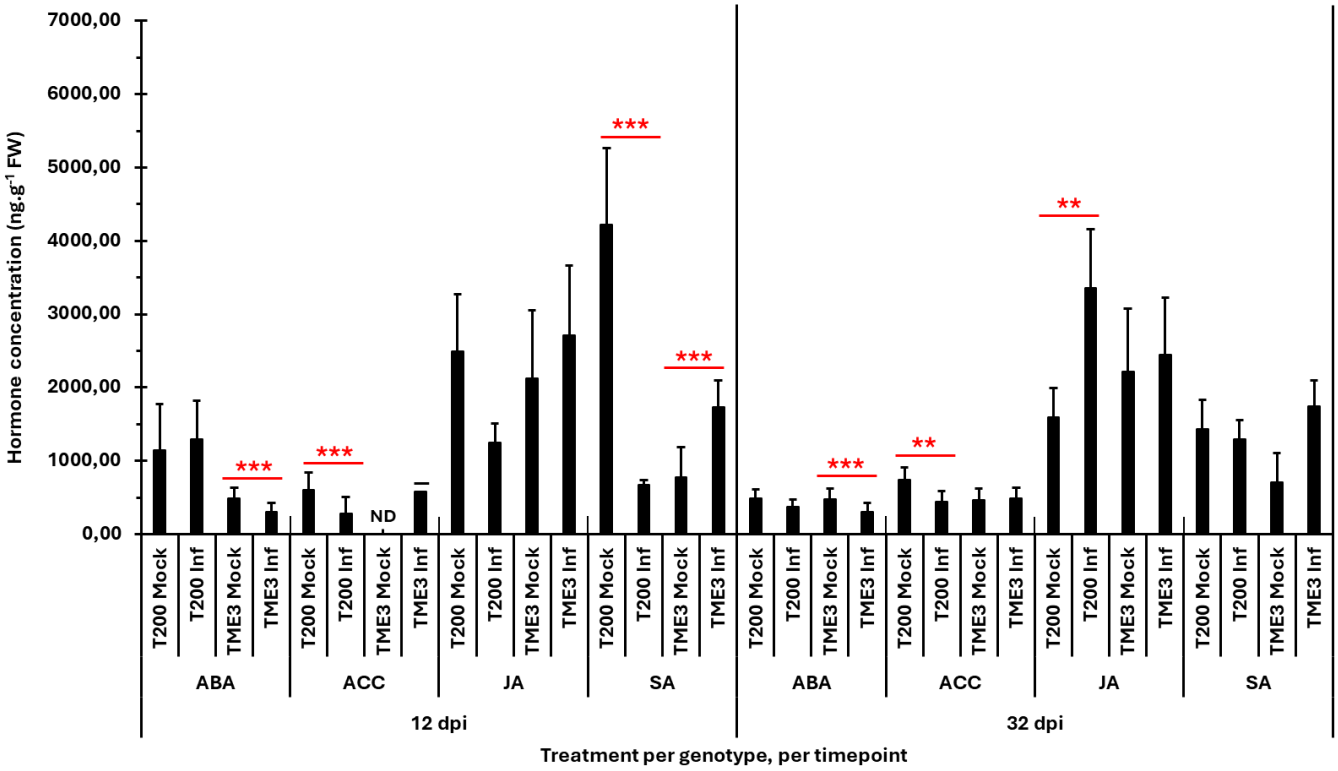


Figure 26: Perturbations in hormone biosynthesis in *South African cassava mosaic virus*-infected T200 and TME3

At 12 dpi, Infected TME3 had a significant decrease in ABA but a significant increase in SA while infected T200 had a significant decrease in ACC and SA. At 32 dpi, infected TME3 had a significant decrease in ABA while infected T200 had a significant decrease in ACC but increase in JA. ACC was not detected in TME3 mock at 12 dpi, which may warrant a repetition of the experiment. For statistical analysis, one-way ANOVA was used and a *p-value* < 0.05 was considered significant. Significance was denoted with asterisks: * *p-value* < 0.05, ** *p-value* < 0.01, and *** *p-value* < 0.001 for comparison between the mock and infected treatment within the genotype. Error bars represent standard deviation of mean (n=3)

4.5.2. Comparison of hormone production in SACMV-infected T200 and SACMV-infected TME3 at 12- and 32-dpi

The production ABA, ACC, JA, and SA was compared between SACMV-infected T200 and SACMV-infected TME3, assessing 12 dpi and 32 dpi.

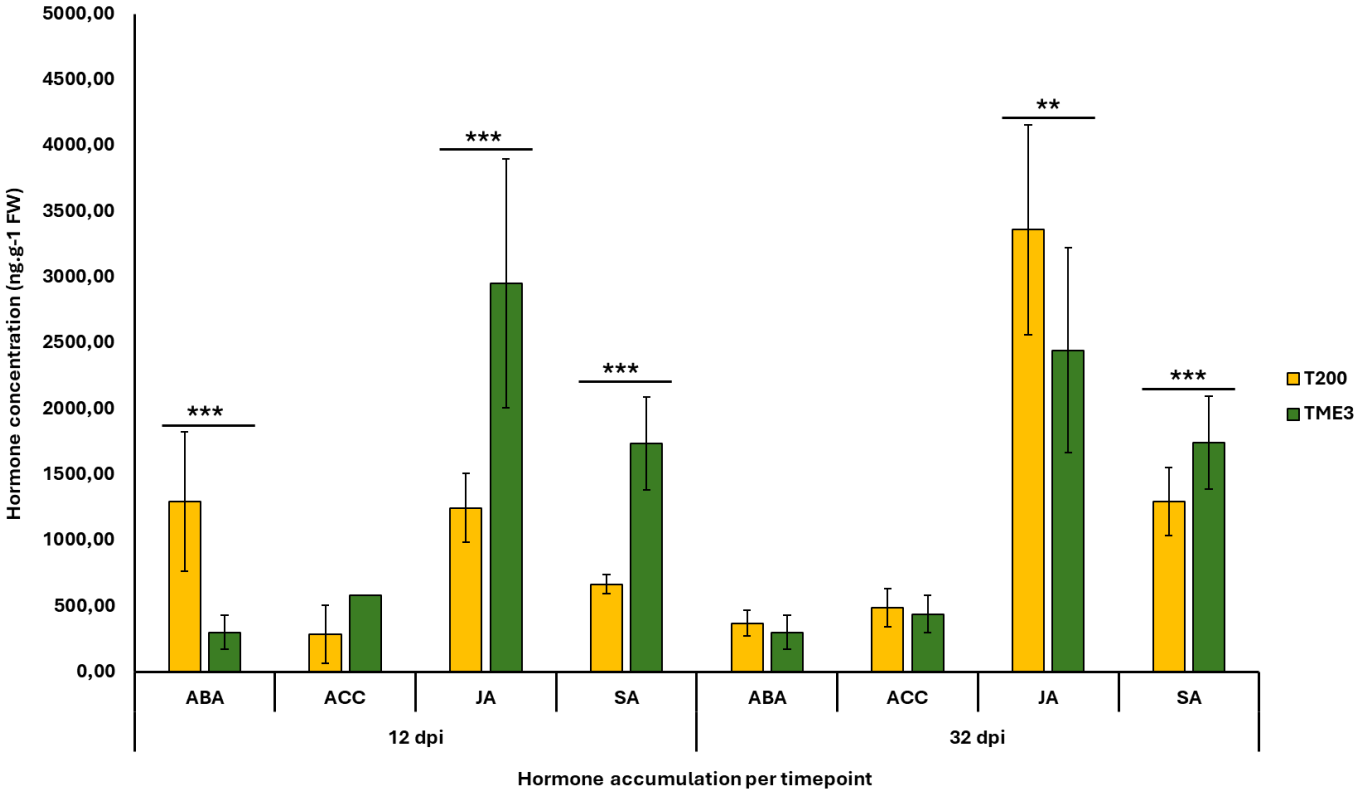


Figure 27: Hormone production influences the response of cassava to *South African cassava mosaic virus* infection

At 12 dpi, T200 showed a significant accumulation of ABA while TME3 showed significant accumulation of both JA and SA. At 32 dpi, T200 then showed a significant accumulation of JA while SA levels in TME3 were still similar to 12 dpi levels and were still significantly accumulated, relative to T200. For statistical analysis, one-way ANOVA was used and a *p-value* < 0.05 was considered significant. Significance was denoted with asterisks: * *p-value* < 0.05, ** *p-value* < 0.01, and *** *p-value* < 0.001 for comparison between SACMV-infected T200 and SACMV-infected TME3. Error bars represent standard deviation of mean (n=3)

Chapter 5: Discussion

Cassava, despite its tolerance for moderate drought conditions, as well as nutrient-deficient soil quality (Anikwe & Ikenganyia, 2018; Kawaye & Hutchinson, 2021), is susceptible to infection by CMGs. These viruses have, in the past, caused several CMD outbreaks in cassava producing regions across Africa and southeast Asia, affecting tuber yields and cassava production (Combala *et al*., 2024; Malichan *et al*., 2023). *South African cassava mosaic virus* is a bipartite species of CMGs that is one of the causative agents of CMD in South Africa, which was first noted in fields in Mpumalanga and Swaziland in the 1980s (Berrie *et al*., 1998). As a bipartite begomovirus, the genome of the SACMV consists of two components, which encode for multifunctional genes that are involved in viral replication, suppression of host defence responses, as well as viral transmission (Briddon *et al.*, 2004; Rey & Vanderschuren, 2017). Thus, this study sought to assess the development of CMD in SACMV-infected CMD-susceptible T200 and CMD-tolerant TME3, determine viral load at key stages of CMD development, and relate disease progression and viral load to the expression of SACMV genes. Furthermore, phytohormone production was assessed and related to the expression of hormone biosynthesis and response genes.

5.1. *South African cassava mosaic virus* titre influences CMD development in cassava and is associated with symptom severity and recovery

Initially, both T200 and TME3 showed no observable symptoms in the early stage of infection, but symptom severity progressed as CMD developed. By 32 dpi, both genotypes showed leaf curling, leaf deformation, reduction in leaf size, as well as mosaic patterning (**Figure 20**). However, TME3 managed to recover by 67 dpi, as seen by the reduction and/or absence of symptoms in the young leaves, whereas T200 remained severely symptomatic (**Figure 20**). Viral load quantification revealed that at 32 dpi, both T200 and TME3 had high SACMV titre (**Figure 22**). However, relative to TME3, viral load in T200 was two-fold higher and this was significant (**Figure 22**). By 67 dpi, TME3 had recovered from CMD, as seen by the lack of notable symptoms in its younger leaves, while T200 still remained severely symptomatic (**Figure 20**). Comparison of viral load at 67 dpi revealed that T200 had a three-

fold higher number of viral copies, relative to TME3 (**Figure 22**). Similar observations had been previously made by Allie *et al.* (2014), in that T200 had ten-fold higher levels of SACMV DNA compared to TME3 at both 32 dpi and 67 dpi (Allie *et al*., 2014). However, unlike Allie *et al.* (2014), T200 and TME3 did not have increases in their respective viral loads from 32 dpi to 67 dpi (**Figure 22**). Despite having decreases in their viral loads relative to 32 dpi, T200 was still severely symptomatic compared to TME3, which had recovered.

In the instance of T200, a reduction of viral load but lack of cessation of symptoms may suggest that there was a substantial increase in viral load to facilitate high levels of viral replication and transmission at 12 dpi. However, once systemic infection had been achieved, viral load decreased but not below the threshold required for optimal infection of the host (Gutiérrez *et al*., 2010). Through this alteration of the multiplicity of infection at different stages of CMD in T200, SACMV may be modulating its virulence to ensure that it can dynamically respond to changes in its host (Gutiérrez *et al*., 2010). Furthermore, as susceptibility corresponds to high virus fitness that results in systemic infection and severe symptomology (Paudel & Sanfaçon, 2018), the susceptibility of T200 to SACMV infection may ensure that CMD persists, despite the abovementioned reduction in viral load between 32- and 67-dpi.

In the instance of TME3, viral load suppression could explain the CMD recovery (Allie *et al*., 2014). Recovery from CMD was first observed in ACMV-infected cassava in 1994, wherein some infected genotypes recovered from CMD symptoms but still had detectable levels of ACMV viral particles, suggesting that the virus had become latent (Njock *et al.*, 1996). Disease recovery, through the observable reduction of severe symptoms and reduction in viral load, has been observed in several other plant species infected with GMVs. *Cucurbit leaf crumple virus* (CuLCvV), a bipartite begomovirus, infects cucurbits such as cantaloupe (*Cucumis melo*) and watermelon (*Citrullus lanatus*) (Hagen *et al.*, 2008). Following the infection of cantaloupe and watermelon, severe symptoms developed during systemic infection stage at 10 dpi (Hagen *et al.*, 2008). However, recovery was observed in newer leaves at 20 dpi, the late infection stage (Hagen *et al.*, 2008). Notably, this recovery

coincided with a significant reduction in CuLCvV viral load, indicating that disease correlated recovery with viral load (Hagen *et al.*, 2008). A similar phenomenon was observed with *Pepper golden mosaic virus* (PepGMV), a bipartite begomovirus that infects pepper plants (Carrillo-Tripp *et al.*, 2007). Despite the cessation of severe symptoms ceased in newer leaves at 12 to 15 dpi, indicating that recovery had been achieved, PepGMV DNA was still detectable at 35 dpi, indicating that the virus can escape host defence mechanisms and maintain a small population of viral particles can establish a symptomless, phenotypically undetectable infection (Carrillo-Tripp *et al.*, 2007).

The reduction in CMD symptoms is an indicator of cassava recovery from CMD (Chaowongdee *et al*., 2023). Resistance to CMD is regulated by either the CMD1 locus, which is polygenic due to *CMD1* being recessive, or by the CM2 locus, wherein *CMD2* is dominant (Akano *et al*., 2002). While TME3 possesses the CM2 locus (Akano *et al*., 2002), which enables cultivars of cassava to have resistance to cassava mosaic viruses, TME3 still develops CMD due to SACMV infection (Chaowongdee *et al*., 2023). As such, TME3 is tolerant to CMD, which is characterised by the maintenance of a significant virus titre while symptom severity is minimal or absent, and plant growth is slightly affected (Paudel & Sanfaçon, 2018).

5.2. Differential expression of viral pathogenicity determinants can be associated with CMD progression and symptom development

5.2.1. Expression of pathogenicity determinants involved in viral replication and cell cycle progression

The replication initiator protein (Rep; AC1) is the sole protein responsible for the initiation of geminivirus replication (Maio *et al*., 2020). To achieve this, initiates the reprogramming of terminally differentiated cells to promote the activation of DNA replication machinery and cell cycle progression (Kong & Hanley-Bowdoin, 2002; Bagewadi *et al.*, 2004). Cell cycle progression in plant cells is negatively regulated by the Retinoblastoma-related protein (RBR), which represses the transcription factor E2F and its positive regulation of the mitotic

cycle in plants (Kong & Hanley-Bowdoin, 2002; Bagewadi *et al.*, 2004). Additionally, the negative regulation of the mitotic cycle by RBR enables for cell differentiation to occur, resulting in terminal differentiation of potential hosts (Kong *et al*., 2000). Rep interacts with and inhibits RBR, resulting in the expression of E2F-regulated cell cycle promoting genes (Bagewadi *et al*., 2004). Furthermore, the interaction between RBR and the Rep proteins of geminiviruses has been shown to be conserved (Rodríguez-Negrete *et al*., 2013). In addition to cell cycle progression, Rep induces the transcription of and mediates the activation of Proliferating Cell Nuclear Antigen (PNCA), a processivity factor for the GMV-preferred DNA polymerase, DNA polymerase δ, which mediates DNA replication or DNA repair (Kong *et al*., 2000; Wu *et al*., 2021). As it is capable of oligomerisation, Rep forms complexes with PCNA and its interacting partner Replication Factor C (RFC) for form a replisome complex that mediates viral replication (Bagewadi *et al*., 2004; Jin *et al*., 2008; Wu *et al*., 2021).

Higher expression of *Rep* in T200 at 12-, 32-, and 67-dpi (**Figure 23**) may have potentiated rolling circle replication and contributed to the accumulation of viral ssDNA genome copies, resulting in the significantly higher viral load detected in T200 at 32- and 67-dpi, compared to TME3 (**Figure 22**). Cassava expressing *AC1*, isolated from ACMV-Kenya, as a transgene showed reduced accumulation of ACMV, EACMV, and SLCMV DNA during separate infection trials (Chellappan *et al.*, 2004). The presence of the transgene led to the generation of siRNAs that facilitated PTGS during virus challenge, specifically targeting the homologous (ACMV) and heterologous (EACMV and SLCMV) *AC1* gene, which encodes for GMV Rep (Chellappan *et al.*, 2004). Consequently, the loss of Rep activity led to loss of viral replication and the reduction of viral load, resulting in recovery (Chellappan *et al.*, 2004). As such, in the context of both SACMV-infected TME3, significantly lower *AC1* expression was key in ensuring lower SACMV titre, resulting in a decrease in SACMV replication and systemic spread, facilitating recovery and tolerance.

The transcription activator protein (TrAP; AC2) promotes cytokinin (CK) responsive genes to positively regulate cytokinin-driven cell proliferation and prevents the catabolism of activated cytokinins (Baliji *et al.*, 2010; Liu *et al.*, 2014). As geminiviruses reprogramme

terminally differentiated cells to initiate replication, TrAP represses the transcription of and/or represses the protein activity of Adenosine Kinase (ADK), an enzyme involved in catabolism and turnover of active CKs (Baliji *et al.*, 2010). TrAP also downregulates the expression of chromatin remodelling protein, *PICKLE*, which hinders accessibility to CK-responsive genes, promoting CK-driven cell proliferation and enhancing susceptibility to GMV infection. Across 12-, 32-, and 67-dpi, *TrAP* had significantly higher expression in T200 compared to TME3, and this correlates with the significantly higher viral load in T200 at 32- and 67-dpi (**Figure 22**). TrAP promotes the expression of *AV1* (core coat protein) and *BV1* (nuclear shuttle protein), which are late genes (Baliji *et al.*, 2010; Liu *et al.*, 2014). Due to its inability to binds dsDNA, TrAP does not function as a canonical TF (Lacatus & Sunter, 2009) and recruits specific host TFs to promote the expression of these two genes (Liu *et al*., 2014). Across 12- and 67-dpi in SACMV-infected T200, significantly higher expression of *TrAP* coincided with significantly higher expression of *AV1* and *BV1* (**Figure 23**), facilitating SACMV DNA encapsulation and nuclear export, enabling for systemic transmission of viral particles and the persistence of CMD.

The replication enhancer protein (REn; AC3) acts as an accessory protein to Rep, interacting with and the enhancing protein-protein interactions between Rep and host proteins such PCNA and RFC to form large multimeric complexes that enhance viral DNA replication and mediate the simultaneous occurrence of activities that favour viral survival (Sunter *et al.*, 1990; Settlage *et al.*, 2001; Castillo *et al.*, 2003; Settlage *et al.*, 2005). At 32- and 67-dpi, T200 has significantly higher expression of REn compared to TME3, with no significant difference at 12 dpi. As viral load was two and three-fold higher in T200 at 32-dpi and 67-dpi, respectively, compared to TME3 (**Figure 22**), REn could be promoting interactions between Rep, along with the host factors involved in geminivirus replication, enhancing the accumulation of viral DNA.

The viral suppressor of RNA silencing (VSR; AC4/C4) promotes cell cycle progression (Lai *et al*., 2009; Mei *et al*., 2018). By promoting the expression of *RKP*, AC4 promotes the degradation of cell cycle inhibitors. As a RING finger protein, RKP mediates the degradation

of proteins via the 26S proteasomal degradation pathway (Lai *et al.*, 2009; Chen & Hellmann, 2013). Furthermore, AC4 interferes with brassinosteroid (BR) signalling by redirecting Shaggy-like kinase (SKn), an ortholog of the BR signalling regulator Brassinosteroid Insensitive 2 (BIN2), from the nucleus to the plasma membrane. The loss of regulation of BR-responsive gene expression leads to developmental abnormalities (Mei *et al*., 2018). The expression of *AC4* was significantly higher in TME3 at 32 dpi compared to T200. However, by 67 dpi, *AC4* expression was significantly higher in T200. The significant accumulation of *AC4* at 67 dpi in T200 may be a contributing factor to the unaltered severe symptoms such as leaf curling and leaf deformation, resulting due to dysregulated cell proliferation and growth (**Figure 20**). As study by Walsh *et al.* (2019) found that the expression of an AC1/AC4-targeting hairpin-RNA (precursor for siRNA) in cassava 60444, a CMD-susceptible genotype, led to decreased symptom severity and significantly reduced SACMV load at 67 dpi (Walsh *et al.*, 2019). This led to cassava 60444 recovery of CMD, akin to the CMD-tolerant landrace TME3 (Walsh *et al.*, 2019). This shows that the reduction the reduction of *AC4* expression in SACMV-infected TME3 was pivotal in the establishment of the recovery phenotype, due to the maintenance of the regulation of cell proliferation and growth in the younger leaves observed at 67 dpi.

The core coat protein (CP; AV1) regulates the accumulation of viral ssDNA copies by promoting and then later facilitating the repression of viral replication, and complexes with the synthesised viral ssDNA to encapsulate it (Unseld *et al.*, 2004; Malik *et al.*, 2005). The expression of *AV1* was significantly upregulated in T200 and TME3 at 12- and 32-dpi, with there being no significant difference at 67 dpi. The upregulation of *AV1* may have contributed to enhanced viral replication that resulted in the accumulation of high SACMV copies at 32- and 67-dpi in T200 (**Figure 22**). However, there was no significant difference in *AV1* expression at 67 dpi (**Figure 23**), but T200 was still symptomatic. Interestingly, In the youngest apical leaves of PepGMV-infected pepper plants that were isolated following disease recovery, there was an unusually high expression of PepGMV *Rep*, despite a reduction in viral load in the recovered plants (Carrillo-Tripp *et al.*, 2007). This suggested that PepGMV maintains a small viral population in young, rapidly growing tissue, allowing for systemic dissemination of the virus as the plant grows, despite recovery having taken

place (Carrillo-Tripp *et al.*, 2007). As the apex of the plant is concentrated with replicating cells as the plant grows, this enables for detectable levels of viral DNA and RNA to be detected in young leaves, despite the virus not inducing host defence responses that would manifest as disease symptoms (Carrillo-Tripp *et al.*, 2007). This would explain why TME3, despite recovering and not showing CMD symptoms, had both SACMV DNA (**Figure 22**) as well as a high expression of *AV1* (*Rep*) relative to the other SACMV pathogenicity determinants (**Figure 23**).

5.2.2. Inhibition of hormone signalling and dysregulation of global metabolism

Geminivirus pathogenicity determinants target hormone signalling and the regulation of global metabolism to enhance susceptibility to infection, wherein the mean latent period and the viral load required to initiate a successful infection are reduced (Sunter *et al.*, 2001).

The precoat protein (AV2) enhances susceptibility to geminivirus infection by inhibiting antioxidant production, and simultaneously suppressing salicylic acid (SA) production and accumulation (Roshan *et al*., 2018). The production of ROS contributes to symptom development, due to oxidative stress (Roshan *et al*., 2018). However, ROS production triggers the biosynthesis of SA, which is antiviral (Ghosh & Chakraborty, 2021; Lukan & Coll, 2022). As such, AV2 also suppresses the expression of *EDS1*, which potentiates SA biosynthesis and creates a positive feedback loop (Roshan *et al*., 2018). The expression of *AV2* was significantly higher in T200 across 12-, 32-, and 67-dpi, compared to TME3, with T200 also having higher viral loads and severe symptoms at 32-dpi and 67-dpi. This suggested that AV2 could have contributed to the impairment of SA-regulated antiviral immunity in T200.

The AC4 VSR interferes with the hormone signalling pathways of gibberellic acid (GA) and brassinosteroids (BRs) (Li *et al*., 2022; Mei *et al*., 2018). Both BR and GA can potentiate SA accumulation and signalling through direct and indirect mechanisms. BR accumulation

inhibits jasmonic acid (JA) signalling, enhancing disease susceptibility due to the defence-regulating role of JA (He *et al*., 2017). However, BRs can also promote SA responses by both inhibiting BIN2, which inhibits SA-responsive signalling components by phosphorylating them (Kim *et al*., 2022), or by suppressing JA signalling (He *et al*., 2017). Due to the antagonism between JA and SA, this can promote SA antiviral immunity (Yan & Xie, 2015). In the case of GA, GA signalling can promote the accumulation of SA (Li *et al*., 2022). AC4 interferes with BR signalling by translocating SKn from the nucleus to the plasma membrane, impeding BR signalling (Mei *et al*., 2018). Additionally, AC4 also inhibits GA signalling by preventing the degradation of GA Insensitive (GAI), a signalling inhibitor, through the 26S proteasome-mediated degradation (Li *et al*., 2022). GA signalling can activate the expression of *ICS1* and *NPR1*, involved in biosynthesis and response, respectively (Li *et al*., 2022). Considering that the expression of *AC4* was significantly higher in TME3 at 32 dpi compared to T200 (**Figure 23**), this may indicate attempts by SACMV through AC4 to dysregulate GA and BR signalling in TME3 to impede SA accumulation and enhance susceptibility. At 67 dpi, *AC4* expression was significantly higher in T200, and this correlates with symptoms that have not ceased (**Figure 20**), alongside a significantly higher viral load in T200 (**Figure 22**).

TrAP interferes with the regulation of global metabolism and perturbs JA signalling (Hao *et al*., 2003; Lozano-Durán *et al*., 2011). Sucrose non-fermenting-related kinase 1 (SnRK1) is a regulator of global metabolism in plants, regulating metabolically-taxing defence pathways while limiting the availability of amino acids and nucleotides, stifling viral infection (Hao *et al*., 2003). TrAP proteins interact with and inhibit the kinase activity of SnRK1, leading to enhanced susceptibility due to the dysregulation of global metabolism (Hao *et al*., 2003). TrAP also impedes JA signalling by dysregulating the activity of the SCF E3 ligase complexes that mediate JA signalling through the degradation of the signalling repressors, JA-ZIM-domain (JAZ) proteins (Lozano-Durán *et al*., 2011). Inhibition of degradation of JAZ proteins leads to loss of jasmonate signalling. (Lozano-Durán *et al*., 2011). The expression of *TrAP* in T200 was significantly higher at 12-, 32-, and 67-dpi, compared to TME3 (**Figure 23**). The dysregulation of hormone signalling and global metabolism may have enhanced the susceptibility of T200 to SACMV.

5.2.3. Virus intercellular movement and systemic spread

The precoat protein (AV2) serves a redundant role in intercellular transport (Rothenstein *et al*., 2007). Due to the relatedness of monopartite and bipartite geminiviruses, AV2 has retained this function as a relic of the evolution of bipartite begomoviruses from monopartite begomoviruses (Rothenstein *et al*., 2007). In T200, there was significantly higher expression of *AV2* at 12-, 32-, and 67-dpi, relative to TME3 (**Figure 23**). Considering the significantly higher viral load in T200 relative to TME3 (**Figure 22**) and T200 being severely symptomatic at 67 dpi while TME3 had recovered (**Figure 20**), AV2 could have enhanced susceptibility in T200 by potentiating virus spread.

Regarding the movement proteins, the movement protein (MP; BC1) redirects nuclear-exported viral ssDNA-CP protein complexes to the cell periphery and modifies the size exclusion limit of the plasmodesmata (PD) to facilitate virus intercellular movement (Noueiry *et al.*, 1994; Sanderfoot & Lazarowitz, 1995). In T200, the expression of *BC1* was significantly higher at 12 dpi and 67 dpi, relative to TME3, whereas TME3 showed a significantly higher expression at 32 dpi (**Figure 23**). Despite the higher expression of *BC1* in TME3 at 32 dpi, viral load was still significantly lower compared to T200 (**Figure 23**), suggesting that the upregulation was to achieve a different outcome, other than enhancing virus intercellular transport. Conversely, the nuclear shuttle protein (NSP; BV1) promotes the nuclear export of viral ssDNA-CP complexes (Noueiry *et al.*, 1994; Carvalho *et al.*, 2006), and it potentiates GMV infection by interfering with PRR-mediated antiviral defences, enhancing susceptibility (Florentino *et al*., 2006; Fontes *et al*., 2004). NSP specifically interacts with NSP-Interacting Kinases (NIKs), inhibiting their kinase activity and disrupting signalling cascades that regulate PAMP-triggered immunity (Fontes *et al*., 2004). The inhibition of NIK activity or repression of *NIK* genes results in enhanced susceptibility to geminivirus infection (Florentino *et al*., 2006). At 32 dpi, *BV1* expression was significantly higher in TME3, as compared to T200. Given the role of BV1 is suppressing NIK-mediated immunity (Fontes *et al*., 2004) and the role of BC1 in the intracellular transport of BV1 to the plasma membrane (Sanderfoot & Lazarowitz, 1995), BC1-BV1 may be targeting membrane-bound NIKs to suppress their signalling and impede host defence.

5.2.4. Suppression of DNA methylation and RNA silencing

Due to the efficiency of DNA methylation and RNA silencing in antiviral defence, the pathogenicity determinants of viruses have evolved to target and suppress these mechanisms (Buchmann *et al*., 2009). In the case of DNA and histone methylation, TrAP simultaneously promotes SAM Decarboxylase (SAMDC1) stabilisation (Zhang *et al*., 2011), targets and inhibits *S*-adenosyl homocysteine hydrolase (SAHH) (Buchmann *et al*., 2009), and inhibits histone methyltransferase (SUVH4/KYP). Firstly, SAMDC1 catabolises *S*-adenosylmethionine (SAM), the methyl group donor for DNA methylation, into the decarboxylated SAM, repressing methylation (Zhang *et al*., 2011). Conversely, SAHH generates SAM, allowing for *de novo* DNA methylation or the maintenance of methylation (Buchmann *et al*., 2009). Lastly, SUVH4/KYP is a histone methyltransferase that transcriptionally represses viral gene expression through methylation of the viral dsDNA-associated histone proteins (Castillo-González *et al*., 2015). In T200, the expression of *TrAP* was significantly higher at 12-, 32-, and 67-dpi, relative to TME3 (**Figure 23**). Additionally, viral load was significantly higher in T200 at 32- and 67-dpi (**Figure 22**). By circumventing the methylation and transcriptional repression of its viral minichromone, SACMV overcomes DNA methylation in T200, resulting in unperturbed viral replication and the maintenance of systemic infection.

In studies assessing the role of DNA methylation in GMV infections, CuLCvV DNA isolated from recovered CuLCvV-infected watermelon plants showed a high degree of methylation compared to unrecovered plants, indicating that recovery is mediated by transcriptional gene silencing (Hagen *et al.*, 2008). Additionally, the recovery of pepper plants infected with PepGMV has been shown to be due to TGS mediated by 24 nucleotide (nt) virus-derived siRNAs that were homologous genome viral intergenic regions (Rodríguez-Negrete *et al.*, 2009). A study by Rogans *et al.* (2016) showed that at 67 dpi, SACMV-infected TME3 had significantly higher accumulation of 24 nt siRNAs compared to SACMV-infected T200, suggesting TGS was targeted towards SACMV during recovery and tolerance. Additionally, a study by Seutane (2022) found that SACMV pathogenicity determinants target cassava methylation pathways through both gene repression and the inhibition of enzyme activity of proteins that are involved in DNA methylation. SACMV infection in T200 and TME3 resulted

in the downregulation of genes involved *de novo* methylation, resulting in genome hypomethylation, a key factor in enhancing susceptibility. Interestingly, at 67 dpi, TME3 showed upregulation of *ARGONAUTE 5* (*AGO5*), a protein involved in RNA-directed DNA methylation (RdDM) that leads to TGS. Thus, the recovery of TME3 is due to a significant reduction in viral load, potentially driven by RdDM-mediated TGS, resulting in tolerance of SACMV and the cessation of severe symptoms.

In the case of RNA silencing , TrAP targets adenosine kinase (ADK), which indirectly regulates the amplification and accumulation of short interfering RNAs (siRNAs) (Wang *et al*., 2005). SiRNAs are homologous to the genes that they target, resulting in the degradation of the targeted RNA (Wang *et al*., 2005). Moreover, siRNAs facilitate RdDM by targeting the DNA from which the siRNA was derived (Buchmann *et al*., 2009), resulting in *de novo* DNA methylation (Trinks *et al*., 2005). The expression of *TrAP* was significantly higher in T200 at 12-, 32-, and 67-dpi, compared to TME3 (**Figure 23**). The potential suppression of RNA silencing, coupled with the loss of DNA methylation, prevents recovery and enables the accumulation of both viral copies and viral transcripts.

In pepper plants that showed recovery to PepGMV infection, Rodríguez-Negrete *et al.* (2009) found that PTGS was mediated by 21 to 22 nt virus-derived siRNAs that were homologous to *Rep*, *TrAP*, *REn*, *MP*, and *NSP* (Rodríguez-Negrete *et al.*, 2009). Additionally, a study by Rogans *et al.* (2016) profiled the siRNAs that accumulate during SACMV infection in T200 and TME3. At 12 dpi, SACMV-infected TME3 had a significantly higher accumulation of 21 nt siRNAs while T200 had a significantly higher accumulation of 24 nt siRNAs, suggesting that while TME3 has an early PTGS response, T200 attempts TGS (Rogans *et al.*, 2016). Interestingly, at 67 dpi, SACMV-infected T200 had a higher number of virus-derived siRNAs, indicating that there was a higher viral load, which correlated to the persistently severe CMD symptoms. This also suggested that in T200, there is a failure in gene silencing mechanisms suppressing viral replication and transcription, resulting in the susceptibility phenotype associated with T200.

The precoat protein (AV2) also interferes with RNA silencing by repressing the expression of RNA-dependent RNA polymerase 1 (*RdRP1*) (Basu *et al*., 2018). By interfering in the accumulation of virus-derived siRNAs, AV2 prevents recovery from geminivirus infection (Basu *et al*., 2018). *AV2* expression was also significantly higher in T200 at 12-, 32-, and 67-dpi, compared to TME3, suggesting that it may be repressing the expression of *RdRP1*, given the lack of recovery and continuation of severe symptoms in T200 at 67 dpi (**Figure 19**). However, considering that SACMV-infected T200 accumulated more virus-derived siRNAs than SACMV-infected TME3 at 67 dpi (Rogans *et al*., 2016), this suggests that both PTGS and TGS in TME3 are more efficient in RNA silencing and DNA methylation, respectively.

5.3. Differential expression of hormone associated genes and the production of phytohormones highlights the contrasting responses of T200 and TME3 against SACMV

5.3.1. Dynamics of gene expression and hormone production during early infection

With regards to hormone biosynthesis genes at 12 dpi, SACMV-infected T200 had significant upregulation, relative to mock, and significantly higher expression, relative to SACMV-infected TME3, of ET (*ACS4*, *ACO10*), JA (*AOS*, *AOC1*), ABA (*NCED*, *AAO3*), SA (*ICS1*) and BR (*BRD1*) (**Figure 24**). Conversely, SACMV-infected TME3 has significantly downregulated *ACO10*, *AOC1*, *NCED*, *ICS1*, *EPS1*, and *BRD1*, with no significant change in *ACS4* and *AOS*. Only *AAO3* was upregulated (**Figure 24**). However, in terms of response at 12 dpi, SACMV-infected TME3 had upregulated and significantly higher expression of *ERF1*, unchanged *EIN3* expression, no downregulation of SA signalling components, and a downregulation of *ARF19* (**Figure 25**). As an EIN3-activated TF, ERF1 promotes the expression of plant defence genes such *b-CHI* and *PDF1.2* (Solano *et al*., 1998).

Despite SACMV-infected T200 expressing the biosynthesis genes of ABA, JA, ET, and SA (**Figure 24**), there was no significant change in the respective hormones, relative to the mock T200 (**Figure 26**). In the case of SACMV-infected TME3 (**Figure 24**), only the ABA gene *AAO3* was upregulated relative to mock TME3, although this had no significance on the level of

hormone, relative to mock TME3 (**Figure 26**). Interestingly, the basal levels of SA and JA in infected TME3 were significantly higher than those in T200 (**Figure 27**). Notably, TME3 has upregulation of *HSP90.0* and unaltered expression of *Hsf8* and *SRS1* (**Figure 25**). In cassava, heat shock factor 8 (Hsf8) is a stress-inducible TF and it activates the expression of *HSP90.0*, with HSP90.0 complexing with SRS1, a SHORT INTERNODES (SHI)-related sequence (SRS) TF, to promote the expression of *PBS3*, an SA biosynthesis gene (Wei *et al*., 2021). This leads to SA accumulation. HSP90.0 also suppresses the accumulation of auxins by mediating their degradation through interactions with a cassava WRKY TF (Wei *et al*., 2021). This may explain the significant downregulation of ARF19 in TME3 at 12 dpi (**Figure 25**), given that ARF19 is an auxin-responsive transcriptional activator of auxin regulated genes (Peres *et al*., 2019). T200 showed upregulation of *ARF19* (**Figure 25**), a promoter of leaf senescence, which can enhance susceptibility to pathogens (Barna, 2022; Huang *et a.l*, 2022). Notably, both T200 and TME3 showed significant downregulation of *JAR1* (**Figure 25**), a positive regulator of JA signalling (Suza & Staswick, 2008), despite not showing a significant alteration in their respective basal levels of JA (**Figure 26**). Interestingly, T200 also showed a significant upregulation and higher expression of *AAR15* (**Figure 25**), a negative regulator of cytokinin signalling (Kiba *et al*., 2003).

Hormone quantification revealed that at 12 dpi, SACMV-infected TME3 had significantly higher levels of JA and SA relative to SACMV-infected T200 (**Figure 27**). In *N. benthamiana* infected with *Plum pox virus* (PPV), cooperation between SA-mediated defence mechanisms such as *PR* gene expression and SA-enhanced RNA silencing, through upregulation of *NtRDR1*, facilitated restriction of PPV and prevented systemic infection (Alamillo *et al*., 2006). Additionally, a study by Sade *et al*., 2014 found that an early response of SA accumulation and *PR* gene expression could promote the establishment of tolerance in TYLCV-infected tomato. Furthermore, in *A. thaliana* infected with *Sri Lankan cassava mosaic virus* (SLCMV), there was a downregulation of *JAR1* but upregulation of SA biosynthesis and response genes (Wang *et al*., 2020), similar to what was observed in SACMV-infected TME3. However, during *Rice stripe virus* (RSV) infection in rice, JA accumulation and the subsequent JA-Ile signalling were shown to enhance RNA silencing by activating *AGO18* transcription, relieving the repression of *AGO1* and thus facilitating AGO1-mediated RNA silencing (Yang *et*

al., 2020). This may suggest that while *JAR1* repression impedes JA-Ile signalling, JA accumulation in SACMV-infected TME3 at 12 dpi may enhance PTGS.

5.3.2. Establishment of systemic acquired resistance during systemic infection

The response genes expressed at 32 dpi highlight key genotype-specific responses to SACMV. While T200 showed upregulation and significantly higher expression of ET-responsive genes (*ERF1*, *ETR1*, *EIN3*, *ERF096*) but downregulation of SA-responsive genes (*PR7*, *PR9, HSP90.0*, and *Hsf8*) (**Figure 25**). Conversely, TME3 showed no significant change in *PR7*, *PR9, HSP90.0*, and *Hsf8*, and had significantly high expression of *SRS1* (**Figure 25**), suggesting that SA plays a key role in responses to SACMV at 32 dpi. The overexpression of both *Hsf8* and *HSP90.9* in cassava has a significant and positive effect on plant disease resistance through the upregulation of SA-responsive PR gene expression, accumulation of SA, and suppression of Auxin accumulation (Wei *et al*., 2021). PR7 proteins function as endoproteases that mediate pathogen cell wall degradation while PR9 proteins function as lignin-forming peroxidases and mediate plant cell wall fortification (Irigoyen *et al*., 2020). The expression of *ETR1* in TME3 at 32 dpi without the ET-responsive TFs *EIN3* and *ERF096* (**Figure 25**) would suggest that TME3 is suppressing ET-responsive gene expression (Mur *et al*., 2013), which is particularly important as in some instances, such as *Tobacco mosaic virus* (TMV) or *Rice dwarf virus* (RDV) in plants, the lack of ET accumulation promotes tolerance to infection and disease (Ghosh & Chakraborty, 2021). The continued expression of *ERF1* in TME3 at 32 dpi could be promoting the accumulation of defence proteins (Solano *et al*., 1998). Furthermore, SACMV-infected TME3 had upregulation and significantly higher expression of *JAR1*, a regulator of JA-regulated defence.

During the systemic infection stage of SACMV infection, T200 and TME3 expressed the hormone biosynthesis genes of ET, JA, and ABA in a similar manner, with TME3 not expressing any SA biosynthesis gene (**Figure 24**). Infected TME3 showed a significant reduction in ABA accumulation, relative to its mock, while infected T200 showed a significant reduction in ACC accumulation, relative to its mock (**Figure 26**). However, infected T200 showed a significant increase in JA accumulation, relative to its mock (**Figure 26**). This

increase enabled for infected T200 to have significantly higher levels of JA, as compared to infected TME3, whereas the basal levels of SA in infected TME3 were still significantly higher than those of infected T200 (**Figure 27**). The antiviral roles served by SA, such as interfering with viral cell-to-cell movement, systemic infection, and viral replication, in addition to regulating SAR and *PR* gene expression while modulating the RNAi pathway, may have been initiated during this stage of CMD in infected TME3 (Doughari, 2015; Zhao & Li, 2021). This was potentially coupled with the reduction in ABA , which modulates *ARGONAUTE 1* (*AGO1*) expression and the RNAi pathway (Zhao & Li, 2021), ensuring that PTGS was maintained by SA during SAR.

The concurrent signalling of *JAR1* and SA-regulated defence factors in TME3 (**Figure 25**) and the significantly higher levels of SA in Infected TME3 relative to infected T200 (**Figure 27**) may suggest that at 32 dpi, TME3 relies of systemic acquired resistance (SAR), with dual JA-SA defence signalling enhancing its efficiency (Zhu *et al*., 2014). Importantly, SA has been shown to induce resistance in TYLCV-susceptible tomato, showing the antiviral role that SA plays during GMV pathogenesis (Li *et al*., 2019). Thus, as both SA and JA were involved in the plant defence response at 32 dpi, the crosstalk between both hormones was important for cassava-SACMV interactions and the establishment of recovery.

5.3.3. Recovery from CMD and tolerance through induced systemic resistance

At the late stage of CMD in T200 and TME3, T200 remained severely symptomatic while TME3 had already recovered from CMD (**Figure 20**), which was coupled with significantly lower viral load in infected TME3 and no significant expression of SACMV genes, relative to infected T200 (**Figure 22**). At 67 dpi, both T200 and TME3 expressed hormone biosynthesis genes in a similar manner as at 32 dpi (**Figure 24**). However, the expression of response genes differed (**Figure 25**). In T200, there was the upregulation and significantly higher expression of *ERF1*, *JMT*, and *BAK1*, whereas TME3 showed upregulation and higher expression of *ETR1*, *EIN3*, *JAR*, and *PYR1* (**Figure 25**). In TME3, the regulation of ET-signalling by *ETR1*, coupled with *EIN3*-mediated regulation of JA signalling (Ma *et al*., 2020; Song *et al*., 2014), the *JAR1*-regulated production of chemical defence, and the regulation of JA-SA

antagonism by *PYR1* all could have facilitated the induction of induced systemic resistance (ISR). In plants, ISR is primarily regulated by JA and ET (Vallad & Goodman, 2004; Zhao & Li, 2021). Interestingly, T200 showed upregulation and significantly higher expression of *JMT* and *ERF1*, which regulate systemic defence signalling and defence protein production (Solano *et al.*, 1998; Cheong & Choi, 2003). However, symptoms remained severe (**Figure 20**), viral load was significantly higher compared to TME3 (**Figure 22**), and the expression of SACMV genes was also significantly higher compared to TME3 (**Figure 23**).

Interestingly, in pepper tissues that had recovered from PepGMV infection, there was differential expression of genes involved in JA-ET mediated defence responses (Góngora-Castillo *et al*., 2012). The *EIN3* TF was downregulated in symptomatic plants , similar to infected T200, while in both recovered and symptomatic plants, there was upregulated *ACO*. Furthermore, in both recovered and symptomatic plants, there was upregulation of JA biosynthesis genes and plant defence genes (*b-Chi)* (Góngora-Castillo *et al*., 2012). Importantly, following recovery, the expression of SA-responsive defence genes such *PR* genes returned to basal levels (Góngora-Castillo *et al*., 2012). The production of JA has been shown to decrease viral DNA titre during geminivirus infection, particularly *Beet curly top virus* (Zhao & Li, 2021). Additionally, ET accumulation and subsequent signalling via ERFs during TYLCV infection in tomato have been identified as the possible avenue through which ET contributes to recovery and tolerance (Ghosh & Chakraborty, 2021). The accumulation of ET in response to viral infection enables ET to act as a systemic signal and to also establish the foundation for ISR, which it regulates alongside JA (Vallad & Goodman, 2004; Pattyn *et al.*, 2021). Lastly, ABA promotes callose deposition at the PD, impeding the intercellular movement of viral particles (Alazem & Lin, 2017). Thus, in recovered TME3, the accumulation of ET, JA, and ABA, alongside *ETR1*, *EIN3*, *JAR1*, and *PYR1* expression enabled for the establishment of ISR, resulting in the maintenance of SACMV tolerance.

Chapter 6: Conclusions

6.1. Key findings of the study

The main aim of this research project was to quantify the phytohormone levels of SA, JA, ABA, and ET in the CMD-susceptible T200 and CMD-tolerant TME3 across the three stages of SACMV infection to determine if these phytohormones contribute to either susceptibility or recovery. The research sought to address if there was a distinction between T200 and TME3 in response to CMD cause by SACMV, if phytohormone where an underlying mechanism by which TME3 recovers from CMD, and if SACMV pathogenicity determinants promote the progression of CMD in T200 and TME3.

This study has shown that the expression of SACMV pathogenicity determinants determines the outcome of CMD progression in either T200 or TME3. At all stages of CMD, T200 mostly had higher expression of the multifunctional pathogenicity determinants and this correlated with dysregulation of cell proliferation and growth (*AC1*, *AC2*, *AC3*, and *AC4*), promotion of viral replication (*AC1*, *AC3*, and *AV1*), promotion of viral systemic transmission (*AC2*, *AV1*, *AV2*, *BC1*, and *BV1*), suppression of hormone biosynthesis (*AC2*, *AC4*, and *AV2*), disruption of global metabolism (*AC2*), disruption of chemical and protein-mediated defences (*AC2*, *BC1*, and *BV1*), and the suppression of PTGS and TGS (*AC2*). The expression of these pathogenicity determinants correlated with viral load, with both being significantly higher in T200 at 32 dpi and 67 dpi, relative to TME3.

Furthermore, this study identified the hormone-response defence pathways and processes that are involved in the recovery of TME3 from CMD and subsequent tolerance. As an early response, TME3 potentially relied on *ERF1*/*EIN3*-driven PTI, SA-responsive *PR*-gene expression, and PTGS of viral transcripts, mediated by ABA and JA. During systemic infection, TME3 had no change in its SA- and ET-driven response but there was the expression of *JAR1*. This suggested that TME3 relied on SAR established via SA-responsive *PR*-gene expression, PTI, PTGS, and JAR1-regulated defence signalling, allowing for recovery from CMD. However, at the late stage of infection, *ETR1*/*EIN3*-driven regulation of ET signalling, *JAR1*-driven

regulation of JA defence signalling, and ABA signalling via PYR1 led to the establishment of ISR, facilitating tolerance.

6.2. Implications of the study

This study assessed the production of four plant hormones (SA, JA, ACC, and ABA) in cassava during CMD in-tandem with assessing the expression of biosynthesis and response genes associated with these hormones, as well as assessing the role of SACMV load and the expression of SACMV pathogenicity determinants. By relating hormone production to the expression of host hormone-related genes, SACMV load, and the expression of SACMV ORFs across the three stages of CMD in T200 and TME3, this study has identified the potential hormone crosstalk that is involved in the recovery of TME3 from CMD and the establishment of tolerance. This hormone crosstalk, which regulates plant protein and chemical defences, TGS and PTGS and the limiting of viral replication and transmission, allows for the establishment of tolerance in TME3 during CMD. This is accomplished through finetuning of host responses to SACMV, preventing the activation of metabolically-taxing defence pathways that may lead to symptom development. Furthermore, the expression of ET biosynthesis genes was identified as a potential enhancer of the susceptibility of T200 to SACMV infection, due to the antagonism between SA and ET, and given how the response of TME3 at 12- and 32-dpi is reliant on SA.

6.3. Limitations

A major limitation was that hormone production was not assessed at 67 dpi in both TME3 and T200 during SACMV infection. However, based on the gene expression studies, it is anticipated that SACMV-infected TME3 will have significantly higher production of JA and ET compared to SACMV-infected T200. As SA-driven defence is not required during ISR, SA levels in SACMV-infected TME3 will be at basal levels.

6.4. Future work

The suggested future work includes hormone quantification at 67 dpi, given that this is the stage in which TME3 becomes tolerant whilst T200 remains severely symptomatic. Secondly, quantification assays for hydrogen peroxide and nitric oxide in SACMV-infected T200 and TME3 could be conducted to assess the redox-state of cassava and how oxidative stress may contribute to susceptibility or signalling that establishes recovery. Reactive oxygen species and nitric oxide species modulate and regulate host stress responses and hormone biosynthesis and contribute to symptom development. Thirdly, hormone production could be assessed from 1 day post infection (dpi) to 7 dpi. The assessment of hormone accumulation at the earliest points of SACMV infection could elucidate the initial mechanisms that enable for SACMV infectivity and the development of CMD in cassava. Lastly, infect T200- and TME3-derived protoplasts with SACMV and assess structural changes in a time course experiment. Geminiviruses are known to initiate their replication in terminally differentiated cells, transcriptionally reprogramming the host to enter the mitotic cycle or endoreplication. The latter leads to endoreduplication, wherein genomic material is replicated without mitotic division, resulting in endoploidy and a substantial increase in cell size. Assessing SACMV-infected protoplasts will help determine if SACMV also triggers endoreduplication in infected cells. In addition to assessing endoploidy during SACMV infection, hormone treatment trials could be undertaken with the infected protoplasts to assess the influence of phytohormone in enhancing or halting endoreduplication in cells during SACMV infection.

References

Akano, A., Dixon, A., Mba, C., Barrera, E., Fregene, M., 2002. Genetic Mapping of a Dominant Gene Conferring Resistance To Cassava Mosaic Disease. *Theoretical and Applied Genetics* 105, 521–525. https://doi.org/10.1007/s00122-002-0891-7

Alamillo, J.M., Saénz, P., García, J.A., 2006. Salicylic Acid-Mediated and RNA-silencing Defense Mechanisms Cooperate in the Restriction of Systemic Spread of *Plum pox virus* in Tobacco. *The Plant Journal* 48, 217–227. https://doi.org/10.1111/j.1365-313X.2006.02861.x

Alazem, M., Lin, N.-S., 2017. Antiviral Roles of Abscisic Acid in Plants. *Frontiers in Plant Science* 8. https://doi.org/10.3389/fpls.2017.01760

Allie, F., Pierce, E.J., Okoniewski, M.J., Rey, C., 2014. Transcriptional Analysis of *South African cassava mosaic virus*-infected Susceptible and Tolerant Landraces of cassava Highlights Differences in resistance, basal defense and Cell Wall Associated Genes During Infection. *BMC Genomics* 15, 1006. https://doi.org/10.1186/1471-2164-15-1006

Amelework, A.B., Bairu, M.W., Maema, O., Venter, S.L., Laing, M., 2021. Adoption and Promotion of Resilient Crops for Climate Risk Mitigation and Import Substitution: A Case Analysis of Cassava for South African Agriculture. *Frontiers in Sustainable Food Systems* 5. https://doi.org/10.3389/fsufs.2021.617783

Anikwe, M.A.N., Ikenganyia, E.E., 2018. Ecophysiology and Production Principles of Cassava (*Manihot* species) in Southeastern Nigeria, in: Waisundara, V. (ed.). *Cassava*. IntechOpen. https://doi.org/10.5772/intechopen.70828

Bagewadi, B., Chen, S., Lal, S.K., Choudhury, N.R., Mukherjee, S.K., 2004. PCNA Interacts with *Indian mung bean yellow mosaic virus* Rep and Downregulates Rep Activity. *Journal of Virology* 78, 11890–11903. https://doi.org/10.1128/jvi.78.21.11890-11903.2004

Baliji, S., Lacatus, G., Sunter, G., 2010. The Interaction between Geminivirus Pathogenicity Proteins and Adenosine Kinase Leads to Increased Expression of Primary Cytokinin Responsive Genes. *Virology* 402, 238–247. https://doi.org/10.1016/j.virol.2010.03.023

Balint-Kurti, P., 2019. The Plant Hypersensitive Response: Concepts, Control And Consequences. *Molecular Plant Pathology* 20, 1163-1178. https://doi.org/10.1111/mpp.12821

Barna, B., 2022. Manipulation of Senescence of Plants to Improve Biotic Stress Resistance. *Life (Basel)* 12, 1496. https://doi.org/10.3390/life12101496

Basu, S., Kumar Kushwaha, N., Kumar Singh, A., Pankaj Sahu, P., Vinoth Kumar, R., Chakraborty, S., 2018. Dynamics of a Geminivirus-Encoded Pre-Coat Protein and Host RNA-Dependent RNA Polymerase 1 In Regulating Symptom Recovery In Tobacco. *Journal of Experimental Botany* 69, 2085–2102. https://doi.org/10.1093/jxb/ery043

Behnam, B., Bohorquez-Chaux, A., Castaneda-Mendez, O.F., Tsuji, H., Ishitani, M., Becerra Lopez-Lavalle, L.A., 2019. An optimized Isolation Protocol Yields High-Quality RNA From Cassava Tissues (*Manihot esculenta* Crantz). *FEBS Open Bio* 9, 814–825. https://doi.org/10.1002/2211-5463.12561

Berrie, L.C., Palmer, K.E., Rybicki, E.P., Rey, M.E.C., 1998. Molecular Characterisation of a Distinct South African Cassava Infecting Geminivirus. *Archives of Virology* 143, 2253–2260. https://doi.org/10.1007/s007050050457

Berrie, L.C., Rybicki, E.P., Rey, M.E.C., 2001. Complete Nucleotide Sequence And Host Range of *South African cassava mosaic virus*: Further Evidence For Recombination Amongst Begomoviruses. *Journal of General Virology* 82, 53–58. https://doi.org/10.1099/0022-1317-82-1-53

Bigeard, J., Colcombet, J., Hirt, H., 2015. Signaling Mechanisms in Pattern-Triggered Immunity (PTI). *Molecular Plant* 8, 521–539. https://doi.org/10.1016/j.molp.2014.12.022

Boher, B., Verdier, V., 1994. Cassava Bacterial Blight in Africa: The State Of Knowledge And Implications For Designing Control Strategies. *African Crop Science Journal* 2, 505–509.

Briddon, R.W., Patil, B.L., Bagewadi, B., Nawaz-ul-Rehman, M.S., Fauquet, C.M., 2010. Distinct Evolutionary Histories of the DNA-A and DNA-B Components of Bipartite Begomoviruses. *BMC Evolutionary Biology* 10, 97. https://doi.org/10.1186/14712148-10-97

Briddon, R.W., Robertson, I., Markham, P.G., Stanley, J., 2004. Occurrence of *South African cassava mosaic virus* (SACMV) in Zimbabwe. *Plant Pathology* 53, 233–233. https://doi.org/10.1111/j.0032-0862.2004.00963.x

Buchmann, R.C., Asad, S., Wolf, J.N., Mohannath, G., Bisaro, D.M., 2009. Geminivirus AL2 and L2 Proteins Suppress Transcriptional Gene Silencing and Cause Genome-Wide Reductions in Cytosine Methylation. *Journal of Virology* 83, 5005–5013. https://doi.org/10.1128/jvi.01771-08

Carrillo-Tripp, J., Lozoya-Gloria, E., Rivera-Bustamante, R.F., 2007. Symptom Remission and Specific Resistance of Pepper Plants After Infection by *Pepper golden mosaic virus*. *Phytopathology* 97, 51–59. https://doi.org/10.1094/PHYTO-97-0051

Carvalho, M.F., Turgeon, R., Lazarowitz, S.G., 2006. The Geminivirus Nuclear Shuttle Protein NSP Inhibits the Activity of AtNSI, a Vascular-Expressed Arabidopsis Acetyltransferase Regulated with the Sink-to-Source Transition. *Plant Physiology* 140, 1317–1330. https://doi.org/10.1104/pp.105.075556

Castillo, A.G., Collinet, D., Deret, S., Kashoggi, A., Bejarano, E.R., 2003. Dual Interaction of Plant PCNA with Geminivirus Replication Accessory Protein (Ren) and Viral Replication Protein (Rep). *Virology* 312, 381–394. https://doi.org/10.1016/S0042-6822(03)00234-4

Castillo-González, C., Liu, X., Huang, C., Zhao, C., Ma, Z., Hu, T., Sun, F., Zhou, Y., Zhou, X., Wang, X.-J., Zhang, X., 2015. Geminivirus-encoded TrAP Suppressor Inhibits the Histone Methyltransferase SUVH4/KYP to Counter Host Defense. *eLife* 4, e06671. https://doi.org/10.7554/eLife.06671

Ceballos, H., de la Cruz, G., 2012. Cassava Taxonomy and Morphology, in: Ospina Patiño, B.; Ceballos, H. (eds.). *Cassava in the Third Millennium: Modern Production, Processing, Use, and Marketing Systems*. Centro Internacional de Agricultura Tropical, Cali, pp. 15–28.

Chaowongdee, S., Malichan, S., Pongpamorn, P., Paemanee, A., Siriwan, W., 2023. Metabolic Profiles of *Sri Lankan cassava mosaic virus*-Infected and Healthy Cassava (*Manihot esculenta* Crantz) Cultivars with Tolerance and Susceptibility Phenotypes. *BMC Plant Biology* 23, 178. https://doi.org/10.1186/s12870-023-04181-3

Chellappan, P., Masona, M.V., Vanitharani, R., Taylor, N.J., Fauquet, C.M., 2004. Broad Spectrum Resistance to ssDNA Viruses Associated with Transgene-Induced Gene

Silencing in Cassava. *Plant Molecular Biology* 56, 601–611. https://doi.org/10.1007/s11103-004-0147-9

Chen, L., Hellmann, H., 2013. Plant E3 Ligases: Flexible Enzymes in a Sessile World. *Molecular Plan*t 6, 1388–1404. https://doi.org/10.1093/mp/sst005

Cheng, M.-C., Liao, P.-M., Kuo, W.-W., Lin, T.-P., 2013. The Arabidopsis ETHYLENE RESPONSE FACTOR1 Regulates Abiotic Stress-Responsive Gene Expression by Binding to Different *cis*-Acting Elements in Response to Different Stress Signals. *Plant Physiology* 162, 1566–1582. https://doi.org/10.1104/pp.113.221911

Cheong, J.-J., Choi, Y.D., 2003. Methyl Jasmonate as a Vital Substance in Plants. *Trends in Genetics* 19, 409–413. https://doi.org/10.1016/S0168-9525(03)00138-0

Chilton, M.-D., Currier, T.C., Farrand, S.K., Bendich, A.J., Gordon, M.P., Nester, E.W., 1974. *Agrobacterium tumefaciens* DNA and PS8 Bacteriophage DNA Not Detected in Crown Gall Tumors. *Proceedings of the National Academy of Sciences* 71, 3672–3676. https://doi.org/10.1073/pnas.71.9.3672

Combala, M., Pita, J.S., Gbonamou, M., Samura, A.E., Amoakon, W.J.-L., Kouakou, B.S.M., Onile-ere, O., Sawadogo, S., Eboulem, G.R., Otron, D.H., Seka, J.S.S., Eni, A., Ndougonna, C., Tiendrébéogo, F., 2024. An Alarming Eastward Front of Cassava Mosaic Disease in Development in West Africa. *Viruses* 16, 1691. https://doi.org/10.3390/v16111691

Dempsey, D.A., Klessig, D.F., 2017. How Does the Multifaceted Plant Hormone Salicylic Acid Combat Disease in Plants and Are Similar Mechanisms Utilized In Humans? *BMC Biology* 15, 1–11. https://doi.org/10.1186/s12915-017-0364-8

Denny, R.C.H., Marquart-Pyatt, S.T., Ligmann-Zielinska, A., Olabisi, L.S., Rivers, L., Du, J., Liverpool-Tasie, L.S.O., 2018. Food Security in Africa: A Cross-Scale, Empirical Investigation Using Structural Equation Modeling. *Environment Systems & Decisions* 38, 6–22. https://doi.org/10.1007/s10669-017-9652-7

Doughari, J., 2015. An Overview of Plant Immunity. *Journal of Plant Pathology and Microbiology* 6. https://doi.org/10.4172/2157-7471.1000322

du Toit, D.C., Ramonyai, M.D., Lubbe, P.A., Ntushelo, V., 2011. Food Security By Directorate Economic Services: Production Economics Unit. Department of Agriculture, Forestry & Fisheries, Pretoria, South Africa.

El-Sharkawy, M.A., Cock, J.H., 1987. C3-C4 Intermediate Photosynthetic Characteristics of Cassava (*Manihot esculenta* Crantz). *Photosynthesis Research* 12, 219–235. https://doi.org/10.1007/BF00055122

Florentino, L.H., Santos, A.A., Fontenelle, M.R., Pinheiro, G.L., Zerbini, F.M., Baracat-Pereira, M.C., Fontes, E.P.B., 2006. A PERK-Like Receptor Kinase Interacts with the Geminivirus Nuclear Shuttle Protein and Potentiates Viral Infection. *Journal of Virology* 80, 6648–6656. https://doi.org/10.1128/JVI.00173-06

Fontes, E.P.B., Santos, A.A., Luz, D.F., Waclawovsky, A.J., Chory, J., 2004. The Geminivirus Nuclear Shuttle Protein is a Virulence Factor that Suppresses Transmembrane Receptor Kinase Activity. *Genes & Development* 18, 2545–2556. https://doi.org/10.1101/gad.1245904

Frederickson Matika, D.E., Loake, G.J., 2014. Redox Regulation in Plant Immune Function. *Antioxidants & Redox Signaling* 21, 1373–1388. https://doi.org/10.1089/ars.2013.5679

Freeborough, W., Gentle, N., Rey, M.E.C., 2021. WRKY Transcription Factors in Cassava Contribute to Regulation of Tolerance and Susceptibility to Cassava Mosaic Disease through Stress Responses. Viruses 13, 1820. https://doi.org/10.3390/v13091820

Garcia-Ruiz, H., 2019. Host Factors Against Plant Viruses. *Molecular Plant Pathology* 20, 1588–1601. https://doi.org/10.1111/mpp.12851

Gautam, J.K., Giri, M.K., Singh, D., Chattopadhyay, S., Nandi, A.K., 2021. MYC2 Influences Salicylic Acid Biosynthesis and Defense Against Bacterial Pathogens in *Arabidopsis thaliana*. *Physiologia Plantarum* 173, 2248–2261. https://doi.org/10.1111/ppl.13575

Ghosh, D., Chakraborty, S., 2021. Molecular Interplay Between Phytohormones and Geminiviruses: A Saga of a Never-Ending Arms Race. *Journal of Experimental Botany* 72, 2903–2917. https://doi.org/10.1093/jxb/erab061

Gilroy, S., Suzuki, N., Miller, G., Choi, W.-G., Toyota, M., Devireddy, A.R., Mittler, R., 2014. A Tidal Wave of Signals: Calcium and ROS at the Forefront of Rapid Systemic Signaling. *Trends in Plant Science* 19, 623–630. https://doi.org/10.1016/j.tplants.2014.06.013

Góngora-Castillo, E., Ibarra-Laclette, E., Trejo-Saavedra, D.L., Rivera-Bustamante, R.F., 2012. Transcriptome Analysis of Symptomatic and Recovered Leaves of Geminivirus-Infected Pepper (*Capsicum annuum*). *Virology Journal* 9, 295. https://doi.org/10.1186/1743-422X-9-295

Gupta, K., Rishishwar, R., Dasgupta, I., 2022. The Interplay of Plant Hormonal Pathways and Geminiviral Proteins: Partners in Disease Development. *Virus Genes* 58, 1–14. https://doi.org/10.1007/s11262-021-01881-6

Gustavsson, J. (Ed.), 2011. Global Food Losses and Food Waste: Extent, Causes and Prevention; Study Conducted For The International Congress Save Food! at Interpack 2011, [16 - 17 May], Düsseldorf, Germany. Presented at the International Congress Save Food!, Food and Agriculture Organization of the United Nations, Rome.

Gutiérrez, S., Yvon, M., Thébaud, G., Monsion, B., Michalakis, Y., Blanc, S., 2010. Dynamics of the Multiplicity of Cellular Infection in a Plant Virus. *PLOS Pathogens* 6, e1001113. https://doi.org/10.1371/journal.ppat.1001113

Hagen, C., Rojas, M.R., Kon, T., Gilbertson, R.L., 2008. Recovery from *Cucurbit leaf crumple virus* (Family *Geminiviridae*, Genus *Begomovirus*) Infection Is an Adaptive Antiviral Response Associated with Changes in Viral Small RNAs. *Phytopathology®* 98, 1029–1037. https://doi.org/10.1094/PHYTO-98-9-1029

Hao, L., Wang, H., Sunter, G., Bisaro, D.M., 2003. Geminivirus AL2 and L2 Proteins Interact with and Inactivate SNF1 Kinase. *The Plant Cell* 15, 1034–1048. https://doi.org/10.1105/tpc.009530

He, Y., Zhang, H., Sun, Z., Li, J., Hong, G., Zhu, Q., Zhou, X., MacFarlane, S., Yan, F., Chen, J., 2017. Jasmonic Acid-Mediated Defense Suppresses Brassinosteroid-Mediated Susceptibility to *Rice black streaked dwarf virus* Infection in Rice. *New Phytologist* 214, 388–399. https://doi.org/10.1111/nph.14376

Huang, C., 2021. From Player to Pawn: Viral Avirulence Factors Involved in Plant Immunity. *Viruses* 13, 688. https://doi.org/10.3390/v13040688

Huang, P., Li, Z., Guo, H., 2022. New Advances in the Regulation of Leaf Senescence by Classical and Peptide Hormones. *Frontiers in Plant Science* 13. https://doi.org/10.3389/fpls.2022.923136

Irigoyen, M.L., Garceau, D.C., Bohorquez-Chaux, A., Lopez-Lavalle, L.A.B., Perez-Fons, L., Fraser, P.D., Walling, L.L., 2020. Genome-wide analyses of cassava Pathogenesis-related (PR) gene families reveal core transcriptome responses to Whitefly Infestation, Salicylic Acid And Jasmonic Acid. *BMC Genomics* 21, 93. https://doi.org/10.1186/s12864-019-6443-1

Jalmi, S.K., Sinha, A.K., 2015. ROS Mediated MAPK Signaling in Abiotic and Biotic Stress-Striking Similarities and Differences. *Frontiers in Plant Science* 6. https://doi.org/10.3389/fpls.2015.00769

Jarvis, A., Ramirez-Villegas, J., Herrera Campo, B.V., Navarro-Racines, C., 2012. Is Cassava the Answer to African Climate Change Adaptation? *Tropical Plant Biology*. 5, 9–29. https://doi.org/10.1007/s12042-012-9096-7

Jin, M., Li, C., Shi, Y., Ryabov, E., Huang, J., Wu, Z., Fan, Z., Hong, Y., 2008. A Single Amino Acid Change in a Geminiviral Rep Protein Differentiates Between Triggering a Plant Defence Response and Initiating Viral DNA Replication. *Journal of General Virology* 89, 2636–2641. https://doi.org/10.1099/vir.0.2008/001966-0

Kawaye, F.P., Hutchinson, M.F., 2021. Maize, Cassava, and Sweet Potato Yield on Monthly Climate in Malawi, in: Oguge, N., Ayal, D., Adeleke, L., da Silva, I. (eds.), *African Handbook of Climate Change Adaptation*. Springer International Publishing, Cham, pp. 617–637. https://doi.org/10.1007/978-3-030-45106-6_120

Kiba, T., Yamada, H., Sato, S., Kato, T., Tabata, S., Yamashino, T., Mizuno, T., 2003. The Type-A Response Regulator, ARR15, Acts as a negative regulator in the Cytokinin-Mediated Signal Transduction in *Arabidopsis thaliana. Plant and Cell Physiology* 44, 868–874. https://doi.org/10.1093/pcp/pcg108

Kim, Y.-W., Youn, J.-H., Roh, J., Kim, J.-M., Kim, S.-K., Kim, T.-W., 2022. Brassinosteroids Enhance Salicylic Acid-Mediated Immune Responses by Inhibiting BIN2 Phosphorylation of Clade I TGA Transcription Factors in *Arabidopsis*. *Molecular Plant* 15, 991–1007. https://doi.org/10.1016/j.molp.2022.05.002

Kong, L.-J., Hanley-Bowdoin, L., 2002. A Geminivirus Replication Protein Interacts with a Protein Kinase and a Motor Protein That Display Different Expression Patterns during Plant Development and Infection. *The Plant Cell* 14, 1817–1832. https://doi.org/10.1105/tpc.003681

Kong, L.-J., Orozco, B.M., Roe, J.L., Nagar, S., Ou, S., Feiler, H.S., Durfee, T., Miller, A.B., Gruissem, W., Robertson, D., Hanley-Bowdoin, L., 2000. A Geminivirus Replication Protein Interacts with the Retinoblastoma Protein Through a Novel Domain to Determine Symptoms and Tissue Specificity of Infection in Plants. *The EMBO Journal* 19, 3485–3495. https://doi.org/10.1093/emboj/19.13.3485

Lacatus, G., Sunter, G., 2009. The Arabidopsis PEAPOD2 Transcription Factor Interacts with Geminivirus AL2 Protein and the Coat Protein Promoter. *Virology* 392, 196–202. https://doi.org/10.1016/j.virol.2009.07.004

Lai, J., Chen, H., Teng, K., Zhao, Q., Zhang, Z., Li, Y., Liang, L., Xia, R., Wu, Y., Guo, H., Xie, Q., 2009. RKP, a RING Finger E3 Ligase Induced by BSCTV C4 Protein, Affects Geminivirus Infection by Regulation of the Plant Cell Cycle. *The Plant Journal* 57, 905–917. https://doi.org/10.1111/j.1365-313X.2008.03737.x

Lebot, V., 2009. Tropical Root and Tuber Crops: Cassava, Sweet Potato, Yams and Aroids, *Crop Production Science In Horticulture Series*. CABI, Wallingford, UK ; Cambridge, MA.

Lefevere, H., Bauters, L., Gheysen, G., 2020. Salicylic Acid Biosynthesis in Plants. *Frontiers in Plant Science* 11. https://doi.org/10.3389/fpls.2020.00338.

Legg, J.P., Fauquet, C.M., 2004. Cassava Mosaic Geminiviruses in Africa. *Plant Molecular Biology* 56, 585–599. https://doi.org/10.1007/s11103-004-1651-7

Legg, J.P., Owor, B., Sseruwagi, P., Ndunguru, J., 2006. Cassava Mosaic Virus Disease in East and Central Africa: Epidemiology and Management of a Regional Pandemic, in: Maramorosch, K., Shatkin, A.J., Thresh, J. M. (eds.), *Advances in Virus Research, Plant Virus Epidemiology*. Academic Press, pp. 355–418. https://doi.org/10.1016/S0065-3527(06)67010-3

León, J., Costa-Broseta, Á., 2020. Present Knowledge and Controversies, Deficiencies, and Misconceptions on Nitric Oxide Synthesis, Sensing, and Signaling in Plants. *Plant, Cell & Environment* 43, 1–15. https://doi.org/10.1111/pce.13617

Li, P., Guo, L., Lang, X., Li, M., Wu, G., Wu, R., Wang, L., Zhao, M., Qing, L., 2022. Geminivirus C4 Proteins Inhibit GA Signaling Via Prevention of NbGAI Degradation, to Promote Viral Infection and symptom Development in *N. benthamiana*. *PLOS Pathogens* 18, e1010217. https://doi.org/10.1371/journal.ppat.1010217

Li, T., Huang, Y., Xu, Z.-S., Wang, F., Xiong, A.-S., 2019. Salicylic Acid-Induced Differential Resistance to the *Tomato yellow leaf curl virus* Among Resistant and Susceptible Tomato Cultivars. *BMC Plant Biology* 19, 173. https://doi.org/10.1186/s12870-019-1784-0

Li, Y., Loake, G.J., 2016. Chapter 24 - Redox-Regulated Plant Transcription Factors, in: Gonzalez, D.H. (ed.), *Plant Transcription Factors*. Academic Press, Boston, pp. 373–384. https://doi.org/10.1016/B978-0-12-800854-6.00024-5

Liu, L., Chung, H.Y., Lacatus, G., Baliji, S., Ruan, J., Sunter, G., 2014. Altered Expression of *Arabidopsis* Genes in Response to a Multifunctional Geminivirus Pathogenicity Protein. *BMC Plant Biology* 14, 302. https://doi.org/10.1186/s12870-014-0302-7

Lozano, J.C., 1986. Cassava Bacterial Blight: A Manageable Disease. *Plant Disease* 70, 1089–1093.

Lozano-Durán, R., Rosas-Díaz, T., Gusmaroli, G., Luna, A.P., Taconnat, L., Deng, X.W., Bejarano, E.R., 2011. Geminiviruses Subvert Ubiquitination by Altering CSN-Mediated Derubylation of SCF E3 Ligase Complexes and Inhibit Jasmonate Signaling in *Arabidopsis thaliana*. *The Plant Cell* 23, 1014–1032. https://doi.org/10.1105/tpc.110.080267

Luan, J.-B., Yao, D.-M., Zhang, T., Walling, L.L., Yang, M., Wang, Y.-J., Liu, S.-S., 2013. Suppression of terpenoid synthesis in plants by a virus promotes its mutualism with vectors. *Ecology Letters* 16, 390–398. https://doi.org/10.1111/ele.12055

Lukan, T., Coll, A., 2022. Intertwined Roles of Reactive Oxygen Species and Salicylic Acid Signaling Are Crucial for the Plant Response to Biotic Stress. *International Journal of Molecular Sciences* 23, 5568. https://doi.org/10.3390/ijms23105568

Ma, F., Yang, X., Shi, Z., Miao, X., 2020. Novel Crosstalk Between Ethylene- and Jasmonic Acid-Pathway Responses to a Piercing–Sucking Insect in Rice. *New Phytologist* 225, 474–487. https://doi.org/10.1111/nph.16111

Maio, F., Helderman, T.A., Arroyo-Mateos, M., van der Wolf, M., Boeren, S., Prins, M., van den Burg, H.A., 2020. Identification of Tomato Proteins That Interact With Replication Initiator Protein (Rep) of the Geminivirus TYLCV. *Frontiers in Plant Science* 11. https://doi.org/10.3389/fpls.2020.01069

Malichan, S., Vannatim, N., Chaowongdee, S., Pongpamorn, P., Paemanee, A., Siriwan, W., 2023. Comparative Analysis of Salicylic Acid Levels and Gene Expression in Resistant, Tolerant, and Susceptible Cassava Varieties Following Whitefly-Mediated SLCMV Infection. *Scientific Reports* 13, 13610. https://doi.org/10.1038/s41598-023-40874-3

Malik, P.S., Kumar, V., Bagewadi, B., Mukherjee, S.K., 2005. Interaction Between Coat Protein and Replication Initiation Protein of *Mung bean yellow mosaic India virus* Might Lead

to Control of Viral DNA Replication. *Virology* 337, 273–283. https://doi.org/10.1016/j.virol.2005.04.030

Maruthi, M.N., Hillocks, R.J., Mtunda, K., Raya, M.D., Muhanna, M., Kiozia, H., Rekha, A.R., Colvin, J., Thresh, J.M., 2005. Transmission of *Cassava brown streak virus* by *Bemisia tabaci* (Gennadius). *Journal of Phytopathology* 153, 307–312. https://doi.org/10.1111/j.1439-0434.2005.00974.x

McCarthy, U., Uysal, I., Badia-Melis, R., Mercier, S., O'Donnell, C., Ktenioudaki, A., 2018. Global Food Security – Issues, Challenges and Technological Solutions. *Trends in Food Science & Technology* 77, 11–20. https://doi.org/10.1016/j.tifs.2018.05.002

Mei, Y., Wang, Y., Hu, T., Yang, X., Lozano-Duran, R., Sunter, G., Zhou, X., 2018. Nucleocytoplasmic Shuttling of Geminivirus C4 Protein Mediated by Phosphorylation and Myristoylation Is Critical for Viral Pathogenicity. *Molecular Plant* 11, 1466–1481. https://doi.org/10.1016/j.molp.2018.10.004

Müllender, M., Varrelmann, M., Savenkov, E.I., Liebe, S., 2021. Manipulation of Auxin Signalling by Plant Viruses. *Molecular Plant Pathology* 22, 1449–1458. https://doi.org/10.1111/mpp.13122

Mur, L.A.J., Prats, E., Pierre, S., Hall, M.A., Hebelstrup, K.H., 2013. Integrating Nitric Oxide into Salicylic Acid and Jasmonic Acid/Ethylene Plant Defense Pathways. *Frontiers in Plant Science*. 4. https://doi.org/10.3389/fpls.2013.00215

Murashige, T., Skoog, F., 1962. A Revised Medium for Rapid Growth and Bio Assays with Tobacco Tissue Cultures. *Physiologia Plantarum* 15, 473–497. https://doi.org/10.1111/j.1399-3054.1962.tb08052.x

Ng, L.M., Melcher, K., Teh, B.T., Xu, H.E., 2014. Abscisic Acid Perception and Signaling: Structural Mechanisms and Applications. *Acta Pharmacologica Sinica* 35, 567–584. https://doi.org/10.1038/aps.2014.5

Njock, T.E., Atiri, G.I., Thottappilly, G., Thresh, J.M., 1996. Disease Development and Recovery in Resistant and Susceptible Cassava Genotypes Infected by *African cassava mosaic geminivirus*. *African Plant Protection* 2, 97–102.

Noueiry, A.O., Lucas, W.J., Gilbertson, R.L., 1994. Two Proteins of a Plant DNA Virus Coordinate Nuclear and Plasmodesmal Transport. *Cell* 76, 925–932. https://doi.org/10.1016/0092-8674(94)90366-2

Nuwamanya, E., Baguma, Y., Rey, C., 2017. The African Perspective: Developing an African Bio-Resource Based Industry: The Case for Cassava, in: Virgin, I., Morris, E.J. (eds.), *Creating Sustainable Bioeconomies: The Bioscience Revolution in Europe and Africa*. Routledge (Taylor & Francis Group) Publishers, Oxfordshire.

Parmar, A., Sturm, B., Hensel, O., 2017. Crops that Feed the World: Production and Improvement of Cassava for Food, feed, and Industrial Uses. *Food Security*. 9, 907–927. https://doi.org/10.1007/s12571-017-0717-8

Patil, B.L., Fauquet, C.M., 2009. Cassava Mosaic Geminiviruses: Actual Knowledge and Perspectives. *Molecular Plant Pathology* 10, 685–701. https://doi.org/10.1111/j.1364-3703.2009.00559.x

Pattyn, J., Vaughan-Hirsch, J., Van de Poel, B., 2021. The Regulation of Ethylene Biosynthesis: A Complex Multilevel Control Circuitry. *New Phytologist* 229, 770–782. https://doi.org/10.1111/nph.16873

Paudel, D.B., Sanfaçon, H., 2018. Exploring the Diversity of Mechanisms Associated With Plant Tolerance to Virus Infection. *Frontiers in Plant Science* 9. https://doi.org/10.3389/fpls.2018.01575

Peres, A.L.G.L., Soares, J.S., Tavares, R.G., Righetto, G., Zullo, M.A.T., Mandava, N.B., Menossi, M., 2019. Brassinosteroids, the Sixth Class of Phytohormones: A Molecular View from the Discovery to Hormonal Interactions in Plant Development and Stress Adaptation. *International Journal of Molecular Sciences* 20, 331. https://doi.org/10.3390/ijms20020331

Ray, D.K., West, P.C., Clark, M., Gerber, J.S., Prishchepov, A.V., Chatterjee, S., 2019. Climate Change Has Likely Already Affected Global Food Production. *PLOS ONE* 14, e0217148. https://doi.org/10.1371/journal.pone.0217148

Rey, C., Vanderschuren, H., 2017. Cassava Mosaic and Brown Streak Diseases: Current Perspectives and Beyond. *Annual Review of Virology* 4, 429–452. https://doi.org/10.1146/annurev-virology-101416-041913

Reynolds, T.W., Waddington, S.R., Anderson, C.L., Chew, A., True, Z., Cullen, A., 2015. Environmental Impacts and Constraints Associated with the Production of Major Food Crops in Sub-Saharan Africa and South Asia. *Food Security* 7, 795–822. https://doi.org/10.1007/s12571-015-0478-1

Ritchie, H., Rosado, P. and Roser, M., 2023. Agricultural Production, *Our World in Data* [Preprint]. Available at: https://ourworldindata.org/agricultural-production (Accessed: 2 March 2025).

Rodríguez-Negrete, E.A., Carrillo-Tripp, J., Rivera-Bustamante, R.F., 2009. RNA Silencing against Geminivirus: Complementary Action of Posttranscriptional Gene Silencing and Transcriptional Gene Silencing in Host Recovery. *Journal of Virology* 83, 1332–1340. https://doi.org/10.1128/jvi.01474-08

Rodríguez-Negrete, E., Lozano-Durán, R., Piedra-Aguilera, A., Cruzado, L., Bejarano, E.R., Castillo, A.G., 2013. Geminivirus Rep Protein Interferes with the Plant DNA Methylation Machinery and Suppresses Transcriptional Gene Silencing. *New Phytologist* 199, 464–475. https://doi.org/10.1111/nph.12286

Rogans, S.J., Allie, F., Tirant, J.E., Rey, M.E.C., 2016. Small RNA and Methylation Responses in Susceptible and Tolerant Landraces of Cassava Infected with *South African cassava mosaic virus*. *Virus Research* 225, 10–22. https://doi.org/10.1016/j.virusres.2016.08.011

Rosas-Díaz, T., Macho, A.P., Beuzón, C.R., Lozano-Durán, R., Bejarano, E.R., 2016. The C2 Protein from the Geminivirus *Tomato Yellow Leaf Curl Sardinia* Virus Decreases Sensitivity to Jasmonates and Suppresses Jasmonate-Mediated Defences. *Plants* 5, 8. https://doi.org/10.3390/plants5010008

Roshan, P., Kulshreshtha, A., Kumar, S., Purohit, R., Hallan, V., 2018. AV2 Protein of *tomato leaf curl Palampur virus* Promotes Systemic Necrosis in *Nicotiana benthamiana* and Interacts with Host Catalase2. *Scientific Reports* 8, 1273. https://doi.org/10.1038/s41598-018-19292-3

Rothenstein, D., Krenz, B., Selchow, O., Jeske, H., 2007. Tissue and Cell Tropism of *Indian cassava mosaic virus* (ICMV) and its AV2 (Precoat) Gene Product. *Virology* 359, 137–145. https://doi.org/10.1016/j.virol.2006.09.014

Roumagnac, P., Lett, J.-M., Fiallo-Olivé, E., Navas-Castillo, J., Zerbini, F.M., Martin, D.P., Varsani, A., 2022. Establishment of Five New Genera in the Family *Geminiviridae*: *Citlodavirus*, *Maldovirus*, *Mulcrilevirus*, *Opunvirus*, and *Topilevirus*. *Archives of Virology* 167, 695–710. https://doi.org/10.1007/s00705-021-05309-2

Sade, D., Sade, N., Shriki, O., Lerner, S., Gebremedhin, A., Karavani, A., Brotman, Y., Osorio, S., Fernie, A.R., Willmitzer, L., Czosnek, H., Moshelion, M., 2014. Water Balance, Hormone Homeostasis, and Sugar Signaling Are All Involved in Tomato Resistance to *Tomato yellow leaf curl virus*. *Plant Physiology* 165, 1684–1697. https://doi.org/10.1104/pp.114.243402

Sage, R.F., 2016. A Portrait of the C4 Photosynthetic Family on the 50th Anniversary of its Discovery: Species Number, Evolutionary Lineages, and Hall of Fame. *Journal of Experimental Botany* 67, 4039–4056. https://doi.org/10.1093/jxb/erw156

Sanderfoot, A.A., Lazarowitz, S.G., 1995. Cooperation in Viral Movement: The Geminivirus BL1 Movement Protein Interacts with BR1 and Redirects It from the Nucleus to the Cell Periphery. *The Plant Cell* 7, 1185–1194. https://doi.org/10.1105/tpc.7.8.1185

Sasaki, Y., Asamizu, E., Shibata, D., Nakamura, Y., Kaneko, T., Awai, K., Amagai, M., Kuwata, C., Tsugane, T., Masuda, T., Shimada, H., Takamiya, K., Ohta, H., Tabata, S., 2001. Monitoring of Methyl Jasmonate-responsive Genes in *Arabidopsis* by cDNA Macroarray: Self-activation of Jasmonic Acid Biosynthesis and Crosstalk with Other Phytohormone Signaling Pathways. *DNA Research* 8, 153–161. https://doi.org/10.1093/dnares/8.4.153

Sasson, A., 2012. Food Security for Africa: An Urgent Global Challenge. *Agriculture & Food Security* 1, 2. https://doi.org/10.1186/2048-7010-1-2

Schaller, A., Stintzi, A., 2009. Enzymes in Jasmonate Biosynthesis – Structure, Function, Regulation. *Phytochemistry* 70, 1532–1538. https://doi.org/10.1016/j.phytochem.2009.07.032

Seo, M., Koiwai, H., Akaba, S., Komano, T., Oritani, T., Kamiya, Y., Koshiba, T., 2000. Abscisic Aldehyde Oxidase in Leaves of *Arabidopsis thaliana*. *The Plant Journal* 23, 481–488. https://doi.org/10.1046/j.1365-313x.2000.00812.x

Settlage, S.B., Miller, A.B., Gruissem, W., Hanley-Bowdoin, L., 2001. Dual Interaction of a Geminivirus Replication Accessory Factor with a Viral Replication Protein and a Plant Cell Cycle Regulator. *Virology* 279, 570–576. https://doi.org/10.1006/viro.2000.0719

Settlage, S.B., See, R.G., Hanley-Bowdoin, L., 2005. Geminivirus C3 Protein: Replication Enhancement and Protein Interactions. *Journal of Virology* 79, 9885–9895. https://doi.org/10.1128/jvi.79.15.9885-9895.2005

Seyfferth, C., Tsuda, K., 2014. Salicylic Acid Signal Transduction: The Initiation of Biosynthesis, Perception and Transcriptional Reprogramming. *Frontiers in Plant Science* 5. https://doi.org/10.3389/fpls.2014.00697

Shamrai, S.N., 2014. Plant Immune System: Basal immunity. *Cytology and Genetics* 48, 258–271. https://doi.org/10.3103/S0095452714040057

Solano, R., Stepanova, A., Chao, Q., Ecker, J.R., 1998. Nuclear Events in Ethylene Signaling: A Transcriptional Cascade Mediated by ETHYLENE-INSENSITIVE3 and ETHYLENE-RESPONSE-FACTOR1. *Genes & Development* 12, 3703–3714. https://doi.org/10.1101/gad.12.23.3703

Song, S., Huang, H., Gao, H., Wang, J., Wu, D., Liu, X., Yang, S., Zhai, Q., Li, C., Qi, T., Xie, D., 2014. Interaction between MYC2 and ETHYLENE INSENSITIVE3 Modulates Antagonism between Jasmonate and Ethylene Signaling in *Arabidopsis*. *The Plant Cell* 26, 263–279. https://doi.org/10.1105/tpc.113.120394

Statistics South Africa, 2019. The Extent of Food Security in South Africa | Statistics South Africa [WWW Document]. Available at: https://www.statssa.gov.za/?p=12135 (Accessed: 01 June 2022).

Sunter, G., Hartitz, M.D., Hormuzdi, S.G., Brough, C.L., Bisaro, D.M., 1990. Genetic Analysis of *Tomato golden mosaic virus*: ORF AL2 is Required for Coat Protein Accumulation while ORF AL3 is Necessary for Efficient DNA Replication. *Virology* 179, 69–77. https://doi.org/10.1016/0042-6822(90)90275-V

Sunter, G., Sunter, J.L., Bisaro, D.M., 2001. Plants Expressing *Tomato Golden Mosaic Virus* AL2 or *Beet Curly Top Virus* L2 Transgenes Show Enhanced Susceptibility to Infection by DNA and RNA Viruses. *Virology* 285, 59–70. https://doi.org/10.1006/viro.2001.0950

Suza, W.P., Staswick, P.E., 2008. The Role of JAR1 in Jasmonoyl-L-Isoleucine Production during *Arabidopsis* Wound Response. *Planta* 227, 1221–1232. https://doi.org/10.1007/s00425-008-0694-4

Taylor, N.J., Fauquet, C.M., Tohme, J., 2012. Overview of Cassava Special Issue. *Tropical Plant Biology* 5, 1–3. https://doi.org/10.1007/s12042-012-9098-5

Tilman, D., Balzer, C., Hill, J., Befort, B.L., 2011. Global Food Demand and the Sustainable Intensification of Agriculture. *Proceedings of the National Academy of Sciences of the United States of America*. U.S.A. 108, 20260–20264. https://doi.org/10.1073/pnas.1116437108

Trinks, D., Rajeswaran, R., Shivaprasad, P.V., Akbergenov, R., Oakeley, E.J., Veluthambi, K., Hohn, T., Pooggin, M.M., 2005. Suppression of RNA Silencing by a Geminivirus Nuclear Protein, AC2, Correlates with Transactivation of Host Genes. *Journal of Virology* 79, 2517–2527. https://doi.org/10.1128/jvi.79.4.2517-2527.2005

Uchechukwu-Agua, A.D., Caleb, O.J., Opara, U.L., 2015. Postharvest Handling and Storage of Fresh Cassava Root and Products: A Review. *Food and Bioprocess Technology* 8, 729–748. https://doi.org/10.1007/s11947-015-1478-z

Unseld, S., Frischmuth, T., Jeske, H., 2004. Short Deletions in Nuclear Targeting Sequences of *African cassava mosaic virus* Coat Protein Prevent Geminivirus Twinned Particle Formation. *Virology* 318, 90–101. https://doi.org/10.1016/j.virol.2003.09.003

Vallad, G.E., Goodman, R.M., 2004. Systemic Acquired Resistance and Induced Systemic Resistance in Conventional Agriculture. *Crop Science*. 44, 1920–1934. https://doi.org/10.2135/cropsci2004.1920

Vidhyasekaran, P., 2014. Nitric Oxide Signaling System in Plant Innate Immunity, in: Vidhyasekaran, P. (ed.), *PAMP Signals in Plant Innate Immunity: Signal Perception and Transduction*. Springer Netherlands, Dordrecht, pp. 307–329. https://doi.org/10.1007/978-94-007-7426-1_6

Walsh, H.A., Vanderschuren, H., Taylor, S., Rey, M.E.C., 2019. RNA silencing of *South African cassava mosaic virus* in transgenic cassava expressing AC1/AC4 hp- RNA induces tolerance. *Biotechnology Reports* 24, 1–13. https://doi.org/10.1016/j.btre.2019.e00383

Wang, C., Wang, C., Zou, J., Yang, Y., Li, Z., Zhu, S., 2019. Epigenetics in the Plant–Virus Interaction. *Plant Cell Reports* 38, 1031–1038. https://doi.org/10.1007/s00299-019-02414-0

Wang, D., Zhang, X., Yao, X., Zhang, P., Fang, R., Ye, J., 2020. A 7-Amino-Acid Motif of Rep Protein Essential for Virulence Is Critical for Triggering Host Defense Against *Sri Lankan cassava mosaic virus*. MPMI 33, 78–86. https://doi.org/10.1094/MPMI-06-19-0163-FI

Wang, H., Buckley, K.J., Yang, X., Buchmann, R.C., Bisaro, D.M., 2005. Adenosine Kinase Inhibition and Suppression of RNA Silencing by Geminivirus AL2 and L2 Proteins. *Journal of Virology* 79, 7410–7418. https://doi.org/10.1128/JVI.79.12.7410-7418.2005

Wasilewska, A., Vlad, F., Sirichandra, C., Redko, Y., Jammes, F., Valon, C., Frey, N.F. dit, Leung, J., 2008. An Update on Abscisic Acid Signaling in Plants and More… . *Molecular Plant* 1, 198–217. https://doi.org/10.1093/mp/ssm022

Wei, Y., Zhu, B., Liu, W., Cheng, X., Lin, D., He, C., Shi, H., 2021. Heat Shock Protein 90 Co-Chaperone Modules Fine-Tune the Antagonistic Interaction between Salicylic Acid and Auxin Biosynthesis in Cassava. *Cell Reports* 34, 108717. https://doi.org/10.1016/j.celrep.2021.108717

Wu, M., Wei, H., Tan, H., Pan, S., Liu, Q., Bejarano, E.R., Lozano-Durán, R., 2021. Plant DNA Polymerases α and δ Mediate Replication of Geminiviruses. *Nature Communications* 12, 2780. https://doi.org/10.1038/s41467-021-23013-2

Yan, C., Xie, D., 2015. Jasmonate in Plant Defence: Sentinel or Double Agent? *Plant Biotechnology Journal* 13, 1233–1240. https://doi.org/10.1111/pbi.12417

Yang, Z., Huang, Y., Yang, J., Yao, S., Zhao, K., Wang, D., Qin, Q., Bian, Z., Li, Yan, Lan, Y., Zhou, T., Wang, H., Liu, C., Wang, W., Qi, Y., Xu, Z., Li, Yi, 2020. Jasmonate Signaling Enhances RNA Silencing and Antiviral Defense in Rice. *Cell Host & Microbe* 28, 89-103.e8. https://doi.org/10.1016/j.chom.2020.05.001

Ye, J., Coulouris, G., Zaretskaya, I., Cutcutache, I., Rozen, S., Madden, T.L., 2012. Primer-BLAST: A Tool to Design Target-Specific Primers for Polymerase Chain Reaction. *BMC Bioinformatics* 13, 134. https://doi.org/10.1186/1471-2105-13-134

Zang, Y., Pei, Y., Cong, X., Ran, F., Liu, L., Wang, C., Wang, D., Min, Y., 2024. Single-cell RNA-Sequencing Profiles Reveal the Developmental Landscape of the *Manihot esculenta* Crantz leaves. *Plant Physiology* 194, 456–474. https://doi.org/10.1093/plphys/kiad500

Zerbini, F.M., Briddon, R.W., Idris, A., Martin, D.P., Moriones, E., Navas-Castillo, J., Rivera-Bustamante, R., Roumagnac, P., Varsani, A., ICTV Report Consortium, 2017. ICTV Virus Taxonomy Profile: *Geminiviridae*. *Journal of General Virology* 98, 131–133. https://doi.org/10.1099/jgv.0.000738

Zhang, P., Vanderschuren, H., Futterer, J., Gruissem, W., 2005. Resistance to Cassava Mosaic Disease in Transgenic Cassava Expressing Antisense RNAs Targeting Virus Replication Genes. *Plant Biotechnology Journal* 3, 385–397. https://doi.org/10.1111/j.1467-7652.2005.00132.x

Zhang, Z., Chen, H., Huang, X., Xia, R., Zhao, Q., Lai, J., Teng, K., Li, Y., Liang, L., Du, Q., Zhou, X., Guo, H., Xie, Q., 2011. BSCTV C2 Attenuates the Degradation of SAMDC1 to Suppress DNA Methylation-Mediated Gene Silencing in *Arabidopsis*. *Plant Cell* 23, 273–288. https://doi.org/10.1105/tpc.110.081695

Zhao, S., Li, Y., 2021. Current Understanding of the Interplays between Host Hormones and Plant Viral Infections. *PLOS Pathogens* 17, e1009242. https://doi.org/10.1371/journal.ppat.1009242

Zhao, Y., 2012. Auxin Biosynthesis: A Simple Two-Step Pathway Converts Tryptophan to Indole-3-Acetic Acid in Plants. *Molecular Plant* 5, 334–338. https://doi.org/10.1093/mp/ssr104

Zhu, F., Xi, D.-H., Yuan, S., Xu, F., Zhang, D.-W., Lin, H.-H., 2014. Salicylic Acid and Jasmonic Acid are Essential for Systemic Resistance Against *Tobacco mosaic virus* in *Nicotiana benthamiana*. *Molecular Plant-Microbe Interactions* 27, 567–577. https://doi.org/10.1094/MPMI-11-13-0349-R

Zhu, T., Zhou, X., Zhang, J., Zhang, W., Zhang, L., You, C., Jameson, P.E., Ma, P., Guo, S., 2022. Ethylene-induced *NbMYB4L* is Involved in Resistance Against *tobacco mosaic virus* in *Nicotiana benthamiana*. *Molecular Plant Pathology* 23, 16–31. https://doi.org/10.1111/mpp.13139